Fakultät für Physik der Universität Bielefeld

The First Second of Leptons

Maik Stuke
Wersterstr. 27
32549 Bad Oeynhausen
May 2011

Supervisor:
Prof. Dr. Dominik J. Schwarz

Vorgelegt der
Fakultät für Physik der Universität Bielefeld
zur Erlangung des akademischen Grades
Doktor der Naturwissenschaften
(Dr. rer. nat.)

Gedruckt auf alterungsbeständigem Papier (ISO 9706)

Contents

Eigenständigkeitserklärung

Hiermit erkläre ich, dass ich die vorliegende Arbeit mit dem Titel THE FIRST SECOND OF LEPTONS selbstständig und ohne unerlaubte fremde Hilfe angefertigt habe. Es wurden ausschließlich die angegebenen Quellen und Hilfen benutzt.

Bielefeld, June 29, 2011

Maik Stuke

The work presented here is based upon some Articles written during the last three years. In the following they are listed chronologically. Parts of them have already been published, see number 4 and 2 below. Also listed here is a popular review of our work at the NewScientist.
The article listed at number 1 has not been submitted, yet.
The article number 3 is published, but not part of this thesis, since it is dealing with a different subject of cosmology, the CMB physics.

1. G. D. Starkman, D. J. Schwarz, M. Stuke,
"Relic WIMP abundance and lepton (flavour-) asymmetries,"
to be submitted.

2. M. Stuke,
"Particle asymmetries in the early universe,"
Proceedings of the 32nd Erice Workshop 2010,
Prog.Part.Nucl.Phys.,**66**,220-225,2010
arXiv:1011.6282 [hep-ph]

3. T. S. Pereira, A. Yoho, M. Stuke, G. D. Starkman,
"Effects of a Cut, Lorentz-Boosted sky on the Angular Power Spectrum,"
arXiv:1009.4937 [astro-ph]

   Citations: 1

4. D. J. Schwarz, M. Stuke,
"Lepton asymmetry and the cosmic QCD transition,"
JCAP **0911** (2009) 025. and Erratum *JCAP* **E01** (2010) 032
arXiv:0906.3434 [hep-ph].

   Citations: 13 (12 (NASA) / 11 (Spires))

A popular review about the work *Lepton asymmetry and the cosmic QCD transition* can be found in the following journal:

R. Courtland
"Did the universe bubble and boil?"
NewScientist **2761 (May 22, 2010) 8.**

June 29, 2011

Danksagung

Diese Arbeit wäre ohne die Mithilfe vieler Personen nie entstanden. Einigen möchte ich an dieser Stelle danken.
Der größte Dank gebührt meiner Familie und deren unbedingter Unterstützung. Sie haben mich stets in dem was ich tat bestärkt. Vielen Dank für Alles!

Entstanden ist diese Arbeit in der Arbeitsgruppe der theoretischen Hochenergiephysik an der Universität Bielefeld. Vielen Dank für die gute Arbeitsatmosphäre und die Ermöglichung der Teilnahme an den vielen Workshops, Konferenzen und Block Kursen im In- und Ausland. Ein besonderer Dank an Susi v. Reder und Gudrun Eichmeyer für Alles! Ein besseres und kreativeres Arbeitsumfeld als das mir durch meinen Betreuer Prof. Dr. Dominik J. Schwarz gebotene, ist wohl nur schwer möglich. Vielen Dank für die geduldige Anleitung zum wissenschaftlichen Arbeiten.

Finanziert wurde diese Arbeit durch ein Stipendium der Friedrich- Ebert-Stiftung der ich für das in mich gesetzte Vertrauen danken möchte. Insbesondere die vielen Workshops, Diskussionen und Freundschaften waren sehr stuimulierent. Besonderes möchte ich mich bei dem für meine Betreuung zuständigem Team um Sohel Ahmand bedanken.

I am grateful to all people I met in the physics department at the University of Bielefeld. Thank you for all the discussions and help. In particular Aravind Natarajan, Christian Byrnes, Olaf Kaczmarek, Edwin Laermann, Anthony Francis, Marcel Müller for discussions, proof readings and help with the numerics of this work.

Also I am very grateful to the physics faculty of the Case Western Reserve University Cleveland, Ohio. In particular to Glenn D. Starkman, who made my visit possible and showed me a whole new perspective on the physics. It was a very inspiring time! Thanks for opening a new field to me, the CMB physics. A big thanks to Amanda Yoho and Thiago S. Pereira for answering all my questions so patiently. I enjoyed the help and discussions with Craig Copi, Pascal M. Vaudrevange, Dimitry Podolsky, Yi-Zhen Chu, Francesco Petrogalli, David M. Jacobs, Eric Greenwood, Yifung Ng, Tanmay Vachaspati and Harsh Mathur. Thanks to everyone for everything! A special thanks to Lori Morton and Patricia Bacevice for helping me with all the administrative stuff, especially the visa!

Sentiti ringraziamenti anche a Giovanni Falcone, che mi ha invitato all´ Universitá della Calabria per il mio primo seminario.

Mille grazie a Rossella Falcone. Senza te non posso fare niente. Un grande bacio!

Abstract

We study the influence of lepton asymmetries on the evolution of the early Universe. The lepton asymmetry l is poorly constrained by observations and might be orders of magnitudes larger than the observed baryon asymmetry $b \simeq 10^{-10}$, $|l|/b \leq 2 \times 10^{9}$.
We find that lepton asymmetries large compared to the tiny baryon asymmetry, can influence the dynamics of the QCD phase transition significantly. The cosmic trajectory in the $\mu_B - T$ phase diagram of strongly interacting matter becomes a function of lepton (flavour) asymmetry. For tiny or vanishing baryon and lepton asymmetries lattice QCD simulations show that the cosmic QCD transition is a rapid crossover. However, for large lepton asymmetry, the order of the cosmic transition remains unknown.
We find that a large asymmetry in one or more lepton flavour changes the number of helicity degrees of freedom of all particles in equilibrium g_* significantly. For the relic abundance of WIMPs, depending on g_* of all particles at the freeze out temperature 40 GeV $> T_{\mathrm{fo}} >$ 0.4 GeV we find a decreasing of few percent depending on l_f. For an asymmetry of $l_f = 0.1$ in all three flavour we found a decrease of the relic WIMP abundance for a given freeze out temperature of almost 20%.

Chapter 1

Introduction

What happens to a thermodynamic ensemble if one changes its boundary conditions? One would say, that in general the system evolves differently. Depending on the size of change and sensitivity of the ensemble to the changed condition, the difference in evolution might also become large. In this work, we investigate the evolution of the ensemble of all Standard Model particles in the early universe by varying boundary conditions within the frame of observational data. The boundary conditions for particle interactions are charge conservation, and the ratio between matter and anti-matter. The latter one is the conservation of baryon and lepton flavour number. There is a time span in the early universe where these conditions are conserved and where we investigate the evolution for different lepton (flavour) numbers.

The recent results from the WMAP[1] 7-year data analysis of the cosmic microwave background (CMB) confirmed ones more the basic predictions of the inflationary Λ-cold dark matter cosmological model providing an improved determination of several cosmological key parameters [K$^+$11]. One of them is the asymmetry between baryons and anti-baryons. Not only our local everyday experience tells us that there are more Protons and Neutrons than anti-Protons and anti-Neutrons, also on larger scales we have clear evidences for the excess of matter. Observations of cosmic rays show that our galaxy is predominantly made of matter. If there would be galaxies or even larger regions of anti-matter, we would observe an γ-ray spectrum from the annihilation between matter and anti-matter at the boundaries of these regions. This is not observed and we can safely assume, that the universe is globally matter dominated and there are no huge anti-matter regions [CDRG98]. The excess of baryons over anti-baryons in an expanding universe is described as

[1] Wilkinson microwave anisotropy probe

a density normalized with the conserved entropy s. The asymmetry is given as the number of baryons N_B minus the number of anti-baryons $N_{\bar{B}}$ and measured by WMAP as [N$^+$10]

$$b = \frac{N_B - N_{\bar{B}}}{s} = (8.85 \pm 0.24) \times 10^{-11}. \tag{1.1}$$

The inflationary Λ-CDM model predicts another background, the cosmic neutrino background (CNB), consisting of the three types of neutrinos decoupling earlier then the photons. But since neutrinos interact only weakly, their background avoided so far any attempt to be measured. Nevertheless, the neutrinos make up approximately 40 per cent of todays radiation energy density and one would like to have more knowledge, how they are distributed. One can define the asymmetry in leptons in the same way as for the baryons

$$l = \sum_f \frac{(N_f - N_{\bar{f}}) + (N_{\nu_f} - N_{\bar{\nu_f}})}{s}, \tag{1.2}$$

where we sum over all flavour $f = e,\ \mu,\ \tau$ and count the charged (anti-) fermions ($\bar{f}$) f and (anti-) neutrinos ($\bar{\nu}$) ν respectively. Since our universe is globally charge neutral [SF06a], the asymmetry between the charged leptons can not exceed the one in baryons. But what about the asymmetry in the neutrinos? Are there more neutrinos or anti neutrinos in our universe? Is the asymmetry between neutrinos much larger then the baryon asymmetry?

Unfortunately theory provides only little help in solving these questions. The mechanism to produce the observed matter anti-matter asymmetry is unknown. After the universe underwent the inflationary expansion in very early times, any existing asymmetry in matter would have been exponentially diluted. So there must have been a mechanism generating the asymmetry after this period. This and the goal to predict the today measured baryon asymmetry led to a large number of different models at different energy scales. The most famous results in this field are the Sakharov conditions [Sak67]. Successful baryogensis happens out of equilibrium, allows for baryon number B violating processes and violates C and CP symmetries. For example this can be achieved by a heavy particle decaying in the early universe, as suggested in grand unified theories (GUT) [Cli06]. With these models it seems to be difficult to generate large asymmetries.
In contrast to this, supersymmetric theories provide an even *natural* mechanism to produce large particle asymmetries [AD85, MOS92, McD00, McD99]. The supersymmetric partners of the Standard Model particles can have a large asymmetry which can be transferred at supersymmetry breaking to the Standard Model particles.

However an asymmetry after the inflationary phase is produced, it has also to survive the B and L violating Sphaleron transition. In the electroweak theory, like in any non abelian theory, the ground states are separated by potential barriers. The thermally induced transitions between two adjacent vacua, called sphaleron transitions, change the baryon and lepton number but conserve (B-L). This process might be in equilibrium at the electroweak scale $T_{ew} \simeq 200\text{GeV}$ and equilibrate or even wash out an existing asymmetry in baryons and leptons [Cli06][2]. Hence, it seems to be natural to expect the lepton asymmetry to be of the same order as the baryon asymmetry. This led to commonly assumed prejudice, that if a lepton asymmetry exist, it is of the same order then the baryon asymmetry, In the Standard Model

$$B = -\frac{51}{28}L, \tag{1.3}$$

both with $\mathcal{O}(10^{-10})$ tiny and negligible in most thermodynamic calculations.

However, in the literature are too many different scenarios resulting in different asymmetries. The widely believed Spahlerons have so far not been observed, since no collider is currently able to produce the needed energies. In the literature it is known, that one can prevent the Sphalerons to be in equilibrium by introducing a large enough current, as for example a neutrino asymmetry would be [Lin76]. This would prevent the dilution or equilibration effects of baryon and lepton flavour effects [CCG99]. Several suggested models are able to reproduce the right baryon asymmetry with a large lepton asymmetry [CCG99, CGMO99, McD99].

Since direct detections fail, we have to rely on indirect effects of large neutrino asymmetries. And indeed, observational data suggests a larger asymmetry in the Neutrinos. The recently published numbers of effective Neutrinos from primordial Helium-4 abundance [IT10] and from Atacama Cosmology Telescope [DHS$^+$10] exceed the standard model value of 3 significantly. Without introducing new particles, the most straight forward way to interpret this is by assuming large neutrino chemical potentials, leading to a neutrino asymmetries of $\mathcal{O}(0.1)$.

We can only give some upper bounds from the big bang nucleosynthesis, the CMB measurements and the formation of large scale structure (LSS). If we assume, that the three neutrinos can change their flavour and oscillate before these events as shown for example in [HMM$^+$02], all three flavour might have the same asymmetry $l_{\nu_e} = l_{\nu_\mu} = l_{\nu_\tau}$. The strong bound on

[2]Tunneling between different vacua are anomalous processes, called Instantons. With increasing temperature they become more and more efficient, while nowadays these anomalous processes are strongly suppressed.

the asymmetry of the electron neutrino from the abundance of primordial ^{4}Helium then applies to all flavour[3]. Again this leads to $l \leq \mathcal{O}(0.1)$, up to ten orders of magnitudes larger then the baryon asymmetry. The situation even worsens if the three flavour do not equilibrate their asymmetries via oscillations. The bounds on the μ- and τ-neutrino can be even larger. For all cosmological observations l/b up to $\mathcal{O}(10^9)$ is allowed.

If we conclude all the different theories and observational data, it is safe to assume the conservation of baryon and lepton flavour number within the Standard Model for the early universe after the electroweak transition and before the onset of Neutrino oscillations. The distribution of a possible large lepton asymmetry on the lepton flavour remains unknown and it might be, that the total lepton asymmetry is of the same order as the baryon asymmetry $\sum_f l_f \simeq b$, but the individual lepton flavour l_f are still orders of magnitudes larger. For example $l_e = b$ but $l_\mu = -l_\tau = \mathcal{O}(0.1)$ as discussed in [CGMO99].

The impact of possible large lepton (flavour) asymmetries have so far only been discussed in the literature in the context of neutrino oscillations [HMM$^+$02, Won02], big bang nucleosynthesis, and the cosmic microwave background [Ste07].

In this work we describe the evolution of the early universe between the electroweak transition at $T_{ew} \simeq 200$ GeV and the onset of nucleosynthesis at $T \simeq 1$ MeV. Between these two events, two more major events might be affected by large chemical potentials. At first the chemical decoupling of a possible WIMP dark matter particle χ with mass TeV $\geq m_\chi \geq 10$ GeV from the plasma of the standard model particles at 40 GeV $> T_{\text{fo}} > 0.4$ GeV. After the interaction rate of the dark matter particle falls behind the Hubble rate at T_{fo}, their number density is only diluted by expansion of the universe and in principle measurable today.
The second event at $T_{QCD} \simeq 170$ MeV is the cosmic QCD transition, where quarks confine to hadrons. It is unclear how this phase transition occurs. Neglecting leptons and their chemical potential, it was stated that the cosmic QCD transition is a rapid change in thermodynamical variables instead of a transition.
These events have only been described for the special case of $l = l_f = 0$. We describe the influence of leptons on these two events in detail, especially the influence of asymmetries between leptons and anti-leptons and their flavour.

The timescale of cosmology is defined as the Hubble time $t_H = \frac{1}{H}$, the interval where thermodynamic variables, curvature, and the expansion changes

[3]The weak current interaction $p + e \leftrightarrow \nu_e + n$ triggers the ratio of protons to neutrons depending on the (anti-)electron neutrinos.

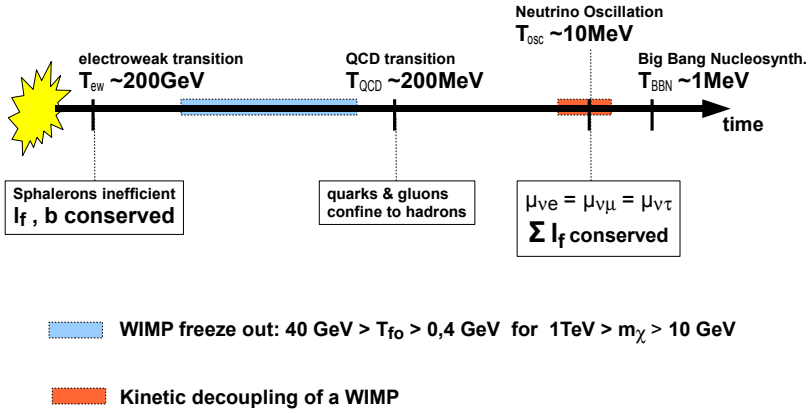

Figure 1.1: Sketch of the evolution of the early universe relevant for this work.

significantly. The corresponding Hubble times for the electroweak phase transition is 10 ps and the onset of nucleosynthesis is at $t_H \simeq 1$ s. In that sense we trace the evolution of leptons through the first second of the universe. We will put a new spotlight on these events and investigate them under the influence of leptons and their possible asymmetries, however they might have been generated.

For this purpose we calculate the temperature evolution of all Standard Model particles for temperatures 200 GeV $> T >$ 10 MeV in an electrical neutral and current free universe for the observed baryon asymmetry and different lepton flavour asymmetries. Since this gives a set of five coupled nonlinear integral equations, one can only solve it numerically. We wrote a software which calculates the thermodynamical variables for any given ensemble of particles in chemical equilibrium following baryon, lepton flavour number and charge conservation.

The work is structured in the following way. After giving a brief introduction into particle cosmology and develop some standard formulae in chapter 2 we derive the thermodynamic description of the particle evolution in chapter 3. Than we go backwards in history of the universe, explaining how large asymmetries change the standard picture $l = l_f = 0$. We start with observa-

tional hints from large scale structure, the cosmic microwave background and the formation of the first elements, the big bang nucleosynthesis in chapter 4. We review upper bounds on neutrino asymmetries in agreement with the observational data.
In chapter 5 we show how these observational bounds might have been before neutrino oscillations and give some comments on possible generating mechanisms.
The cosmic QCD transition and the triggering via leptons is described in chapter 6. We show how the cosmic trajectory in the different phase diagrams change with increasing lepton asymmetry.
In chapter 7 we show how a large lepton flavour asymmetry changes the relic abundance of a WIMP dark matter particle for several scenarios of lepton flavour asymmetries and different freeze out temperature.
We conclude our findings in chapter 8 and give a short outlook in chapter 9. Details on the used numerics are presented in the appendix.

Throughout this work we will use natural units $\hbar$=c=k_{B}=1. In this system, there is one fundamental dimension [energy]=[mass]=[temperature]=[length]$^{-1}$=[time]$^{-1}$. The unit is GeV = 10^3 MeV = 10^6 keV = 10^9 eV with the conversion factors:

Energy	$1\ \mathrm{GeV} = 1.6022 \times 10^{-3}$ erg
Temperature	$1\ \mathrm{GeV} = 1.1605 \times 10^{13}$ K
Mass	$1\ \mathrm{GeV} = 1.7827 \times 10^{-24}$ g
Length	$1\ \mathrm{GeV}^{-1} = 1.9733 \times 10^{-14}$ cm
Time	$1\ \mathrm{GeV}^{-1} = 6.5822 \times 10^{-25}$ s
Energy	$1\ \mathrm{GeV}^2 = 2.4341 \times 10^{21}$ erg/s.

Chapter 2

Particle Cosmology

2.1 Standard Model of particle physics

The most accurate tested theory in physics, besides classical mechanics, is the Standard Model of particle physics. The aim of it is to describe and predict the behaviour of our world´s building blocks.

Starting with the discovery of the electron in 1897, one particle after another uncovered the Standard Model´s characteristics. With the discovery of the nucleus in 1910 and that it constitutes of neutrons and protons in 1930 the building blocks of our ordinary, everyday experienced matter was discovered and being now able to describe the elements on earth and their chemistry could have been the end of all particle research. But in 1932 the positron has been discovered. This was the first hint that anti-matter exists, a form of matter which is not part of our everyday experience. The questions concerning the constituents of our world became even bigger with the discovery of the muon in 1937, a particle which is not even necessary for our normal world. Finally the third charged lepton, the tau, was discovered in 1977 by Martin L. Perl and his colleagues at the Stanford Linear Collider (SLAC) and the Lawrence-Berkley-Laboratory (LBL) who shared the Nobel price in physics in 1995 with Frederick Reines. The latter received it for the first detection of the Neutrinos together with Clyde Cowen in 1956. After they observed the electron Neutrino it took more than 40 years to observe the last Standard Model Neutrino, the $\tau-$Neutrino, by the DONUT-collaboration in 2000 (see for example [N$^+$10]).

The existence of a particle like the Neutrino was proposed by Wolfgang Pauli in 1930 to explain the continuous energy spectrum of the beta decay [Pau78] and little later, in 1933 this particle was named Neutrino by Enrico

Fermi. Today it is well established that Neutrinos have standard weak interactions mediated by $W^{\pm}$ and Z^0 bosons. Their masses should be either zero or tiny. The fact that we still do not know the masses, shows that the Neutrino still remains a mystery.

The experimental search for more particles led in the 1950´s to the discovery of many so called *strongly interacting* particles, leading to the proposal of quarks by Murray Gell-Mann in 1964. And indeed, one quark after another was discovered in experiments, the last one, the top quark, in 1994.

For many years, the Standard Model accounted for all observed particles and their interactions. It includes 12 spin-1/2 fermions (6 quarks and 6 leptons), 4 spin-1 bosons and the so far unobserved spin-0 Higgs boson. The 6 quarks include the up and down quarks that make up the neutron and proton. The 6 leptons include the electron and its partner, the electron Neutrino.

The Standard Model can be described in terms of symmetries using theories of gauge formalisms describing the interactions. It is based on the $\mathrm{SU}(3)_c \otimes \mathrm{SU}(2)_L \otimes \mathrm{U}(1)_Y$ breaking down via spontaneous symmetry breaking to $\mathrm{SU}(3)_c \otimes \mathrm{U}(1)_Q$. Y and Q stand for hyper charge and (electric) charge respectively. This spontaneous breaking generates the $\mathrm{W}^{\pm}$ and Z bosons and the massive scalar Higgs field.

The leptons and quarks are separated into three generations of SU(2) doublets

$$\begin{pmatrix} \nu_e \\ e \end{pmatrix} \quad \begin{pmatrix} \nu_\mu \\ \mu \end{pmatrix} \quad \begin{pmatrix} \nu_\tau \\ \tau \end{pmatrix} \tag{2.1}$$

$$\begin{pmatrix} u \\ d' \end{pmatrix} \quad \begin{pmatrix} c \\ s' \end{pmatrix} \quad \begin{pmatrix} t \\ b' \end{pmatrix} \tag{2.2}$$

The primed quarks are weak eigenstates related to mass eigenstates via the Cabbibo-Kobayashi-Maskawa matrix:

$$\begin{pmatrix} d' \\ s' \\ b' \end{pmatrix} = \begin{pmatrix} V_{ud} & V_{us} & V_{ub} \\ V_{cd} & V_{cs} & V_{cb} \\ V_{td} & V_{ts} & V_{tb} \end{pmatrix} \begin{pmatrix} d \\ s \\ b \end{pmatrix} . \tag{2.3}$$

Each generation contains two flavours of quarks with baryon number $B = 1/3$ and lepton number $L = 0$ whereas for leptons $B = 0$ and $L = 1$. Each particle has a corresponding anti-particle, equal in mass but opposite in quantum numbers.

The strong interaction is mediated via gluons, while the electroweak interaction is mediated by $\mathrm{W}^{\pm}$, Z^0, photons (γ) and the Higgs boson H^0. The latter is only predicted by the Standard Model and has not yet been observed. It is

needed to give mass to the W and Z bosons, and to be consistent with experimental observations. While photons and gluons have no mass, the W and Z are quite heavy. The Higgs is expected to be even heavier and experimental observations set a lower limit on its mass of 110 GeV [N+10].
All particles of the Standard Model are assumed point-like with a quantized internal spin degree of freedom and can have values of 0, 1/2 or 1. Spin-1/2 particles obey Fermi statistics, while spin-1 and spin-0 particles follow Bose-Einstein statistics.

Today it seems that this theory is a low energy limit to a more fundamental theory and there exists several different extensions, solving several problems of the Standard Model. Some of the unsolved questions in the Standard Model are

- The hierarchy problem – Why is there such an enormous difference between the electroweak and the Planck scale in the presence of a Higgs-field?

- Matter-Antimatter asymmetry – Why is there obviously more baryonic matter than antimatter? The Standard Model itself does not provide an answer to this question.

- Dark matter – Why is there such a discrepancy between the measured matter density and baryonic density? There is no candidate in the Standard Model explaining this

- Neutrino masses[1] – What are the masses of the three Neutrinos?

- Dirac or Majorana Neutrinos – What is the correct description for Neutrinos? Dirac or Majorana spinors? If the Neutrinos are Majorana fermions, lepton number violation is explicitly allowed and one would observe a Neutrinoless double beta decay, where two Neutrinos would not leave the nucleus, but annihilate. This is only possible, if the Neutrino is its own anti-particle, a characteristic of Majorana particles. So far this decay is not observed.

The list of open issues can be extended much further, and we refer to the literature for a detailed discussion.

[1] It is a question of definition, if massive Neutrinos are already an extension of the Standard Model.

		Particle	Mass [MeV]	Electric charge [e]	Spin-states	Color-states	Internal degrees of freedom	Baryon number
Fermions	Leptons	Electron	0.511	1	2	1	2 + 2	0
		Muon	105.658	1	2	1	2 + 2	0
		Tau	1776.99	1	2	1	2 + 2	0
		Electron-neutrinos	$< 2.5 \cdot 10^{-6}$	0	1	1	1 + 1	0
		Muon-neutrinos	< 0.17	0	1	1	1 + 1	0
		Tau-neutrinos	< 18	0	1	1	1 + 1	0
	Quarks	Up	1.5 bis 3.0	2/3	2	3	6 + 6	1/3
		Down	3 bis 7	1/3	2	3	6 + 6	1/3
		Charm	95	2/3	2	3	6 + 6	1/3
		Strange	1250	1/3	2	3	6 + 6	1/3
		Top	172300	2/3	2	3	6 + 6	1/3
		Bottom	4200	1/3	2	3	6 + 6	1/3
	Hadrons	Proton	938.27	1	2	1	2 + 2	1
		Neutron	939.57	1	2	1	2 + 2	1
Bosons	Inter-action bosones	Photon	0	0	2	1	2	0
		W-Boson	80000	1	2	1	2 + 2	0
		Z-Boson	91188	0	1	1	1	0
		Gluon	0	0	2	8	16	0
		Higgs	> 114400	0	1	1	1	0
	Mesones	Pion $\pi^{\pm}$	139.57	1	2	1	2+2	0
		Pion π^{0}	134.98	1	2	1	2+2	0

Figure 2.1: Some properties of the Standard Model particles. Not shown are the lepton numbers, since trivially all leptons have lepton number 1 and all other particles 0. The masses are taken from [N$^+$10]. For mesons we just show the pions here. Note that we quoted here the Neutrino mass bounds from laboratory experiments. Assuming Neutrino oscillation leads to smaller bounds. For more details see [N$^+$10].

2.2 Friedmann-Lemaître-Robertson-Walker cosmology

In the following we want to introduce some basic formulas to describe particles in the expanding universe. A successful cosmological model should describe not only the structure of spacetime but also the dynamics of all components. For further details, we refer the reader to any modern textbook on cosmology, like [Muk05, KT94, Wei72, Ber88]

The basic ingredient to the Standard Model of cosmology is the cosmological principal. It states that a comoving observer can at no time make any difference in spatial directions and there is no exclusive place in the universe. Certainly this ignores the fact of small scale energy differences caused by any structure like stars or galaxies. However, several experiments like the temperature fluctuations of the microwave background or the distribution of galaxies indicate, that for scales larger then 100 Mpc[2] the universe is homogeneous and the kopernican principal is a good approximation.

The description of a comoving system in a homogeneous and isotrop spacetime is realized in the theory of general relativity by describing a four dimensional manifold by a defined metric $g_{\mu\nu}$[3]. The latter one describes the spatial-, time-, and causal connection between two events.
For a comoving observer the cosmological principal was formulated as a metric in 1929 by H.P.Robertson and A.G.Walker. In polar coordinates the Roberston-Walker metric $g_{\mu,\nu}$ is:

$$\mathrm{d}s^2 = g_{\mu\nu}\mathrm{d}x^\mu \mathrm{d}x^\nu = \mathrm{d}t^2 - R^2(t)\left[\frac{\mathrm{d}r^2}{1-kr^2} + r^2(\mathrm{d}\theta^2 + sin^2\theta \mathrm{d}\phi)\right]. \qquad (2.4)$$

The cosmic scale factor $R(t)$ describes the expansion or contraction of the universe. The cosmic time t is the so called Eigenzeit of the comoving observer. The factor k describes the sign of the normalized spatial scalar curvature. It is defined as +1 for spherical, 0 for euclidean and -1 for hyperbolic space.
Combining the metric with Einsteins equation of general relativity

$$\mathcal{R}_{\mu\nu} - \frac{1}{2}g_{\mu\nu}\mathcal{R}^{(4)} = G_{\mu\nu}, \qquad (2.5)$$

[2] 1 pc (parsec) is an astronomical distance unit. It is defined as the distance between the earth and a star at a parallax of one arcsecond. It is approximately 3.3 lightyears or 3.086×10^{16} meters.

[3] Here the sign convention is (+,−,−,−).

one easily derives the Friedmann-Lemaître equations from the time and spatial components of the $G_{\mu,\nu}$ tensor[4] shown briefly below.
The curvature or Ricci tensor is defined as

$$\begin{aligned} \mathcal{R}_{\mu\nu} &= g^{\lambda\kappa}\mathcal{R}_{\lambda\mu\kappa\nu} = \mathcal{R}_{\nu\mu} \\ &= g^{ij}\mathcal{R}_{i\mu j\nu} + g^{00}\mathcal{R}_{0\mu 0\nu}, \end{aligned} \tag{2.6}$$

with the Riemann-Christoffel tensor[5] $\mathcal{R}_{\lambda\mu\kappa\nu}$.
The time and spatial components of the Ricci tensor and the metric in (2.5) combined with (2.4) are then:

$$\mathcal{R}_{00} = g^{ij}\mathcal{R}_{i0j0} = 3\frac{\ddot{R}}{R}, \tag{2.7}$$

$$\mathcal{R}_{ij} = g^{lm}\mathcal{R}_{limj} + g^{00}\mathcal{R}_{0i0j} = -\hat{g}^{ij}(2k + 2\dot{R}^2 + \ddot{R}R), \tag{2.8}$$

$$g_{00} = -1, \tag{2.9}$$

$$g_{ij} = R^2\hat{g}_{ij}. \tag{2.10}$$

where the metric tensor $\hat{g}_{\mu\nu}$ in polar coordinates reads:

$$\hat{g}_{ij} = 0 \quad \text{für } i \neq j, \tag{2.11}$$

$$\hat{g}_{rr} = \frac{1}{1 - kr^2}, \tag{2.12}$$

$$\hat{g}_{\theta\theta} = r^2, \tag{2.13}$$

$$\hat{g}_{\phi\phi} = r^2\sin^2\theta. \tag{2.14}$$

The Ricci scalar $\mathcal{R}^{(4)}$ is defined as the trace of the Ricci tensor:

$$\begin{aligned} \mathcal{R}^{(4)} &= g^{\lambda\nu}g^{\mu\kappa}\mathcal{R}_{\lambda\mu\nu\kappa} = g^{\mu\kappa}\mathcal{R}_{\mu\kappa} = g^{00}\mathcal{R}_{00} + g^{ij}\mathcal{R}_{ij} \qquad (2.15) \\ &= -6\left(\frac{k}{R^2} + \frac{\dot{R}^2}{R^2} + \frac{\ddot{R}}{R}\right). \qquad (2.16) \end{aligned}$$

[4]The tensor $G^{\mu\nu}$ is symmetric and covariantly conserved $G^{\mu\nu}_{;\mu} = 0$.
[5]The Riemann-Christoffel-Tensor is defined as

$$\mathcal{R}_{\alpha\beta\nu\delta} = \frac{1}{2}\left(\frac{\partial^2 g_{\alpha\nu}}{\partial x^\nu \partial x^\delta} - \frac{\partial^2 g_{\beta\nu}}{\partial x^\alpha \partial x^\delta} - \frac{\partial^2 g_{\alpha\delta}}{\partial x^\beta \partial x^\nu} + \frac{\partial^2 g_{\beta\delta}}{\partial x^\alpha \partial x^\nu}\right) + g_{\eta\sigma}(\Gamma^\eta_{\nu\alpha}\Gamma^\sigma_{\beta\delta} - \Gamma^\eta_{\delta\alpha}\Gamma^\sigma_{\beta\nu})$$

where the Christoffel symbols $\Gamma^\mu_{\nu\delta}$ are defined by the metric as $\Gamma^\mu_{\nu\delta} = \frac{1}{2}(g_{\lambda\sigma,\nu} + g_{\nu\lambda,\sigma} - g_{\nu\sigma},\lambda)g^{\lambda\mu}$.

The time and spatial components of $G_{\mu\nu}$ are then:

$$G_{00} = \mathcal{R}_{00} - \frac{1}{2}g_{00}\mathcal{R}^{(4)} = -3\left[\frac{k}{R^2} + \frac{\dot{R}^2}{R^2}\right], \tag{2.17}$$

$$G_{ij} = \mathcal{R}_{ij} - \frac{1}{2}g_{ij}\mathcal{R}^{(4)} = g_{ij}\left[\frac{k}{R^2} + \frac{\dot{R}^2}{R^2} + 2\frac{\ddot{R}}{R}\right]. \tag{2.18}$$

Relating the G_{00} and G_{ij} components with the cosmological constant[6] Λ, Newtons gravitational constant G_N and the energy and pressure densities ρ and P respectively leads to the cosmodynamic Friedmann-Lemaître equations

$$G^{00} = -8\pi G_N\rho - \Lambda = -3\left[\frac{k}{R^2} + \frac{\dot{R}^2}{R^2}\right], \tag{2.19}$$

$$G^{ij} = -8\pi G_N P = \left[\frac{k}{R^2} + \frac{\dot{R}^2}{R^2} + 2\frac{\ddot{R}}{R}\right]. \tag{2.20}$$

With the continuity equation of the energy density ρ

$$\dot{\rho} = -3\frac{\dot{R}}{R}(\rho + P) \tag{2.21}$$

one has a description for a model including dust ($P = 0$) and radiation ($P = 1/3$).

A crucial parameter is the Hubble parameter, defined in this homogeneous and isotropic model as

$$H^2 \equiv \frac{\dot{R}^2}{R^2} = \frac{8\pi}{3}G_N\rho - \frac{k}{R^2} + \frac{1}{3}\Lambda. \tag{2.22}$$

With this definition we can now derive measurable observables like the critical density ρ_c. If one neglects the cosmological constant, the relation between the energy density ρ and the critical density denoted by Ω and describes the sign and size of the curvature term k/R^2

$$\rho_c = \frac{3H^2}{8\pi G_N} \equiv \frac{\rho}{\Omega}. \tag{2.23}$$

The critical density today ρ_{c0} is[N$^+$10]

$$\rho_{c0} = 1.054 \times 10^{-5} h^2 \text{GeV cm}^{-3}. \tag{2.24}$$

[6]The comological constant can be derived of the spatial components of the Riemann tensor $\mathcal{R}_{ijkl} = \Lambda(g_{jk}g_{il} - g_{jl}g_{ik})$. For further details we refer the reader to [Jac07].

The only scale in the above presented Standard Model of cosmology is the Hubble parameter h

$$h \equiv \frac{H_0}{100\text{km sec}^{-1}\text{Mpc}^{-1}} = \frac{\dot{R}_0}{R_0} \times \frac{1}{100\text{km sec}^{-1}\text{Mpc}^{-1}}. \tag{2.25}$$

In general it is possible to measure H_0. But several uncertainties in measuring cosmic distances leading to an approximate value of $h = 0.73^{+0.04}_{-0.03}[\text{N}^+10]$.

The magnitude of the energy or mass density in the expanding universe is usually presented as the dimensionless ratio $\Omega = \rho/\rho_c$. The sum of all constituents to the total energy density is predicted to be approximately 1 by inflationary theories: $\Omega_{tot} = 1.001(12)$ $[\text{N}^+10]$. The components can be observed for example by the WMAP satellite[7], measuring the cosmic microwave background . The baryonic matter contribution

$$\Omega_b = 0.0223(7)h^{-2} \simeq 0.0425 \tag{2.26}$$

is only a small part to the total amount of measured pressureless matter density in the universe

$$\Omega_m = 0.128(8)h^{-2} \simeq 0.24 \tag{2.27}$$

The non-visible or missing mass

$$\Omega_{DM} = \Omega_m - \Omega_b = 0.105(8)h^{-2} \simeq 0.20 \tag{2.28}$$

is called *dark matter* (DM). The radiation component, the density of photons is measured as

$$\Omega_\gamma \simeq 4.6 \times 10^{-5} \tag{2.29}$$

and the Neutrinos contribute

$$0.001 < \Omega_\nu < 0.05. \tag{2.30}$$

The remaining energy density is the so called *dark energy* and is the dominant contribution today

$$\Omega_\Lambda \simeq 0.73. \tag{2.31}$$

The simplest cosmological model to fit almost all measured data is a flat universe with a cosmological constant and non-relativistic (cold) dark matter. The standard cosmological model is the so called inflationary ΛCDM-Standard Model. It incorporates the Standard Model of particles plus an additional cold dark matter component, the cosmological constant Λ and a short inflationary expansion at very early times. For the problem of the accelerated expansion, the *Dark Energy*, we refer the reader to the literature, for example [PR03, Muk05].

[7] **W**ilkinson **M**icrowave **A**nisotropy **P**robe

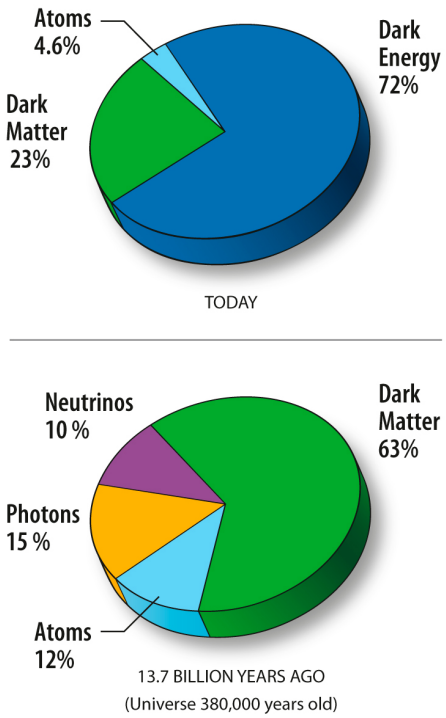

Figure 2.2: Composition of our universe. The upper diagram shows the dark energy domination today, while in former times it was matter dominated shown in the lower diagram. Credit: NASA / WMAP Science Team

2.3 Dark Matter and other mysteries

A wide variety of evidence from particle and astro-physical observations support the idea of a dark matter particle. At galactic and sub-galactic scales the evidence includes galaxy rotation curves [BS01], weak gravitational lensing of distant galaxies by foreground structures and the modulation of the strong lensing around individual massive elliptical galaxies [HYG02, MMBP04]. On the scale of galaxy clusters, observations point to a total cosmological matter density of $\Omega_M \approx 0.2 - 0.3$ [Hoo09] much larger than the density in baryons.

On cosmological scales, the tiny anisotropy of the spectrum of the cosmic microwave background leads to a determination of $\Omega_M h^2 = 0.1358^{+0.0037}_{-0.0036}$, including observations of baryonic acoustic oscillations and type Ia supernovae [Hoo09]. In contrast to this, the same measurements combined with the abundance of light elements leads to a baryonic matter density of $\Omega_B h^2 = 0.02267^{+0.00058}_{-0.00059}$[T$^+$04, Hoo09].
Further information on the nature of the missing mass densities come from

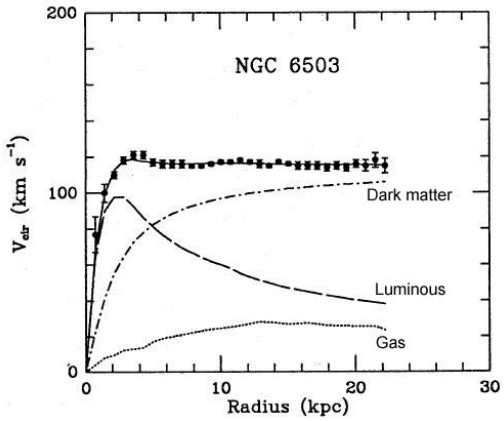

Figure 2.3: An example of a galaxy rotation curve, studied in [BBS91]. Plotted is the distance form the galaxy center on the x-axis versus the velocity on the y-axis. The solid line is the theoretical rotation curve and the dots with error bars show the measured rotation velocity. Also shown are the inferred contributions from gas, luminous matter and dark matter.

simulations of large scale structure formations. These N-body simulations of gravitational clustering of collision less dark matter particles indicates that the dark matter component should be non-relativistic, so called cold dark matter. The prediction of large scale structure formed by a relativistic dark matter component mismatches with the observed large scale structure.
All observations and simulations point to an additional component of the Standard Model of particles, which interacts only by its gravitational force[8].

At a first glance the Standard Model[9] itself provides a reasonable candidate for the dark matter puzzle, the Neutrino. A stable particle, only weakly interacting and massive. The three Standard Model Neutrinos have a relatively small annihilation cross section $\langle\sigma|v|\rangle \simeq 10^{-23}\mathrm{cm}^3/\mathrm{s}$, with small masses $m_\nu < 1$ eV. The freeze out temperature $T_{\mathrm{fo}} \simeq \mathcal{O}(MeV)$ leads to a relic Neutrino density[JKG96, Hoo09]

$$\Omega_{\nu+\bar{\nu}}h^2 \approx 0.1\left(\frac{m_\nu}{9\mathrm{MeV}}\right). \tag{2.32}$$

Since the Neutrino masses are constrained to be well below 9 MeV, the fraction of Neutrinos to the dark matter can only be very small. Furthermore,

[8] Another way to interpret the observational data is by modifying Newtons gravitational law to $F = ma \times \mu a$ in the so called MOND-theories. So far all these theories fail to explain observational data without also introducing a dark matter component[SMFB06, Hoo09].

[9] It is a matter of definition, if massive Neutrinos are part of the Standard Model of particles or already an extension.

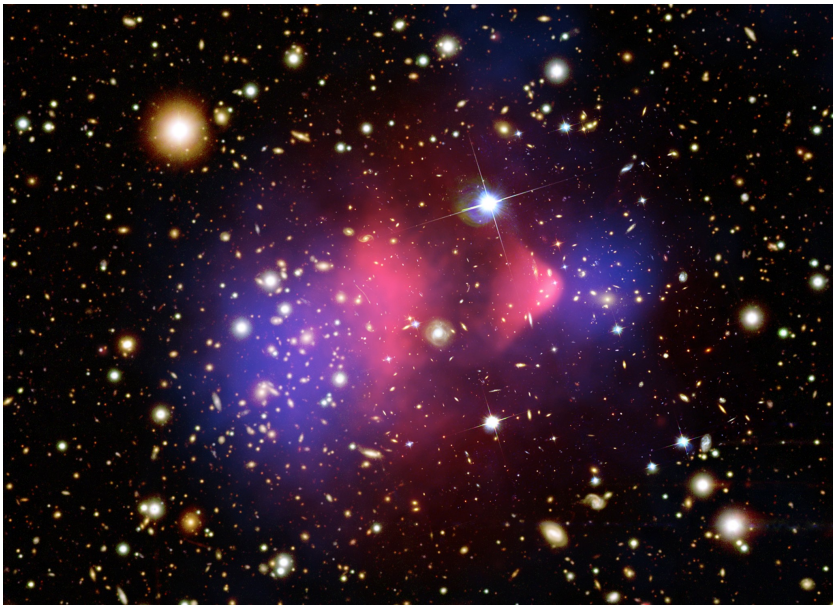

Figure 2.4: The matter in galaxy cluster 1E 0657-56, also known as "bullet cluster". The individual galaxies are seen in the optical image data, but their total mass adds up to far less than the mass of the cluster's two clouds of hot x-ray emitting gas shown in red. Representing even more mass than the optical galaxies and x-ray gas combined, the blue hues show the distribution of dark matter in the cluster. The dark matter was mapped by observations of gravitational lensing of background galaxies. The bullet-shaped cloud of gas at the right was distorted during the collision between two galaxy clusters that created the larger bullet cluster itself. But the dark matter present has not interacted with the cluster gas except by gravity. The clear separation of dark matter and gas clouds is considered direct evidence that dark matter exists. (Composite Credit: X-ray: NASA/CXC/CfA/ M.Markevitch et al.; Lensing Map: NASA/STScI; ESO WFI; Magellan/U.Arizona/ D.Clowe et al. Optical: NASA/STScI; Magellan/U.Arizona/D.Clowe et al.)

even if these constraints would not exist, light Neutrinos would be relativistic at the time of freeze out and thus constitute hot dark matter, which is in conflict with observations of large scale structure[BHS05, Hoo09].

Within the framework of the Standard Model the missing masses on almost all cosmological scales cannot be understood. One has to go beyond the Standard Model.
Maybe the two most popular extensions of the Standard Model to solve the dark matter problem are theories with *extra dimensions* and the *Supersymmetry*.
In the search of unification of the interactions, one can develop theories with extra spatial dimensions, see for example [Che10]. In theories with unified extra dimensions, the lightest of the first excitation states of all Standard Model particles is a viable dark matter candidate.
Even more interesting is the theory of Supersymmetry, believed to be the future extension of the Standard Model by many theorists, even though it is yet experimentally unproven. The idea is a complete symmetry between fermions and bosons. Every Standard Model particle has then a supersymmetric partner and a new symmetry is introduced, the R-parity, $R = (-1)^{3B+L+2S}$ with B, L, and S denoting the baryon number, lepton number and spin. Each Standard Model particle has $R = +1$ and the supersymmetric partner $R = -1$. The conservation of R-parity requires superpartners to be created or destroyed in pairs. Thus, the lightest supersymmetric particle would then be stable even over cosmological timescales [JKG96]. In particular the weak-scale Supersymmetry provides an elegant way to solve the hierarchy problem, enabling grand unification by causing the gauge couplings of the Standard Model to evolve to a common scale, and providing a natural dark matter candidate [Hoo09].
Another popular candidate is the Axion, a particle associated with the Peccei-Quinn symmetry to solve the strong CP-problem of the Quantum-Chromo-Dynamics (QCD)[PQ77, Sik08]. These particles, if they exist, would have a small mass of $m_{\mathrm{A}} \leq 1\mathrm{eV}$ [HMRW10].

2.4 Brief thermal history

The description given above makes it possible to extrapolate the past of our universe based on known physics. The most striking result is, that our universe has not existed forever, but for approximately 14 gyr. What might be before, or shortly after remains unclear and we can only guess.

The different components of energy described in chapter 2.2 evolved differently in the history of the universe. The dependence of the scale factor R of the different energy forms can be derived from energy conservation, $dU = PdV$ with the internal energy U and the equation of state $P = P(\rho) = \omega\rho$. For constant ω, it follows that the energy density scales as $\rho \propto R^{-3(2+\omega)}$. For matter $\omega_{\mathrm{m}} = 0$, for radiation $\omega_{\mathrm{rad}} = 1/3$ and for the cosmological constant $\omega_\Lambda = -1$.
For the different energy densities one gets the following solutions.

- Non-relativistic matter means that $T \ll m$ and thus $\rho = nm \gg nT = P$ and non-relativistic matter is pressure less, $\omega = 0$. The mass is constant and $n \propto 1/R$. It follows, that ρ is just diluted by the expansion of the universe, $\rho_{\mathrm{m}} \propto 1/R^3$.

- Radiation is not only diluted but the energy of photons is also red shifted with $E \propto 1/R$. The energy density of radiation scales as $\rho_{\mathrm{rad}} \propto 1/R^4$.

- The cosmological constant acts like an energy density $\rho_\Lambda = \Lambda/(8\pi G)$, constant in time. This is independent from a possible expansion or contraction of the universe.

We see that for different times the universe was dominated by different energy components. The very early universe was radiation dominated, followed by a period of matter domination. Today the universe is dominated by the cosmological constant (see figure (2.2)).

For a particle cosmologists the scaling of the temperature $T \propto 1/R$ is the most important effect. It leads to the conclusion that any bound states today has been dissolved in the past, when the temperature approximately reaches the binding energy. Or in other words: The higher the temperature gets, or the further backwards in time we go, the heavier particles can be produced. Following approximately the relation between the temperature and a particle with mass m_i $T \geq 2m_i$. The cooling early universe consisted of a plasma containing of all Standard Model particles in thermal equilibrium. A particle decouples from the plasma, when the temperature reaches its mass threshold. An important outcome is that most reaction rates Γ increase faster than the expansion rate of the universe for $t \to 0$. Since the number densities of

relativistic particles evolve like $n \propto T^3$ but the Hubble rate $H \propto \sqrt{\rho_{\rm rad}} \propto T^2$. Reactions that have become ineffective today were important in the early Universe.

This gives us the possibility to extrapolate our Standard Model of particle physics backwards in time. The inflationary-Λ-CDM Standard Model assumes a short period of rapid exponential expansion of the universe, called *inflation*. This epoch is needed to answer some questions appearing in the Standard Model of Cosmology, for example why in the universe causally disconnected regions are still so perfectly homogeneous? Any horizon grows with t, but the scale factor in radiation or matter dominated epoch as $t^{2/3}$ or $t^{1/2}$, respectively. Thus for a scale contained today and completely inside the horizon, in former times it crossed the horizon. A solution to this problem requires that R grows faster than the horizon. With the relation $R \propto t^{2/[3(1+\omega)]}$ one needs $\omega < -1/3$. The horizon problem together with the flatness problem can be solved by introducing Inflation, a short phase of exponentially expansion in the very early universe caused by a field called inflaton. For further details we refer to [Gut81, Lin82].

After the inflationary period, the following events are predicted with increasing temperature (see also figure 2.5):

- At $T \simeq$ 200GeV the gauge symmetry of the Standard Model breaks spontaneously into $\mathrm{SU}(3)_c \otimes \mathrm{U}(1)_Q$. This phase transition is called the *electroweak phase transition*. It happens when the universe is 10ps old and the Hubble radius is circa 10 mm. The order of the transition depends on the effective Higgs potential which in turn depends on the Higgs mass, for more details see for example [Cli06]. Within the Standard Model, the transition is expected to be a smooth crossover, but things are not so clear for extensions of the Standard Model [KLRS96]. For our purpose it is worth noting, that in the Standard Model baryon number B and lepton number L are conserved after the electroweak transition. We assume any asymmetry in baryons and leptons, however produced, survives until today.

- At 40 GeV$< T <$400 MeV a possibly existing weak scale dark matter particle decouples chemically from the particle plasma. The temperature depends on the mass, assumed to be 1 TeV$> m_\chi >$10 GeV[GHS05]. We will discuss this period in greater detail in chapter 7.

- At $T \simeq$ 200MeV the QCD phase transition occurs and quarks and gluons confine to hadrons. Also this event is discussed in greater detail in chapter 6

- At $T \leq 10$MeV Neutrinos start to oscillate and individual lepton flavour numbers are not conserved any more. Still the total lepton number is a conserved quantity.
- At $T \simeq 1$MeV the neutrons freeze out and little later protons and neutrons start to fuse into the first light elements D,^{3}He, ^{4}He, and Lithium. This is called *Big Bang nucleosynthesis* and its agreement between observations and theories is remarkably good.
- At $T \simeq 1$eV the density of matter becomes equal to the density of radiation and the first structures start to form.
- At $T \simeq 0.4$eV the Photons decouple from the plasma and produce the cosmic background radiation, measured for example by the WMAP and PLANCK satellites.

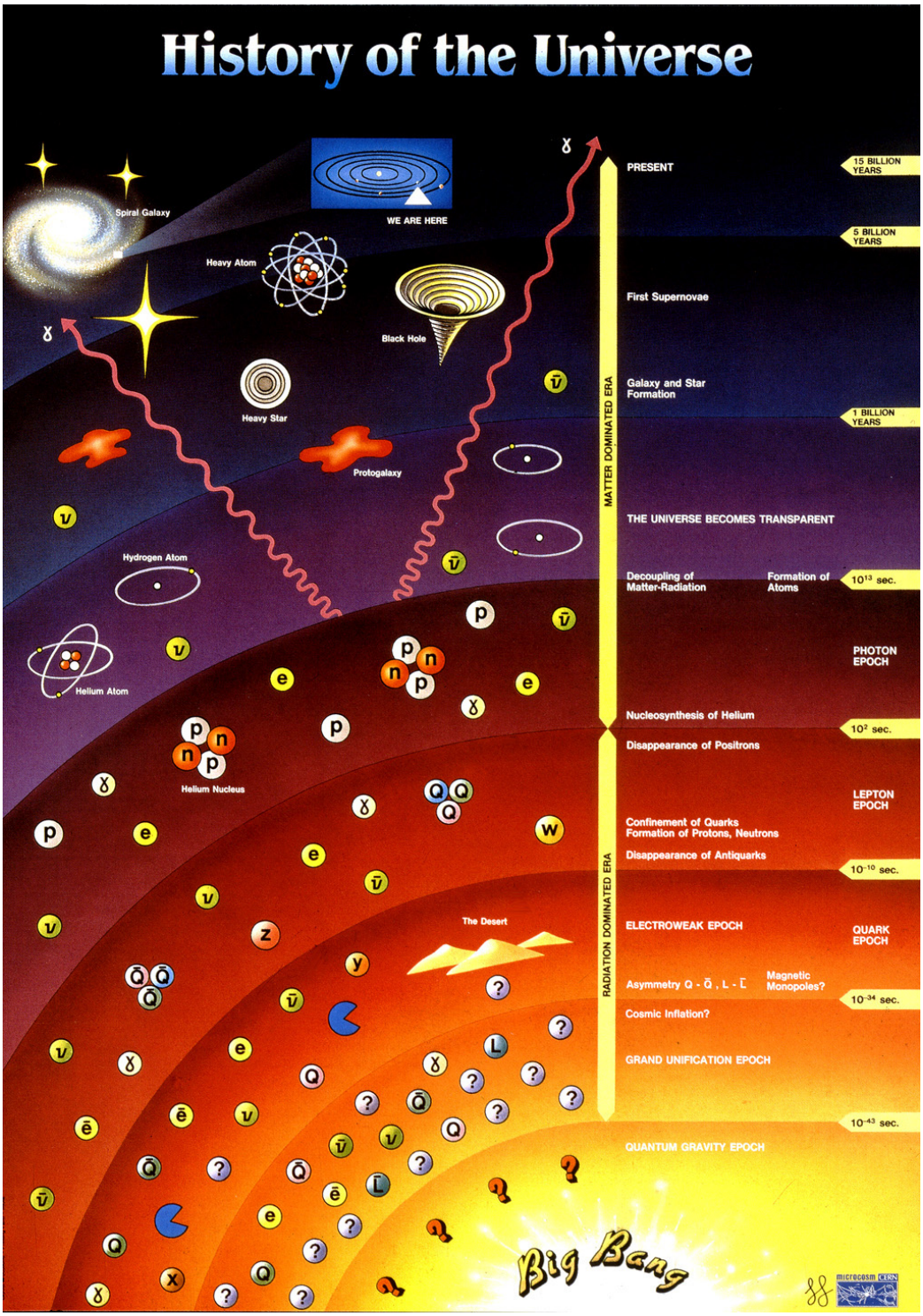

Figure 2.5: Cartoon of the history of the universe. Credits:CERN

Chapter 3

Thermodynamics

3.1 Kinetic theory in the expanding universe

In this work we want to describe the evolution of the Standard Model of particles in the early universe and investigate the influence of chemical potentials, neglected so far in most of the cosmology textbooks. We start developing a thermodynamic description for particle species in cosmological models.
The energy momentum tensor for a perfect fluid is defined as:

$$T_{\mu\nu} = p\, g_{\mu\nu} + (p+\rho) u_\mu\, u_\nu, \tag{3.1}$$

where $u^\mu \equiv \mathrm{d}x^\mu/\mathrm{d}s$ is the four-velocity.
Isotropy and homogeneity gives further:

$$T_{\mu\nu} = \mathrm{diag}(\rho, -P, -P, -P). \tag{3.2}$$

Solving Einstein´s equations including the energy momentum tensor for a perfect fluid

$$\mathcal{R}_{\mu\nu} - \frac{1}{2}\mathcal{R} g_{\mu\nu} - \Lambda g_{\mu\nu} = -8\pi G_N T_{\mu\nu} \tag{3.3}$$

leads to a thermodynamic description of the particle content depending on the energy density ρ and pressure P

The distribution function f of a perfect fluid is defined as a density function in the phase space[1] of the corresponding particle. Homogeneity and isotropy ensures that the distribution function depends only on $\vec{p}$ and t, but not on $\vec{r}$:

$$f = f(|\vec{p}|, t). \tag{3.4}$$

[1]The phase space of a particle in the expanding universe is only well defined for times when the Hubble radius is smaller than the deBroglie wave length of the particle.

The energy momentum tensor depending on f with $p = |\vec{p}|$ reads for a one particle distribution function of an ideal gas:

$$T^{\mu\nu} = \int f \, \frac{p^\mu p^\nu}{p^0} \frac{\mathrm{d}^3 p}{(2\pi)^3}. \tag{3.5}$$

and further for the energy density

$$T^{00} =: \rho = \int f \, p^0 \, \frac{\mathrm{d}^3 p}{(2\pi)^3} \tag{3.6}$$

and the pressure

$$P = T^{ii} = \int f \, \frac{{p^i}^2}{p^0} \, \frac{\mathrm{d}^3 p}{(2\pi)^3}. \tag{3.7}$$

Homogeneity and isotropy ensure that the pressure is the same in all three spatial directions.

Now one can define thermodynamic variables like the particle flow density N^μ. For a particle species one gets:

$$N^\mu = \int f \, \frac{p^\mu}{p^0} \, \frac{\mathrm{d}^3 p}{(2\pi)^3}. \tag{3.8}$$

Isotropy of our spacetime ensures that only the zeroth component is non-vanishing:

$$N^0 =: N = \int f \, \frac{\mathrm{d}^3 p}{(2\pi)^3}, \tag{3.9}$$

where n is the particle density.

Taking particle masses and helicity degrees of freedom g as well into account, one derives for the particle density, the energy density ϵ and the pressure P

$$N = \frac{g}{(2\pi)^3} \int f \, \mathrm{d}^3 p, \tag{3.10}$$

$$\epsilon = \frac{g}{(2\pi)^3} \int \sqrt{p^2 + m^2} \, f \, \mathrm{d}^3 p, \tag{3.11}$$

$$P = \frac{1}{3} \frac{g}{(2\pi)^3} \int \frac{p^2}{\sqrt{p^2 + m^2}} \, f \, \mathrm{d}^3 p. \tag{3.12}$$

Assuming kinetic equilibrium between the particles, one can describe the particle distribution function f as a Fermi-Dirac $(-)$ or Bose-Einstein $(+)$ distribution.

$$f(E, \mu, T) = \frac{1}{\exp(\frac{E-\mu}{T}) \pm 1}. \tag{3.13}$$

The distribution function is depending on the energy E, the chemical potential μ, and the temperature T. The thermodynamic variables in chemical equilibrium then become

$$N(E,\mu,T) = \frac{g}{2\pi^2}\int_m^\infty \frac{E\left(E^2-m^2\right)^{1/2}}{\exp[\frac{\mathrm{E}-\mu}{\mathrm{T}}]\pm 1}\mathrm{dE}, \tag{3.14}$$

$$\epsilon(E,\mu,T) = \frac{g}{2\pi^2}\int_m^\infty \frac{E^2\left(E^2-m^2\right)^{1/2}}{\exp[\frac{\mathrm{E}-\mu}{\mathrm{T}}]\pm 1}\mathrm{dE}, \tag{3.15}$$

$$P(E,\mu,T) = \frac{g}{6\pi^2}\int_m^\infty \frac{\left(E^2-m^2\right)^{3/2}}{\exp[\frac{\mathrm{E}-\mu}{\mathrm{T}}]\pm 1}\mathrm{dE}. \tag{3.16}$$

For our work a central thermodynamical variable is the net particle density, the sum of a particle i minus its anti-particle $\bar{i}$. Assuming that their chemical potentials differ only by the sign $\mu(i) = -\mu(\bar{i})$ we define

$$\begin{aligned} n_i &= N_i - N_{\bar{i}} \\ &= \frac{g}{2\pi^2}\int_{m_i}^\infty E\sqrt{E^2-m_A^2}\left(\frac{1}{\exp(\frac{E-\mu_i}{T})\pm 1} - \frac{1}{\exp(\frac{E-\mu_{\bar{i}}}{T})\pm 1}\right)\mathrm{d}E, \end{aligned} \tag{3.17}$$

For the relativistic and non-relativistic case, one can simplify the expressions for n, ϵ and P. For a particle with mass $m = 0$ (3.14) to (3.16) can be expanded around $\mu/T = 0$:

$$\begin{aligned} \epsilon &= \begin{cases} (\frac{\pi^2}{30}gT^4 + \frac{3}{\pi^2}\zeta(3)gT^3\mu + \frac{1}{4}gT^2\mu^2 + O(\mu^3) & \text{for bosons,} \\ \frac{7}{8}\frac{\pi^2}{30}gT^4 + \frac{9}{4\pi^2}gT^3\mu + \frac{1}{8}gT^2\mu^2 + O(\mu^3) & \text{for fermions} \end{cases} \\ P &= \rho/3 \\ N &= \begin{cases} \frac{1}{\pi^2}\zeta(3)gT^3 + \frac{1}{6}gT^2\mu + O(T\mu^2) & \text{for bosons,} \\ \frac{3}{4\pi^2}\zeta(3)gT^3 + \frac{1}{12}gT^2\mu + O(T\mu^2) & \text{for fermions} \end{cases} \end{aligned} \tag{3.18}$$

where $\zeta(3) \approx 1.202$ is the Riemann-zeta function.
For the non-relativistic case $T \ll m$ the fermions and bosons follow the Stefan-Boltzmann distribution:

$$\begin{aligned} N &= g\left(\frac{mT}{2\pi}\right)^{3/2}\exp\left[-\frac{m-\mu}{T}\right], \\ \epsilon &= mn, \\ P &= nT \qquad (\ll \epsilon). \end{aligned} \tag{3.19}$$

The net particle densities for the relativistic and non-relativistic case become:

$$n_i \overset{(T\gg m,\mu)}{=} \begin{cases} \frac{1}{3}gT^2\mu_i + O(\mu_i^2) \text{ for bosons} \\ \frac{1}{6}gT^2\mu_i + O(\mu_i^2) \text{ for fermions} \end{cases} \tag{3.20}$$

$$\overset{(T\ll m)}{=} 2g\left(\frac{mT}{2\pi}\right)^{3/2} \sinh\left(\frac{\mu}{T}\right) \exp\left(\frac{-m}{T}\right). \tag{3.21}$$

This is only valid, if all reactions are in chemical equilibrium, a perfect approximation for particle reactions in the early universe. The scale of interest in cosmology is the Hubble time $t_H = 1/H$. As long as the particle interaction in the early universe are faster than the Hubble time, they remain in equilibrium. Comparing the Hubble rate with the typical interaction rates shows that until $T \simeq 1\text{MeV}$ all interaction rates of massless particles are larger and though it is an excellent approximation to assume thermal and chemical equilibrium in the early universe (see figure 3.1). The weak interaction rate (Γ_w) falls behind the Hubble rate at $T \simeq 1\text{MeV}$, while the electro-magnetic (Γ_{em}) and strong interaction rates are always faster then the Hubble rate.

The net particle density is zero, if the number of particles equals the number of anti particles. It also vanishes, if the temperature becomes to low to create the particle in reactions like $\gamma + \gamma \rightarrow i + \bar{i}$. As the Universe expands and cools, the particles annihilate at temperatures comparable to their mass and eventually fall out of equilibrium. The annihilation temperature can be approximated by $T_{\text{ann}} \simeq m_i/3T$. If there is no initial and conserved asymmetry between the particle and its anti-particle, the species i annihilates completely.

3.2 Entropy and degrees of freedom

In this section we develop the entropy s, first introduced in 1865 by Rudolf Clausius for the description of closed thermodynamic processes. We assume that the entropy in the early universe is conserved and derive a $s(\mu)$. We also introduce the effective degrees of freedom of a particle plasma in the expanding universe.
The definition of the entropy density current including all quantum mechanical effects in terms of the distribution function f is [Ber88]:

$$S^\mu := -\int \left(f\ln f \mp (1 \pm f)\ln(1 \pm f)\right) \frac{p^\mu}{p^0} \frac{\mathrm{d}^3 p}{(2\pi)^3}, \tag{3.22}$$

where upper and lower signs refer to Bose-Einstein and Fermi-Dirac statistics, respectively.

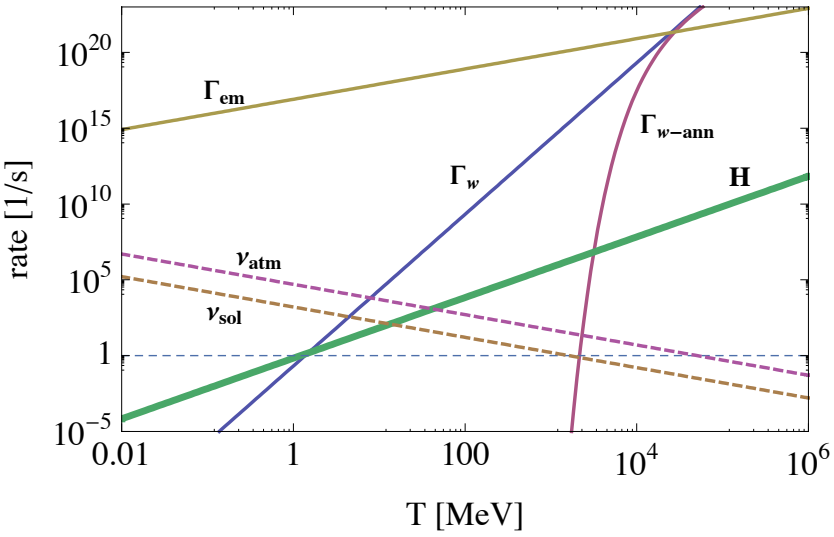

Figure 3.1: Sketch of the evolution of the Hubble rate and the typical interaction rates for temperatures between 0.01 and 10^6 MeV for the Fermi theory and ignoring the running of the coupling constants. The strong interaction would be above the scale of this plot. The solid purple trajectory Γ_{w-ann} shows the WIMP annihilation rate for a WIMP with mass $m_{\mathrm{WIMP}} = 100$ GeV. Such a particle would decouple from the plasma at $T \simeq 2$ GeV. Also shown are the frequencies for Neutrino oscillations (dashed lines) for the solar and atmospheric Neutrino solution. The crossing of these trajectories with the weak interaction indicate the onset of vacuum Neutrino oscillations. Credits: [Sch03].

Calculating the zeroth component with the equilibrium distribution function for massless particles with vanishing chemical potentials and internal degrees of freedom g, we derive the well known entropy density formula

$$s(T) \overset{m,\mu=0}{=} \frac{2\pi^2}{45} T^3 \left(\sum_{i=\text{bos}} g_i + \frac{7}{8} \sum_{i=\text{fer}} g_i \right) \tag{3.23}$$

$$= \frac{2\pi^2}{45} T^3 g_{s*}. \tag{3.24}$$

The abbreviations *bos* and *fer* mean bosons and fermions, respectively. The function g_{s*} counts the effective degrees of freedom [see figure (3.2)]. For the early universe with $T \gg m_i$, this approximation is excellent. Taking the fermionic chemical potentials into account, leads to slightly different solution:

$$s(T, \mu_i) \overset{m=0}{=} \frac{2\pi^2}{45} T^3 \left(\sum_{i=\text{bos}} g_i + \frac{7}{8} \sum_{i=\text{fer}} g_i + \sum_{i=\text{fer}} \frac{g_i}{6} \left(\frac{\mu_i}{T} \right)^2 \right) \tag{3.25}$$

$$= \frac{2\pi^2}{45} T^3 \left(g_{s*} + \Delta g_{s_*} \right). \tag{3.26}$$

where g_i counts the internal degrees of freedom of a particle species. For example, $g_i = 1$ for ν_i, $g_i = 2$ for charged leptons or $g_i = 6$ for quarks. We see that for $\frac{\mu_i}{T} < 1$ the contribution can be neglected and the well known entropy is an excellent approximation.

The entropy s is an important quantity because it is conserved during the evolution of the universe. Conservation implies that $s \propto g_{s*} R^3 T^3$ is constant and we can relate the temperature of the Universe to the scale factor $T \propto g_{s*}^{-1/3} R^{-1}$. We see that as long as g_{s*} is constant, $T \propto 1/R$. But the effective degrees of freedom change, if a particle reaches the mass threshold it annihilates. Then the entropy is transferred to the photons, for example for the electrons $e^+e^- \to \gamma\gamma$ leads formally to a decrease in g_{s*} and for a short period the temperature decreases less slowly.

For this work it is important to note, that the entropy scales as $s \propto R^{-3}$ like the net numbers with conserved charges, for example baryons. If the baryon number B is conserved, also the ration n_b/s is conserved.

Alternatively, one can also derive the effective degrees of freedom from the energy density of all particles in the plasma. The energy density of a species i, the particle and its anti-particle is given as

$$\epsilon_{i,\bar{i}} \overset{m_i=0}{=} \sum_i \frac{g_i}{2\pi^2} \int_0^\infty E^3 \left[f(i) + f(\bar{i}) \right] \mathrm{dE} \tag{3.27}$$

$$\simeq \frac{\pi^2}{15} g_{\epsilon*} T^4. \tag{3.28}$$

For fermions the distribution function in (3.27) reads $f(i) = (\exp[(\mathrm{E} -$

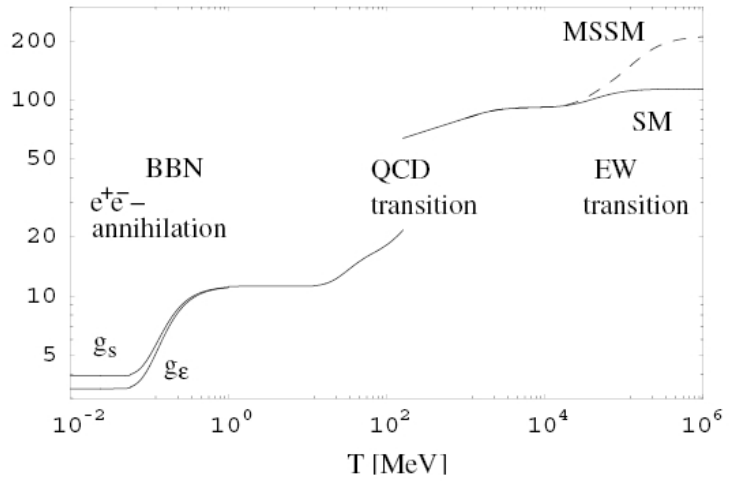

Figure 3.2: Shown here are the effective degrees of freedom on the y-axis and their evolution in T for vanishing chemical potentials. When the temperature reaches $T \approx m_i/T$ the particle i annihilates and the corresponding degrees of freedom disappear. The difference between $g_* = g_\epsilon$ and $g_{*s} = g_s$ in the low temperature regime shows the effect, that the Neutrinos decouple from the plasma before e^+e^--annihilation, but remain relativistic and contribute further. The dashed line shows the extension by the Minimal Supersymmetric Standard Model [Sch03].

$\mu_\mathrm{i})/\mathrm{T}] + 1)^{-1}$ and the integral of the energy density can be solved exactly. Assuming $\mu_i = -\mu_{\bar{i}}$ leads for the energy density to

$$\epsilon_{i,\bar{i}} = \sum_i g_i \left[\frac{7\pi^2}{120}T^4 + \frac{1}{4}T^4\left(\frac{\mu_i}{T}\right)^2 + \frac{1}{8\pi^2}T^4\left(\frac{\mu_i}{T}\right)^4\right], \tag{3.29}$$

and further to

$$g_{\epsilon *} = \frac{15}{\pi^2}\sum_i g_i \left[\frac{7\pi^2}{120} + \frac{1}{4}\left(\frac{\mu_i}{T}\right)^2 + \frac{1}{8\pi^2}\left(\frac{\mu_i}{T}\right)^4\right]. \tag{3.30}$$

The μ_i- depending difference to the standard g_* is

$$\Delta g_{\epsilon *} = \frac{15}{4\pi^2}\sum_i g_i \left[\left(\frac{\mu_i}{T}\right)^2 + \frac{1}{2\pi^2}\left(\frac{\mu_i}{T}\right)^4\right]. \tag{3.31}$$

We see that taking the μ-dependence into account leads to a difference between the degrees of freedom of the entropy and of the energy density.

$$g_{\epsilon *}(T,\mu) \neq g_{s*}(T,\mu). \tag{3.32}$$

While the degrees of freedom in the entropy density depends additionally only on a squared (μ/T)-term, $g_{\epsilon *}$ shows also a $(\mu/T)^4$ term. It is usually assumed, that chemical potentials are tiny and play no role in the evolution of the early universe. This is not necessarily true, as we will show in the next chapters. However, for any $\mu/T < 0.1$, the contribution can be neglected for most purposes. Doing so, leads to the degrees of freedom shown in figure 3.2. We see that with decreasing temperature and annihilating particles the number of effective degrees of freedom in the plasma gets smaller.

For example each quark has 12 degrees of freedom (3 colours, 2 charges and anti quark), where a charged lepton has only four (2 charges, particle-antiparticle). The annihilation of a quark has a bigger impact on the effective degrees of freedom than the annihilation of a lepton. For Standard Model particles (excluding the Higgs particle) g_* starts at temperatures around 200 GeV with 102 degrees of freedom. The first increase from 100 to 10 GeV is due to the annihilation of the top quark, W and Z bosons, where the biggest effect comes from the 12 degrees of freedom of the top quark. The second decrease from $T \approx$3 GeV to $T \approx .5$ GeV is due to the annihilation of charm and bottom quarks and the τ. The increase after the cosmic QCD transition is due to the fact, that the remaining quarks confine to hadrons with much less degrees of freedom. We also see that the thermodynamic effect on the early universe from the QCD transition is much bigger than from the electroweak transition.

3.3 Conserved quantum numbers

In the early Universe, after the electroweak phase transition at $T_{\mathrm{EW}} \sim 200$ GeV and before the onset of Neutrino oscillations at a few MeV, baryon number B and lepton flavour numbers L_f are conserved, since no baryon or lepton number violating processes have been observed, yet. We further assume, conservation of the electrical charge Q and that $Q = 0$. A neutral universe seems to be reasonable, because several observations point to neutrality and lack of currents on large scales. The work of [SF06b] shows that a possible charge asymmetry is annihilated in less than a Hubble time for 100 GeV $\geq T \geq 1$ eV. It is shown too, that currents are damped for all temperatures $T \geq 1$ eV.

We also assume that all globally conserved quantum numbers are also conserved locally. This means that our approximation is applicable at length scales larger than the largest scale on which transport phenomena can show up, given we apply homogeneous initial conditions. The largest mean free path is that of Neutrinos and thus the local physics on scales less than the Neutrino mean free path might differ from the results obtained in this work.

The net particle density n_i is the density of a particle minus the density of its anti-particle. In thermal and chemical equilibrium (and neglecting effects of interactions) it can be described as shown in (3.17).

Lifting the global conservation laws to local ones we obtain equations for the specific lepton flavour asymmetry, specific baryon asymmetry and the charge density:

$$l_f = \frac{n_f + n_{\nu f}}{s} \qquad \text{for } f = e, \mu, \tau, \tag{3.33}$$

$$b = \sum_i \frac{b_i n_i}{s} \qquad \text{with } b_i = \text{baryon number of species i}, \tag{3.34}$$

$$0 = \sum_i q_i n_i \qquad \text{with } q_i = \text{charge of species i}, \tag{3.35}$$

with the entropy density $s = s(T, \mu)$. For any given temperature T, the free variables in this set of equations are the chemical potentials in the net particle densities $n_i(T, \mu_i)$ and the specific lepton flavour asymmetries l_f are three unknown parameters. The baryon number $b \approx (8.85 \pm 0.24) \times 10^{-11}$ is given, based on [N+10].

To solve this set of equations, we have to give some constraints to the chemical potential. This means we have to specify l_f, the asymmetry in the individual lepton flavour. In the next chapter, we give some experimental boundaries derived from the cosmic microwave background, big bang nucleosynthesis and the formation of large scale structure.

Chapter 4

Leptons and BBN,CMB and LSS

Two pillars of modern cosmology are the synthesis of the first light elements, the so called big bang nucleosynthesis, and the measurements of the cosmic microwave background. The first offers the deepest and reliable probe of Standard Model physics in the early universe, while the measurement of the temperature fluctuations of the microwave background photons offers the most accurate results. Possible deviations from standard physics have to be explained within the results of these observations. In this chapter we want to review experimental boundaries on the lepton flavour asymmetries from observations.

The theory of big bang nucleosynthesis predicts the universal abundances of the elements D, ^{3}He, ^{4}He, ^{7}Li, produced in the first three minutes of the universe. The synthesis of these first elements is sensitive to the condition in the early universe at $T \leq 1$MeV, or equivalently $t \simeq$1s. At this time, the weak interaction rate, converting neutrons to protons, $\Gamma_w \simeq G_F^2 T^5$ increases faster then the Hubble rate $H \simeq \sqrt{g_* G_N} T^2$. This results in the freeze out temperature $T_{\rm fo} \simeq (g_* G_N / G_F^4)^{1/6} \simeq 1$ MeV. The ratio between neutron and protons is at this time $n/p = \exp[-\Delta {\rm m}/{\rm T_{fo}}] \simeq 1/6$, with $\Delta m = m_p - m_n \simeq 1.29$eV being the mass difference between the proton and neutrons. This ratio is sensitive to strong and electromagnetic interactions in Δm and the determination of $T_{\rm fo}$ to weak and gravitational interactions. Another impact can be the changing in the effective degrees of freedom in the Hubble rate. The g_* is defined over the energy density in (3.27) and we have shown, that a large chemical potential increases the energy density and the effective degrees of freedom.

The relativistic particles contributing to the energy density at $T \simeq 1$ MeV are the photons, $e^{\pm}$ and the Neutrinos. Since our universe is charge

neutral and the asymmetries in baryons is measured to be $b = \mathcal{O}(10^{-10})$ any asymmetry in the charged leptons today can be at maximum of the same order. Otherwise the condition of global charge neutrality would be violated. The only charged leptons at $T \simeq$ few MeV are electrons, since the τ and μ´s are too heavy. But the lepton flavour asymmetries are the sum of the net particle densities of the charged leptons and their corresponding Neutrinos. A large lepton flavour asymmetry may be hidden in the Neutrinos and we can approximate

$$b \ll l_f = \frac{n_{\nu_f}}{s(T)} \tag{4.1}$$

$$l_f \simeq 0.6 \frac{\mu_{\nu_f}}{T}. \tag{4.2}$$

To receive some information about the possible asymmetry, one can check indirect influences on the evolution of the early universe for $T < 1$ MeV and compare them with the observational data.

After the neutron to proton ratio freezes out, the neutron fraction drops due to the $\beta-$decay until $n/p \simeq 1/7$ and the nucleosynthesis chain begins with the formation of Deuterium. However, photo-dissociation delays the reaction p(n,γ)D until $T \simeq 0.1$ MeV nuclei begin to form. Since the density is already low at this point, $2 \to 2$ processes are the most important. The reactions D(p,γ)^{3}He and ^{3}He(γ)^{4}He are the dominant processes. All β-decay surviving neutrons end up in the stable element[1] ^{4}He. The primordial mass fraction Y_P can be estimated by

$$Y_P = \frac{2(n/p)}{1 + (n/p)} \approx 0.25 \tag{4.3}$$

For a better prediction one has to include a lot more physics, like the full nuclear reaction rates and the exact neutron lifetime. The predicted values can than be compared to the today measured ones. To observe only the primordial elements and not the ones being produced later in stellar evolution, one seeks for astrophysical objects with low metal abundances.

The actual experimental value for ^{4}He fraction given in [IT10] is

$$Y_P = 0.2565 \pm 0.0010(\text{stat.}) \pm 0.0050(\text{syst.}) \ . \tag{4.4}$$

This is remarkably close to the easy approximation given above. However, observing the relic abundances today is always difficult and there may be always systematically errors (see figure 4.2).

[1] Heavier nuclei do not form in any reasonable number, since there are no stable mass number 5 nuclei. The coulomb barrier for the production of ^{7}Li or ^{7}Be is too high for the production of a huge amount.

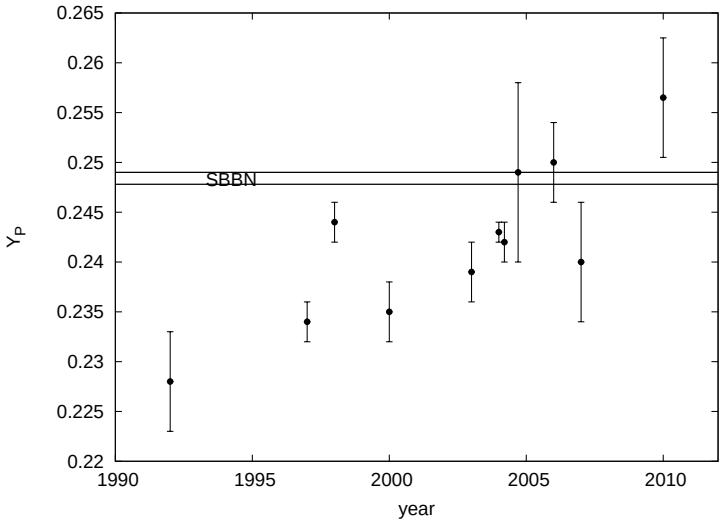

Figure 4.1: Observational ^{4}He abundances published between 1992 and 2010 and the 1 σ band for the predicted standard big bang nucleosynthesis (SBBN). The error bars are the 1 σ uncertainties. The values are taken from [Ste07, IT10]. All data stems from the observation of metal poor HII regions. The recently published indirect measurement (via N_ν^{eff}) of $Y_P = 3.13 \pm 0.044$ by the ATC group is not included in this figure since it relies on measuring the cosmic microwave background.

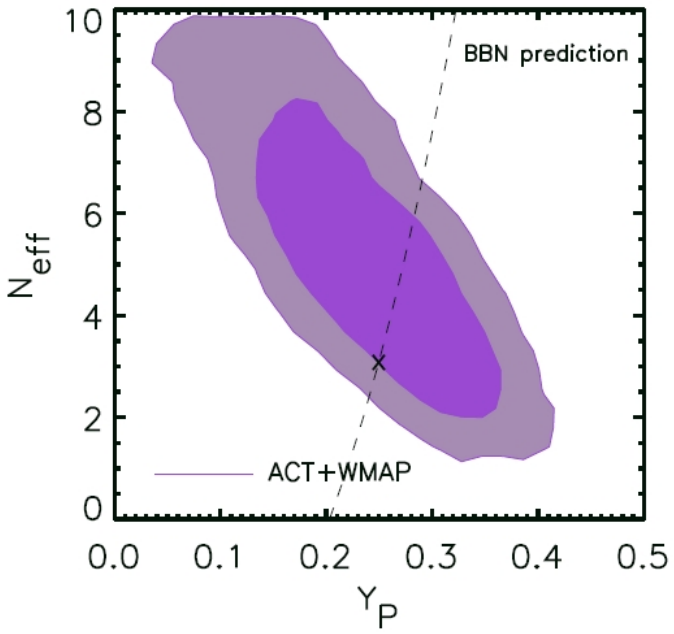

Figure 4.2: The recently published indirect measurement (via N_ν^{eff}) of $Y_P = 3.13 \pm 0.044$ by the ATC group is way above all before published abundances. Shown here are the combined WMAP-ATC data and the 1 and 2 σ contours. We see, that the SBBN prediction for Y_P with $N_\nu^{\text{eff}} = 3.04$ lies on the edge of the 1 σ area. For more details and credits see [DHS$^+$10].

-

The *standard* big bang nucleosynthesis (SBBN) takes three Neutrinos without a chemical potential into account. An asymmetry between the electron- and anti-electron Neutrino effects the neutron to proton ratio. A nonzero $\frac{\mu_e}{T}$ would shift the abundances of neutron and protons:

$$\mathrm{Y}_n = \frac{1}{\exp[\Delta\mathrm{m}/\mathrm{T} + \frac{\mu_{\nu_\mathrm{e}}}{\mathrm{T}}] + 1} \tag{4.5}$$

$$\mathrm{Y}_p = \frac{1}{\exp[-\Delta\mathrm{m}/\mathrm{T} - \frac{\mu_{\nu_\mathrm{e}}}{\mathrm{T}}] + 1} \ . \tag{4.6}$$

For further details and a more detailed calculation see for example [Ste07]. Note, that a possible shift is also sign dependent. The second effect of non-zero Neutrino chemical potentials would be their contribution to the energy density of the universe. At $T \simeq 1$ MeV the radiation energy density consists of photons and Neutrinos. Introducing non zero Neutrino chemical potential is equivalent to additional flavours. From (3.31) it follows for the effective number of Neutrinos:

$$\begin{aligned} N_\nu^{\mathrm{eff}} = &\quad N_\nu + \Delta N_\nu^{\mathrm{eff}} &(4.7)\\ = &\quad 3 + \frac{30}{7\pi^2}\sum_f \left[\left(\frac{\mu_{\nu_f}}{T}\right)^2 + \frac{1}{2\pi^2}\left(\frac{\mu_{\nu_f}}{T}\right)^4\right], &(4.8)\end{aligned}$$

assuming three active Neutrino flavours $N_\nu = 3$. The values given recently in [IT10]: $N_\nu^{\mathrm{eff}} = 3.8^{+0.8}_{-0.7}$ and in [DHS$^+$10]: $N_\nu^{\mathrm{eff}} = 4.6\pm0.8$ indicate clearly deviation, possibly originated by chemical potentials.

An asymmetry in the μ or τ-flavour effects only the energy density and so the expansion rate of the universe. Note that this effect does not distinguish between the flavours nor the sign.

The effect on the Helium would be the following: Increasing $|\frac{\mu_\mu}{T}|$ and/or $|\frac{\mu_\tau}{T}|$ leads to a faster expansion and therefore to a higher freeze out temperature of the weak interaction and so to an increased yield of ^{4}He. Increasing μ_{ν_e}/T affects the expansion rate, but also changes the neutron to proton density and so can lead to a smaller n/p at the freeze out of weak interactions. So the three chemical potential can be played against each others to get the observed ^{4}He abundance, done in [OSTW91].
The production of D+^{3}He and ^{7}Li is much far sensitive to the n/p-ratio, since their abundances is due to competitions between different nuclear reaction rates. The longer the nuclear rates are in equilibrium, the more D and ^{3}He are destroyed.
The bounds on the chemical potentials coming from big bang nucleosynthesis alone are $|\mu_{\nu_e}/T| < 0.1$ and $|\mu_{\nu_{\mu,\tau}}/T| < 0.1$. The bounds coming from the

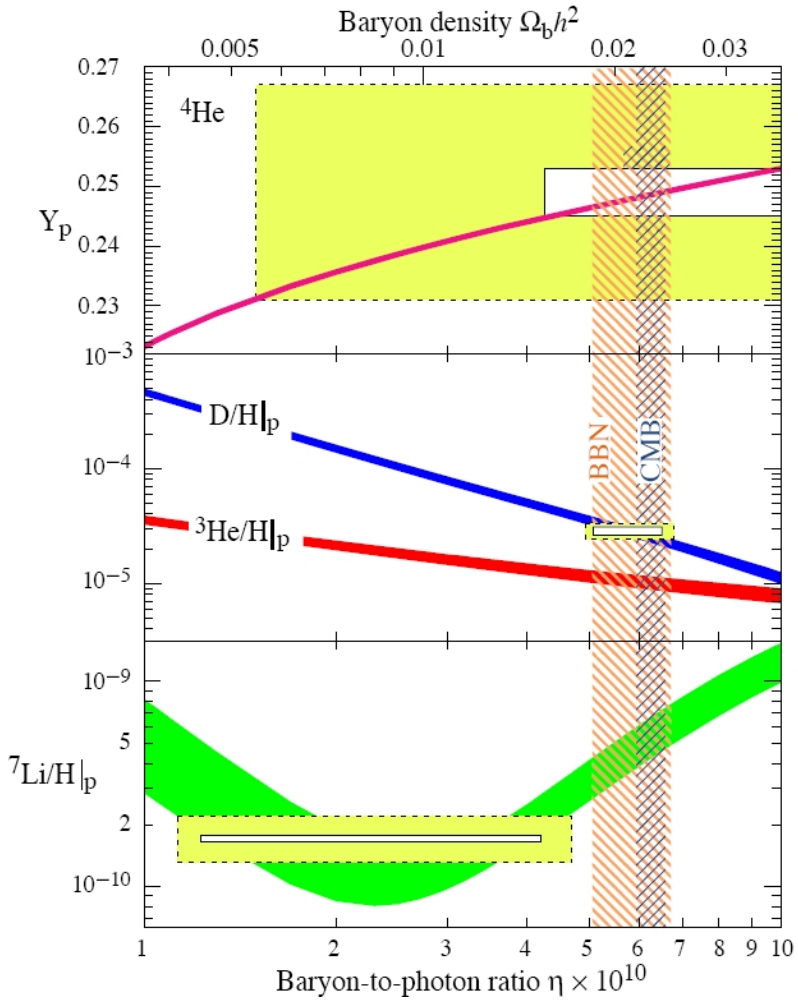

Figure 4.3: The abundance of light elements depending on the baryon density. The coloured lines show the standard BBN predicted abundances with $N_\nu^{\text{eff}} = 3$ The thickness indicates the 95% CL range. The boxes show the measured value, where the smaller, inside ones represent the $\pm 2\sigma$ statistical errors and the larger boxes the $\pm 2\sigma$ statistical and systematical error. The vertical bands show the 95% CL measured cosmic baryon density fom CMB and BBN data respectivly. The Helium-4 and Deuterium abundances overlap perfectly. For the Lithium we see a missmatch of the favoured regions, the so called *Litium problem*. Credits:[N$^+$10]

cosmic microwave background and large scale structure measurements are much looser, since they are more sensitive to the expansion. Since the best measured value for the baryon density comes from CMB, a combination of CMB and BBN (and LSS) is the choice for lepton asymmetries in the early universe at temperatures less than 1 MeV. The concluded values of (μ_{ν_f}/T) depends on the adopted measured relic abundances and N_ν^{eff}. In [SS08] the authors found for $N_\nu^{\text{eff}} = 3.3^{+0.7}_{0.6}$ where $\Delta N_\nu^{\text{eff}} \leq 0.01$ is fixed by the adopted $\text{Y}_\text{p} = 0.240 \pm 0.006$ an asymmetry in the electron Neutrinos of $(\mu_{\nu_e}/T) = 0.056 \pm 0.046$. For the case that[2] $(\mu_{\nu_e}/T) \ll (\mu_{\nu_\mu}/T) = (\mu_{\nu_\tau})/T$ and (μ_{ν_e}/T) is determined by the ^{4}He abundance, we can only make predictions for the cases $(\mu_{\nu_e}/T) \ll (\mu_{\nu_\mu}/T) = (\mu_{\nu_\tau}/T)$ and $(\mu_{\nu_e}/T) = (\mu_{\nu_\mu})/T \ll (\mu_{\nu_\tau}/T)$. One finds $|\xi_{\mu,\tau}| \leq 2.34$. If $(\mu_{\nu_e}/T) = (\mu_{\nu_\mu}/T) \ll (\mu_{\nu_\tau}/T)$ one finds $|\frac{\mu_\tau}{T}| \leq 4.12$ [SS08].
These boundaries would lead to $l_f = \mathcal{O}(1)$, orders of magnitude larger then the asymmetry in the baryon and still in perfect agreement with observational data.

N_ν^{eff}	(μ_{ν_e}/T)	(μ_{ν_μ}/T)	(μ_{ν_τ}/T)	References
≤ 7	$-0.01 \leq (\mu_{\nu_e}/T) \leq 0.22$	$\lvert\mu_{\nu_\mu}/T\rvert \leq 2.6$	$\lvert\mu_{\nu_\tau}/T\rvert \leq 2.6$	[HMM$^+$02]
$3.3^{+0.7}_{-0.6}$	0.023 ± 0.041	$\lvert\mu_{\nu_\mu}/T\rvert \leq 2.34$	$\lvert\mu_{\nu_\tau}/T\rvert \leq 2.34$	[SS08]
$3.3^{+0.7}_{-0.6}$	0.023 ± 0.041	$(\mu_{\nu_\mu}/T) = (\mu_{\nu_e}/T)$	$\lvert\mu_{\nu_\tau}/T\rvert \leq 4.12$	[SS08]
3.3		$(\mu_{\nu_f}/T) = 0.0245 \pm 0.0092$		[SR05]
3.0		$\lvert\mu_{\nu_f}/T\rvert \leq 0.09$		[SS08]
$3.3^{+0.7}_{-0.6}$		$\lvert\mu_{\nu_f}/T\rvert \leq 0.1$		[SS08]
$4.34^{+0.86}_{-0.88}$		$-0.14 \leq (\mu_{\nu_f}/T) \leq 0.12$		[KLS10]

Table 4.1: Observational bounds on Neutrino asymmetries for $T \simeq$few MeV.

[2]Since BBN/CMB can not distinguish between μ- and τ-Neutrinos.

Chapter 5

Lepton Asymmetries Before BBN

Neutrinos travel with almost speed of light through our universe. They were first created at the big bang and continued to be created in nuclear reactions and particle interactions through the evolution of the early universe.
Nowadays, in every cubic meter of space at every instant there should be about 330 millions neutrinos. On average there are roughly one billion times more neutrinos than protons in the universe. Most of the time, neutrinos pass through matter without any interactions since they are only affected by the weak force.

For the standard model of particle physics we know from the combined LEP results [N$^+$10] about the existence of three different neutrino species, shown in figure 5.1. The three fits to the data corresponds to models with different numbers of neutrino families. The width of the curve is determined by the life time t of the Z^0. The more neutrino families, the more decay possibilities and the shorter is t and hence the bigger the width of the decay peak. The best fit to the measurements of the Z^0 decay width gives $N_\nu = 2.993 \pm 0.011$ including all neutral fermions with normal weak couplings to the Z^0 and masses below $m_Z/2 \approx 45$ GeV [Cer06].

In the following chapter we will set the stage to trace neutrinos and their asymmetries in the early universe before the big bang nucleosynthesis. We will show, that Neutrino oscillations might have equilibrated initially different flavour asymmetries and mention some explored scenarios which can generate large lepton, or lepton-flavour asymmetries, but a small baryon asymmetry.

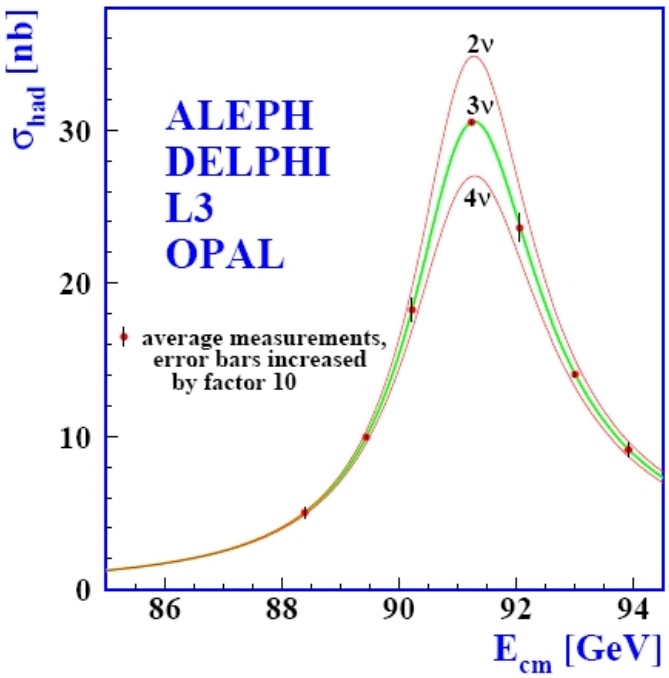

Figure 5.1: The Z^0 decay. Plotted is the center of mass energy versus the cross section σ of the reaction $e^+ + e^- \rightarrow Z^0 \rightarrow$hadrons. The dots show the combined data of the four CERN collaboration mentioned in the figure. The best fit is given by three neutrino families. Credits: [Cer06]

5.1 Neutrino oscillation

In the Standard Model the neutrinos are massless and interact only diagonal in flavour

$$\begin{aligned} \mathrm{W}^+ &\to f^+ + \nu_f, \\ \mathrm{W}^+ &\to f^- + \bar{\nu}_f, \\ \mathrm{Z}^0 &\to \nu_f + \bar{\nu}_f. \end{aligned} \tag{5.1}$$

Traveling at the speed of light, neutrinos can not change their character and remain uninteresting compared to quarks.
But the results of several experiments showed a behaviour of neutrinos, which could not be explained by massless neutrinos. The first hints of neutrino masses showed up more than 40 years ago, when Raymond Davis Jr. and his colleagues discovered a discrepancy between the predicted and measured neutrinos arriving from the sun [DHH68, DEC79]. Also at the detectors at proton decay experiments, measurments of the neutrino background showed a discrepancy between the predicted and observed muon neutrinos, an effect similar to the solar anomaly.
In 1998 the SuperKamiokande team published experimental data [F$^+$99] which led to the conclusion, that neutrinos can change their flavours.
The observation of these behaviours can be most easily explained by introducing neutrino flavour transitions. This would imply, that neutrinos have a mass and there must exist a mixing matrix like in the quark sector, relating the mass Eigenstates $\nu_j = (\nu_1, \nu_2, \nu_3, ...)$ with the flavour states $\nu_\alpha = (\nu_e, \nu_\mu, \nu_\tau, ...)$:

$$|\nu_\alpha\rangle = \mathrm{U}^*_{\alpha\mathrm{j}} \, |\nu_\mathrm{j}\rangle \, , \tag{5.2}$$

with the mixing matrix $\mathrm{U}_{\alpha\mathrm{j}}$.

To determine $\mathrm{U}_{\alpha\mathrm{j}}$ one measures the probability of a neutrino with flavour α converting after a certain distance to the flavour β. It the flavour did not change, the survival probability is given by

$$P(\nu_\alpha \to \nu_\alpha) = \left| \sum_j \mathrm{U}^*_{\alpha\mathrm{j}} \mathrm{exp} \left[-\mathrm{i} \mathrm{m}^2_\mathrm{j} \frac{\mathrm{L}}{2\mathrm{E}} \right] \mathrm{U}_{\alpha\mathrm{j}} \right|^2 \tag{5.3}$$

The factor L/E is the distance traveled divided by the neutrino energy and is characteristic for any given experiment. CPT invariance ensures $P(\nu_\alpha \to \nu_\alpha) = P(\bar{\nu}_\alpha \to \bar{\nu}_\alpha)$.

		L/E in [km MeV^{-1}]	Experiment
$P(\bar{\nu}_e \to \bar{\nu}_e)$	reactor	≈ 15	KamLAND
		≈ 0.5	CHOOZE, Daya Bay
	solar		(Super-)Kamiokande, SNO
$P(\nu_\mu \to \nu_\mu)$		≈ 500	MINOS,K2K,T2K
$P(\nu_\mu \to \nu_e)$		≈ 0.5	T2K
		≈ 0.4	NOνA
$P(\bar{\nu}_\mu \to \bar{\nu}_e)$		$\approx 10^{-5}$	LSND observed MiniBoone not observed

Table 5.1: Incomplete overview of some experimental evidence for neutrino oscillations.

If one assumes 3 light neutrinos with masses $m_i < 1$eV and only two independent $\Delta m^2_{ij} = \Delta m^2_i - m^2_j$ with three active flavours ν_e, ν_μ, ν_τ. The unitary mixing matrix has 3 angles θ_{12}, θ_{23}, θ_{13}, a Dirac phase δ and two Majorana phases (α, β). Except for the so called LSND anomaly, all experimental results can be explained with this parameters.
The mixing matrix becomes

$$\begin{aligned} U = & \begin{pmatrix} c_{13}c_{12} & c_{13}s_{12} & s_{13}e^{-i\delta} \\ -c_{23}s_{12} - s_{13}c_{12}s_{23}e^{i\delta} & c_{23}c_{12} - s_{13}s_{12}s_{23}e^{i\delta} & c_{13}s_{23} \\ s_{23}s_{12} - s_{13}c_{12}c_{23}e^{i\delta} & s_{23}c_{12} - s_{13}s_{12}c_{23}e^{i\delta} & c_{13}s_{23} \end{pmatrix} \times \mathrm{A}(\alpha,\beta) \\ = & \begin{pmatrix} 1 & & \\ & c_{23} & s_{23} \\ & -s_{23} & c_{23} \end{pmatrix} \begin{pmatrix} c_{13} & & s_{13}e^{-i\delta} \\ & 1 & \\ -s_{13}e^{i\delta} & & c_{13} \end{pmatrix} \begin{pmatrix} c_{12} & s_{12} & \\ -s12 & c_{12} & \\ & & 1 \end{pmatrix} \\ & \times \mathrm{A}(\alpha,\beta) \end{aligned} \tag{5.4}$$

where $s_{ij} = \sin\theta_{\mathrm{ij}}$ and $c_{ij} = \cos\theta_{\mathrm{ij}}$ and the matrix $A(\alpha,\beta) = \mathrm{diag}(1, \mathrm{e}^{\mathrm{i}\alpha}, \mathrm{e}^{\mathrm{i}\beta})$ with only non-vanishing entries on the diagonal.

In the decomposed form 5.4 each term can be associated wit different regimes of mixing explored by different classes of experiments. Experiments with atmospheric neutrinos explore the (23)- sector with Δm^2_{atm} while the (12)- sector is identified with the solar Δm^2_{sol}. The transitions (13) describe transitions from the electron flavour on the atmospheric scale which are so far unobserved. The Majorana phases α, β are observable via CP conserving effects in neutrinoless double beta decays. If Neutrinos are Dirac particles instead of Majorana, the neutrinoless double beta decay will not

be observed and the Majorana phases are zero. The Dirac phase δ allows for CP violations.

Currently the best fit values or limits are[Par08, N$^+$10]:

$$\begin{aligned} \sin^2 2\theta_{12} &= 0.87 \pm 0.03 \\ \sin^2 2\theta_{23} &> 0.92 \\ \sin^2 2\theta_{13} &< 0.15 \\ 0 \leq \quad \delta &\geq 2\pi. \end{aligned}$$

Neutrino oscillation experiments can not measure the different neutrino masses directly, but the mass differences:

$$\begin{aligned} |\Delta m^2_{32}| &= 2.43 \pm 0.13 \times 10^{-3} eV^2 \\ |\Delta m^2_{21}| &= 7.59 \pm 0.2 \times 10^{-5} eV^2. \end{aligned}$$

Since the masses of the neutrinos are yet unknown, there are two possible arrangements of this mass differences. The so called *normal* hierarchy, where the electron neutrino is the lightest and the *inverted* hierarchy, where it is the heaviest. Both scenarios are compatible with experimental data. It also remains an open question, if there is any CP violation and hence $\delta \neq 0$.
While these open issues can in principle be solved by oscillation experiments, the question of the mass of the neutrinos can not be answered. It is also impossible for these experiments to distinguish between Majorana and Dirac neutrinos.
But what these experiments can do, is give hints to the answers whether there are more then three neutrinos and if they interact via some exotic interactions. And indeed, the before mentioned LSND anomaly is pointing on these issues. Without going to too many details, the LSND experiment has observed evidence for $\bar{\nu}_\mu \rightarrow \bar{\nu}_e$ oscillations at an L/E which can not be explained within the above described three active neutrino oscillations. The results suggest the possibility of one or more additional neutrinos with a squared mass splitting of the active neutrinos of $\mathcal{O}(1)\mathrm{eV}^2$. These additional light neutrinos can not have SU(2)×U(1) quantum numbers, since they are for example not observable in the Z^0 decay. For that reason they are called *sterile* neutrinos. MiniBoone did not confirm the results but, again without going into details, the results are still compatible with a 3+2 neutrino oscillation (3 active and 2 sterile).

For the purpose of this work, the active neutrino oscillation in the early universe are of crucial interest since they might equilibrate different asymmetries in different flavour. Since we want to remain in the smallest possible

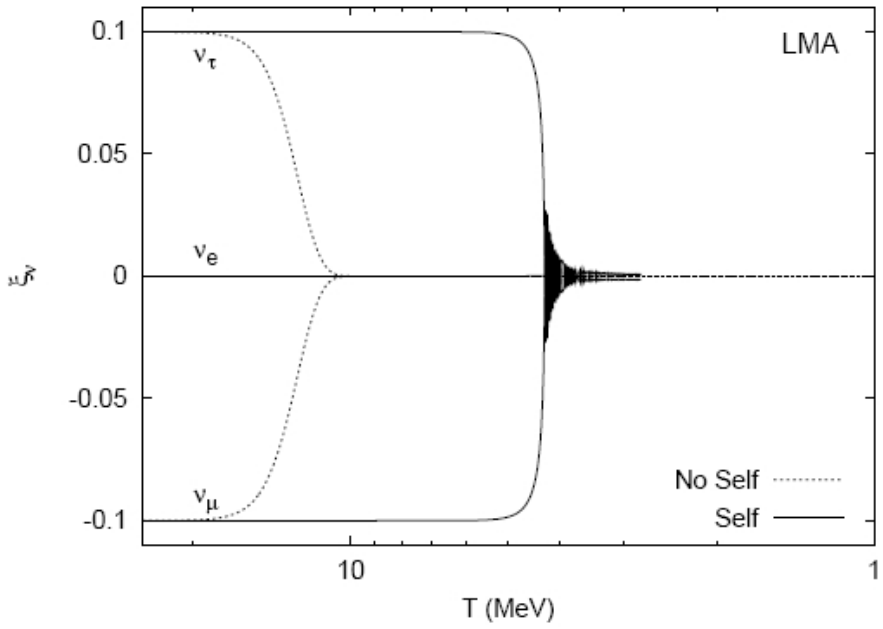

Figure 5.2: Shown here is the evolution $\xi_\nu = \mu_\nu/T$ for initial asymmetries $\mu_{\nu_e}/T = 0$, $\mu_{\nu_\mu} = -0.1$, and $\mu_{\nu_\tau} = 0.1$ for the large mixing angle solution of the neutrino oscillation, solved numerically by [DHP+02]. Also taken into account are the background media effects (e.g. collisonal damping, influence of charged leptons) and possible neutrino self interactions. Note that the total lepton asymmetry $l = \sum_f l_f$ is always zero. Before BBN starts at $T \simeq 1$ MeV, flavour oscillations lead to total equilibration of the asymmetries.

extension of the standard model of particle physics, we neglect in this work oscillations with possibly existing sterile neutrinos. For the interplay of active and sterile neutrinos and their asymmetries, see for example [CC06].

We have seen before, that there are several serious hints that neutrinos can change their flavour by oscillating. The widely believed, but yet unproven solution is the so called *large mixing angle* (LMA) solution [GGdHPGV00], where the first two mixing angles θ_{12} and θ_{23} are large. If this is the case, then different initial flavour asymmetries might have the tendency to equilibrate. For example an initial asymmetry $l_e < l_\mu < l_\tau$ would then be transfered to $l_e = l_\mu = l_\tau$. For three flavour mixing, the equilibration of different initial flavour asymmetries was shown in [DHP+02] and proven analytically in [Won02]. For most of the cases the authors showed a full equilibration, especially for the interesting case, where the sum of all flavour asymmetries is zero, but two flavour have a large but opposite asymmetry. In both works,

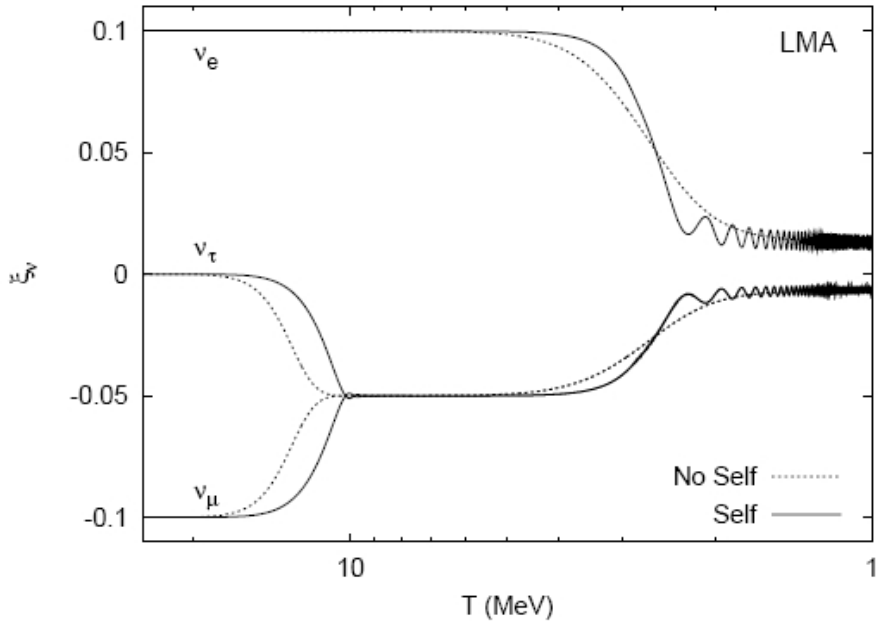

Figure 5.3: Shown here is the evolution $\xi_\nu = \mu_\nu/T$ for initial asymmetries $\mu_{\nu_e}/T = 0.1$, $\mu_{\nu_\mu} = -0.1$, and $\mu_{\nu_\tau} = 0$ for the large mixing angle solution of the neutrino oscillation, solved numerically by [DHP$^+$02]. Also taken into account are the background media effects (e.g. collisonal damping, influence of charged leptons) and possible neutrino self interactions. Again, the total lepton asymmetry is always zero. In this case flavour oscillations lead to almost equilibration of the asymmetries still before BBN.

the authors show, that the partial or complete equilibrium is achieved before big bang nucleosynthesis, if the oscillation parameters are the LMA solution and the third angle is sizeable. If this would be the case, the experimentally much better proven asymmetry between the electron and anti-electron neutrino would apply to all flavour $l_e = l_\mu = l_\tau$.

We have seen in this chapter, that neutrino flavour oscillation might lead to an equilibration of initially different flavour asymmetries. After the neutrino flavour starts to oscillate at $T_{\mathrm{osc}} \simeq$few MeV, only the total lepton number is further conserved. Going further back in time, we might only know the total lepton asymmetry, but not the distribution on the three flavour.

In the following we want to show, if and how a large total lepton asymmetry of large flavour asymmetries can be produced.

5.2 Generation of asymmetries

Why is there more matter than anti-matter? What mechanism generated it and at what time? A definite answer to these questions has not been given, yet. The only known fact is the asymmetry in baryons today, measured as $b \simeq \mathcal{O}(10^{-10})$. A possible asymmetry in leptons must be, due to charge conservation, hidden in the Neutrinos and so far we have no clue about the size nor the sign. But even if we would have experimental data for the l-asymmetry today, we can not be sure about the l_f-asymmetry in earlier times. Neutrino oscillations between active-active or (possibly existing) active-sterile Neutrinos at comparably low temperatures around T few 10 MeV might have changed the flavour asymmetries [CC06, ABFW05, DHP$^+$02, Won02]. To trace the lepton asymmetry one naturally would have to start at the beginning, the generation. Since we do not even know the energy scale of the possible mechanism generating any asymmetry, this is linked to the understanding of discrete symmetries in particle physics.
To get rid of this foggy cloud in the evolution of the early universe it seems to be common to assume the total lepton asymmetry to be of the same order as the baryon asymmetry, based on the assumption, that Sphalerons equilibrate any lepton and baryon asymmetry. Tiny lepton asymmetries means tiny and negligible fermionic chemical potentials and an easier thermodynamic description, as shown in the chapter before.

There are two things to be mentioned here. The first is, that even if the total lepton asymmetry is of the same order as the baryon asymmetry, the individual flavour asymmetries are still free to be orders of magnitudes larger. The second is, that we do not know, if Sphalerons exist, and if they ensured equilibration in the early universe.

In this chapter we will give a short review of some lepto- and baryogenesis scenarios at $T \geq \mathcal{O}(\text{GeV})$ focusing on models predicting large lepton asymmetries with a small baryon asymmetry.

5.2.1 Large lepton asymmetries

More than fifty years ago, Sakharov pointed out, that for a successful generation of a baryon asymmetry three conditions have to be fulfilled:

- The theory should have B-violating interactions.
- These interactions should violate both, C and CP symmetry.

- The process of net baryon number generation should occur in an out-of-equilibrium process.

These three pillars led to constructions of plenty of theories. Unfortunately also to an almost universal theoretical prejudice, that if lepton-chemical potentials exists, they have to be produced in similar non-trivial dynamics. If both asymmetries would be generated by processes matching the Sakharov conditions, it appears unnatural to generate a lepton asymmetry orders of magnitude larger than then the baryon asymmetry. In other words: Given the difficulties in generating the measured baryon asymmetry purely from the electroweak phase transition, a much larger lepton asymmetry is highly unlikely to be a consequence of physics around the electroweak scale.
However, above the electroweak scale, b and l are not conserved, only the term (b-l). This is because of the Sphalreon mediated transitions and the electroweak b and l anomalies. The induced chemical equilibrium by the Sphaleron transition would then enforce the baryon and lepton asymmetry to be of the same order.
To get a lepton asymmetry within the experimental bounds from BBN,CMB and LSS, three possibilities exists:

- The lepton asymmetry is generated below the electroweak scale. A possible candidate are oscillations between active and sterile Neutrinos. It was shown, that asymmetries can be transfered between the active and sterile Neutrino sector[CC06]. However, these oscillations occur at temperatures $\mathcal{O}(\infty\prime)$MeV and since we focus on the earlier universe, we only want to mention this possibility.

- The Sphaleron transition was never in equilibrium below the temperature at which the lepton asymmetry was generated. This was shown and proven by A.Linde [Lin76] and has some interesting consequences for the cosmological dynamics.

- The total asymmetry vanishes, while the individual asymmetries can be large.

In the following we want to give some more details for the last two possibilities.

A natural way of getting large particle asymmetries is included in Supersymmetric theories [McD00], having the intrigue feature of directions on the field space with virtually no potential, so called *flat directions*. Made of squarks or sleptons, these directions can carry baryon and/or lepton number. During Inflation these s-quark and s-leptons are free to fluctuate and form

scalar condensates. Due to their dynamical evolution after Inflation, the condensates can be charged up with a large baryon and/or lepton number. By decaying, these charges are released to the SM particles. This is called the Affleck-Dine mechanism [AD85, CD92].
In the early universe, large asymmetries have to be produced after an inflationary phase, for not getting washed out again.
Another possibility to dilute a large asymmetry is via Sphaleron transitions at high temperatures. But if the asymmetries are larger than a critical value l_c 10^{-2}, electroweak symmetry is never restored and Sphalerons are suppressed for all times [Lin76, McD99]. The large asymmetries would than have survived until today. The underlying reason is that a non-zero Neutrino asymmetry $n_0 = n_\nu - n_{\bar{\nu}}$ breaks explicitly Lorentz invariance and SU(2). This would allow the SU(2) gauge fields to acquire non vanishing vacuum expectation values. For more details see i.e.[LS94].

In [CCG99] the authors combine the Affleck-Dine mechanism with this idea. They consider a model with a sneutrino right condensate to generate large l-asymmetries, $0.2 > l > 1.4$, but no baryon asymmetry. In their specific model they take the MSSM with three right handed Neutrino singlet superfields. For a mass of the lightest Neutrino of $\mathcal{O}(10^{-4})$eV and a preferred mass of the lightest right handed Neutrino of $\mathcal{O}$(TeV) their model leads to asymmetries $l \simeq 10^{-2}$ to 1. This would prevent the electroweak symmetry to be restored and Sphaleron transitions are suppressed for all times.

The correct values of the resulting baryon and lepton asymmetries depends on the model parameter and is here not a subject of discussion. Since there are several models and ways described in the literature, how to get a large lepton asymmetries and the measured baryon asymmetry. We find this idea to be a good motivation to further investigate the cosmological consequences of such large $|l|/b \simeq \mathcal{O}(10^{10})$.

5.2.2 Large lepton flavour asymmetries

In this section we want to motivate another interesting scenario, where the total $l = b$, but the individual lepton flavour can have asymmetries $l_f \simeq \mathcal{O}(0.1)$. Experimental bounds on flavour asymmetries at $T \simeq$few MeV, so after Neutrino oscillation, and the possible equilibration of different flavour asymmetries due to oscillations, allow even flavour asymmetries $l_i \simeq -l_j = \mathcal{O}(1)$ and $l_k \ll l_{i,j}$ [SS08, Won02, HMM$^+$02].

Such a model with $l_i \simeq -l_j = \mathcal{O}(1)$ and $l_k \ll l_{i,j}$, a large asymmetry in the lepton flavour and the asymmetry in the baryons resulting in the physical range of $\mathcal{O}10^{-10}$ is for example discussed in [CGMO99]. It is shown in detail a model with $l_e = -l_\mu$ and $l_\tau = 0$

To have an impact on the thermodynamic variables of the early universe, we need $|l_{i,j}| = \mathcal{O}(1)$ with $l_i \simeq -l_j$ and $\sum_i \left(\frac{1}{3}B - l_i\right) = 0$ with $i, j = e,\, \mu,\, \tau$. In the Affleck-Dine mechanism it can be generated naturally. The flat direction in which such an asymmetry could live would be lifted by supersymmetry breaking effects by an operator of the form [CGMO99]

$$\int \mathrm{d}^4\theta \zeta^* \zeta \frac{\phi^*\phi^*\phi\phi}{\mathrm{M_X^2}} = \tilde{m}\frac{\phi^*\phi^*\phi\phi}{M_X^2} \tag{5.5}$$

where $\zeta = \tilde{m}\theta^2$ are the supersymmetry breaking spurions, ϕ are the matter fields and M_X is the scale of the operator. A $B - 3L_i$ asymmetry can then be generated by

$$\tilde{m}\frac{L_i^* L_j H_u^* H_u}{M_X^2} \tag{5.6}$$

violating the individual flavour asymmetries, but not the total (B-L). The asymmetry generated would correspond to

$$L_i = -L_j \simeq \frac{\phi_0^4 T_{RH}}{m_{3/2} M_X^2 M_*^2} \tag{5.7}$$

where $T_{RH} < 10^9$GeV is the reheating temperature, bounded by thermal gravitino overproduction [MRMR99]. $m_{3/2}$ is the gravitino mass of approximately 1 TeV and $M_* \simeq 10^{18}$GeV is the reduced Planck mass. ϕ_0 is the initial amplitude of s-lepton expectation value. To generate an asymmetry of $\mathcal{O}(1)$ we would need an initial amplitude of $\phi_0 \simeq 10^{18}$. The detailed mechanism for generating ϕ_0 is strongly model dependent. How to regulate the baryon asymmetry in Affleck-Dine mechanisms is discussed in [CGMO99].

Chapter 6

Leptons and Cosmic QCD Transition

Another unknown, although most dramatic event in the early universe is the quark-hadron transition at approximately 10μs after the big bang, where quarks and gluons condense to hadrons. The SM predicts a spontaneous breaking of the chiral symmetry of QCD and a confining of quarks into hadrons at a (pseudo-)critical Temperature T_c. This epoch is one of the most interesting in the early universe, but experimentally only little is known about this QCD transition at $T_c \approx 170$ MeV [Kar09, Kar07]. It is well established in lattice theory, hat the order of the transition depends on the baryon density, or equivalently the baryochemical potential μ_B. It is common to draw a QCD phase diagram in the $\mu_B - T$ plane, in which the cosmic QCD transition is commonly assumed to take place at $T = T_c$ and $\mu_B \approx 0$. In the following we show that this assumption holds only if $|l| = \mathcal{O}(b)$.

The QCD transition is in the focus of the relativistic heavy-ion research programs at RHIC and LHC. These experiments are taking place at very small baryochemical potential and high temperatures, presumably far away from a critical point. More information about a possible first-order transition at large values of μ_B are expected from the future FAIR program. Todays ordinary matter is located at $T \approx 0$ and μ_B equal to the nucleon mass. Extremely dense matter, like the interior of compact stars with $T \leq 10$ MeV, are expected to reach some colour superconducting phase [ASRS08].

For T and μ_B being of the order of the QCD confining scale Λ_{QCD}, the most reliable tool is lattice simulations with quarks. But as a tribute to different possible solutions to the so called 'sign problem' [Ste06, Sch06], different phase diagrams with different T_c and different critical lines have been proposed [Phi07, Ste06, dFP07]. The widely expected shape of the QCD phase diagram in a $\mu_B - T$ plane as a combination of results from

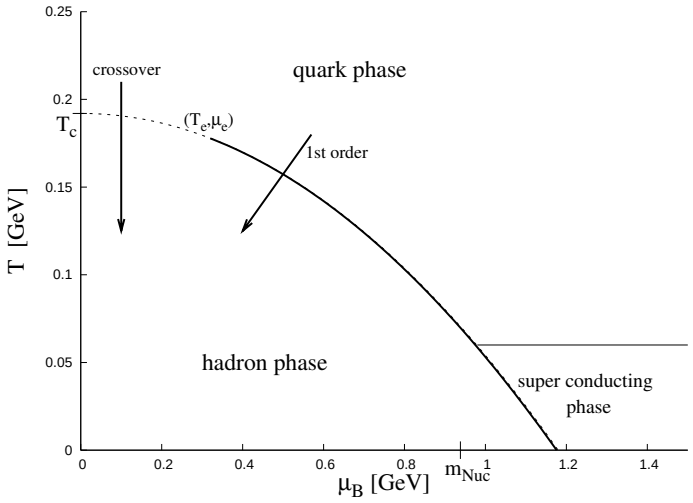

Figure 6.1: Sketch of the phase diagram for physical QCD, based on findings from nuclear physics, lattice QCD and perturbative calculations. Solid lines indicate a first-order phase transition, while the dashed line indicates a crossover. The exact phase diagram with or without a critical end point $(T_\mathrm{e}, \mu_\mathrm{e})$ is still under debate. So is also the (pseudo-)critical temperature $T_\mathrm{c} = 192(7)(4)$ MeV [Kar09, Kar07], which differs from $T_\mathrm{c} = 164 \pm 2$ MeV, the value found in [AFKS06]. While [dFP07] argue that it is still an open question if a critical end point exists at all, [FK04] find $\mu_\mathrm{e} = 360 \pm 40$ MeV and $T_\mathrm{e} = 162 \pm 2$ MeV. The calculations and methods leading to these different results are discussed and compared in [Kar07, AFKS06, dFP07, Ste06].

nuclear physics, perturbative calculations and lattice simulations is shown in figure 6.1.

For cosmology, gaining better knowledge of the QCD transition would be great. The transition sets the initial condition for big bang nucleosynthesis. Standard BBN relies on the assumption that the Universe can be treated as a homogeneous and isentropic radiation fluid at the moment of BBN. Therefore it is of great interest to know exactly what happens at the QCD transition [AH85]. The cosmic QCD transition might also create some relics observable today. Most of them can only be generated during a first-order transition, like quark nuggets or magnetic fields [Wit84, Sch03], while QCD balls could be generated independently of the order of the transition [Zhi03]. The transition might also lead to the formation of cold dark matter (CDM) clumps [SSW97] and definitely leads to a modification of the primordial background

of gravitational waves [Sch98, WK06].

In the following, we trace the baryo-, lepto- and charge chemical potentials in the early Universe as functions of temperature around the QCD phase transition. We assume that the Universe is neutral and that electric charge, baryon and lepton (flavor) numbers are conserved. For vanishing lepton asymmetry this situation has also been studied in [FR02] and in [Zar00].

We introduce the chemical potentials related to the conserved quantum numbers and study the trajectories of the Universe in the corresponding $\mu - T$ planes, depending on the assumed lepton asymmetry.

6.1 Quark phase

In the following we describe the evolution of the net particle densities of all SM particles in the quark phase ($T > T_{QCD}$).

In the early Universe the Hubble expansion rate H is always bigger than the particle interaction rate Γ and the particle densities are usually not high enough for many body reactions. The main processes that keep all particles in thermal and chemical equilibrium are $2 \leftrightarrow 2$-processes. So, all particles in the quark phase and in the hadron phase are in local thermal (LTE) and local chemical equilibrium (LCE). The chemical potentials of photons and gluons are zero $\mu_\gamma = \mu_g = 0$, as they can be produced and annihilated in any number. As a consequence of that, the chemical potentials of a particle i and its anti-particle $\bar{i}$ are equal, but of opposite sign: $\mu_i = -\mu_{\bar{i}}$.

The leptons are then linked via reactions like $f_i + \bar{f}_j \rightleftharpoons \nu_{f_i} + \bar{\nu}_{f_j}$ for all combinations of flavours, leading to relations like

$$\mu_e - \mu_{\nu_e} = \mu_\mu - \mu_{\nu_\mu}. \tag{6.1}$$

Due to flavour mixing in the quark sector, we only need to distinguish between up and down type quarks with chemical potentials $\mu_u = \mu_c = \mu_t$ for the up, charm and top quarks and $\mu_d = \mu_s = \mu_b$ for the down, strange and bottom quarks. These quark chemical potentials are further linked via weak reactions like $u + e^- \rightleftharpoons d + \nu_e$, which leads to $\mu_d = \mu_u + \mu_e - \mu_{\nu_e}$.

The number of independent chemical potentials in the quark phase is thus reduced to four leptonic potentials (μ_e, μ_{ν_e}, μ_{ν_μ}, μ_{ν_τ}) and just one for the quarks (μ_u). For temperatures well below m_W and in chemical and thermal equilibrium, the evolution of the net particle densities as a function

of temperature is described by five conservation equations

$$
\begin{aligned}
0 = \quad & n_e(T,\mu_e) + n_{\nu_e}(T,\mu_{\nu_e}) - l_e s(T), && (6.2)\\
0 = \quad & n_\mu(T,\mu_{\nu_\mu},\mu_e,\mu_{\nu_e}) + n_{\nu_\mu}(T,\mu_{\nu\mu}) - l_\mu s(T), && (6.3)\\
0 = \quad & n_\tau(T,\mu_e,\mu_{\nu_e},\mu_{\nu_\tau}) + n_{\nu_\tau}(T,\mu_{\nu_\tau}) - l_\tau s(T), && (6.4)\\
0 = \quad & n_u(T,\mu_u) + n_d(T,\mu_u,\mu_e,\mu_{\nu_e}) + n_c(T,\mu_u) + n_s(T,\mu_u,\mu_e,\mu_{\nu_e}) && (6.5)\\
& \qquad + n_b(T,\mu_u,\mu_e,\mu_{\nu_e}) - 3bs(T),\\
0 = \quad & n_u(T,\mu_u) + n_c(T,\mu_u) - n_e(T,\mu_e) - n_\mu(T,\mu_{\nu_\mu},\mu_e,\mu_{\nu_e}) && (6.6)\\
& \qquad - n_\tau(T,\mu_e,\mu_{\nu_e},\mu_{\nu_\tau}) - bs(T).
\end{aligned}
$$

The last equation combines the conservation of electric charge and baryon number in a convenient manner. Exact solutions to this system of coupled integral equations must be obtained numerically. However, before doing so, we estimate the evolution of the chemical potentials at high temperatures via an analytic approach.

At $T > T_c$, but close to the QCD transition, we consider the three light quarks u, d and s, as well as electrons and myons with their corresponding neutrinos (the masses of these particles are neglected). Tau leptons annihilate well before the QCD transition (at $T_\tau \sim 600$ MeV), hence tau neutrinos are decoupled at the temperatures of interest. For relativistic particles ($T \gg m_i, \mu_i$) the net number densities become

$$
\begin{aligned}
n_i \quad &= \tfrac{1}{3} g_i T^2 \mu_i + O(\mu_i^3) \quad \text{for bosons,} && (6.7)\\
&= \tfrac{1}{6} g_i T^2 \mu_i + O(\mu_i^3) \quad \text{for fermions,} && (6.8)
\end{aligned}
$$

while we neglect the nonrelativistic particles. With these approximations equations (6.2) to (6.4) become:

$$
\begin{aligned}
l_e s(T) \quad &= \tfrac{1}{3}\left(2\mu_e + \mu_{\nu_e}\right) T^2, && (6.9)\\
l_\mu s(T) \quad &= \tfrac{1}{3}\left(2\mu_\mu + \mu_{\nu_\mu}\right) T^2, && (6.10)\\
l_\tau s(T) \quad &= \tfrac{1}{3}\mu_{\nu_\tau} T^2. && (6.11)
\end{aligned}
$$

Let us further assume (for simplicity) that $l_e = l_\mu = l_\tau = l/3$, which implies, together with (6.1), that electrons and muons, as well as electron and muon neutrinos have equal chemical potentials, while (6.11) fixes $\mu_{\nu_\tau} = ls(T)/T^2$. Consequently, from the complete set of conservation equations, the chemical potentials for all particles can be expressed in terms of the lepton and baryon

asymmetries, l and b (for three quark and two lepton flavours):

$$\frac{\mu_u}{T} = \frac{1}{2}\frac{bs(T)}{T^3} + \frac{1}{6}\frac{ls(T)}{T^3}, \tag{6.12}$$

$$\frac{\mu_d}{T} = \frac{1}{2}\frac{bs(T)}{T^3} - \frac{1}{12}\frac{ls(T)}{T^3}, \tag{6.13}$$

$$\frac{\mu_e}{T} = \frac{1}{2}\frac{\mu_{\nu_e}}{T} = \frac{1}{4}\frac{ls(T)}{T^3}. \tag{6.14}$$

While the chemical potentials for the leptons (6.14) depend on the lepton asymmetry only, the quark chemical potentials given by (6.12) and (6.13) depend on baryon and lepton asymmetry.

We would like to stress that the result (6.12) to (6.14) strongly depends on the number of relativistic quark and lepton flavour. Increasing the temperature to $T \sim 1$ GeV, the inclusion of tau leptons and charm quarks modifies the coefficients in the above result, i.e.

$$\frac{\mu_u}{T} = \frac{9}{32}\frac{bs(T)}{T^3} + \frac{1}{8}\frac{ls(T)}{T^3}, \tag{6.15}$$

$$\frac{\mu_d}{T} = \frac{15}{32}\frac{bs(T)}{T^3} - \frac{1}{8}\frac{ls(T)}{T^3}, \tag{6.16}$$

$$\frac{\mu_e}{T} = \frac{1}{4}\frac{ls(T)}{T^3} + \frac{1}{16}\frac{bs(T)}{T^3}, \tag{6.17}$$

$$\frac{\mu_{\nu_e}}{T} = \frac{1}{2}\frac{ls(T)}{T^3} - \frac{1}{8}\frac{bs(T)}{T^3}. \tag{6.18}$$

It actually turns out that the previously found independence of the chemical potentials of the leptons from the baryon asymmetry is a coincidence of the three quark flavour case. The deeper reason is that the charges of one down and one strange quark just compensate the charge of one up quark. In general, all particle chemical potentials depend on b and l. For three quark flavour this is also the case when the strange quark mass is taken into account.

For physical particle masses (e.g. the strange quark mass and the mass of the muon cannot be neglected during the QCD transition) an analytic solution is not possible. The full numerical solution is presented below.

6.2 Hadron phase

The hadron phase (for $T < T_c$) contains besides hadrons, electrons and muons as well as all three types of neutrinos. At low temperatures all quarks are bound in neutrons and protons, but close to the QCD transition also mesons,

mainly pions, are produced in significant numbers. The conservation of quantum numbers, expressed in terms of the net particle densities depending on four independent chemical potentials, gives rise to the relations:

$$0 = n_e(T,\mu_e) - n_{\nu_e}(T,\mu_{\nu_e}) - l_e s(T), \tag{6.19}$$
$$0 = n_\mu(T,\mu_p,\mu_n,\mu_{\nu_\mu}) - n_{\nu_\mu}(T,\mu_{\nu_\mu}) - l_\mu s(T), \tag{6.20}$$
$$0 = n_p(T,\mu_p) + n_n(T,\mu_n) - bs(T), \tag{6.21}$$
$$0 = n_p(T,\mu_p) - n_e(T,\mu_e) - n_\mu(T,\mu_p,\mu_n,\mu_{\nu_\mu}) - n_\pi(T,\mu_p,\mu_n). \tag{6.22}$$

For a simplified analytic treatment, we neglect all mesons and muons. Only protons, neutrons, electrons and electron neutrinos are taken into account. The leptons are still relativistic (as long as $T > m_e/3$), while protons and neutrons are non-relativistic. Their net particle density is approximated as

$$n_i \simeq 2g_i \left(\frac{m_i T}{2\pi}\right)^{3/2} \sinh\left(\frac{\mu_i}{T}\right) \exp\left(\frac{-m_i}{T}\right). \tag{6.23}$$

The system of equations (6.19), (6.21), and (6.22) then becomes (as above, we assume $l_e = l/3$)

$$ls(T) = 2T^2(2\mu_e + \mu_{\nu_e}), \tag{6.24}$$
$$bs(T) = 4\left(\tfrac{Tm}{2\pi}\right)^{3/2} \exp\left(\tfrac{-m}{T}\right)\left(\sinh\tfrac{\mu_p}{T} + \sinh\tfrac{\mu_n}{T}\right), \tag{6.25}$$
$$0 = 4\left(\tfrac{Tm}{2\pi}\right)^{3/2} \exp\left(\tfrac{-m}{T}\right)\sinh\tfrac{\mu_p}{T} - \tfrac{2}{3}T^2\mu_e, \tag{6.26}$$

where we assumed $m_n \approx m_p \equiv m$. The weak reactions $e + p \rightleftharpoons n + \nu_e$, which are in equilibrium at energies above ~ 1 MeV, (6.24) implies

$$\frac{\mu_e}{T} = \frac{ls(T)}{6T^3} + \frac{\mu_n - \mu_p}{3T}. \tag{6.27}$$

For $\mu_p/T \ll 1$ and $\mu_n/T \ll 1$, we may simplify (6.25) to obtain

$$\frac{\mu_p}{T} + \frac{\mu_n}{T} = \frac{bs(T)}{c(T)} \exp[m/T], \tag{6.28}$$

with $c(T) = 4(\frac{Tm}{2\pi})^{3/2}$. Together with (6.27) and (6.26) the proton chemical potential reads

$$\frac{\mu_p}{T} = \frac{\frac{ls(T)}{4T^3} + \frac{bs(T)}{2c(T)} \exp[m/T]}{1 + \frac{9c(T)}{4T^3} \exp[-m/T]}. \tag{6.29}$$

Note that this expression holds as long as $\mu_p/T \ll 1$. Nevertheless, the expression allows us to understand why the lepton asymmetry does not couple

to the proton and neutron chemical potentials. As T decreases, the influence of the baryon asymmetry eventually overcomes any lepton asymmetry, as the term $\propto b\exp[m/T]$ grows exponentially. Thus, in the low temperature regime, large lepton asymmetries play no role for the proton chemical potential. In the same limit, $\mu_p \approx \mu_n$. From equation (6.27) we find that a large lepton asymmetry results in a large neutrino and electron asymmetries, as $\mu_{\nu_e} \approx \mu_e$.

As the temperature drops further, μ_p/T becomes large and the above approximation breaks down. In that case we can approximate $\sinh(\mu/T)$ in (6.25) by $\exp(\mu/T)/2$ and we finally find that

$$\mu_p \approx m - T\ln[c(T)/2bs(T)]. \tag{6.30}$$

In the low temperature regime μ_p is linear in T and for small T it runs against the mass m. The electron asymmetry finally is just the same as the proton asymmetry and a possible large lepton asymmetry is turning into a large neutrino asymmetry in the late Universe.

Thus, large lepton asymmetries in the low temperature regime of the hadron gas affect only the chemical potentials of leptons and play no role for μ_p and μ_n. The full calculation for all particles of the standard model with physical masses can again only be done numerical. For details of the numerics see the appendix. In the following section we take a closer look at the chemical potentials around the QCD transition.

6.3 Chemical potentials

Each conserved quantum number can be associated with a chemical potential. The particles contribution to the free energy can then be described as

$$\mu_Q n_Q + \mu_B n_B + \sum_f \mu_{L_f} n_{L_f} \overset{T>T_{\mathrm{QCD}}}{=} \sum_q \mu_q n_q + \sum_l \mu_l n_l + \sum_g \mu_g n_g$$
$$\overset{T<T_{\mathrm{QCD}}}{=} \sum_b \mu_b n_b + \sum_m \mu_m n_m + \sum_l \mu_l n_l,$$

with Q denoting charge, B baryon number, and L_f lepton flavour number on the l.h.s. and q quarks, l leptons, g massive gauge bosons (the gluon and photon chemical potentials vanish), b baryons and m mesons.

The particle fluid in the quark phase contains all types of quarks and leptons. The massive gauge bosons are way too heavy to play a crucial rôle at the QCD epoch, nevertheless we keep them in our model. So we get:

$$\begin{aligned} &\mu_Q(\tfrac{2}{3}n_u - \tfrac{1}{3}n_d + \tfrac{2}{3}n_c - \tfrac{1}{3}n_s + \tfrac{2}{3}n_t - \tfrac{1}{3}n_b - n_e - n_\mu - n_\tau + n_W) \\ &\quad +\mu_B\left(\textstyle\sum_q \frac{1}{3}n_q\right) + \textstyle\sum_f \mu_{L_f}(n_f + n_{\nu_f}) \\ = &\quad \textstyle\sum_q \mu_q n_q + \sum_l \mu_l n_l + \mu_W n_W. \end{aligned}$$

The Z-boson does not show up, as at high energies its chemical potential vanishes (like the one of photons and gluons) and there are no Z-bosons at low temperatures. For the W we pick the convention that n_W counts W^+ with a plus sign. A comparison of the coefficients in front of the net particle densities gives:

$$\mu_u = \mu_c = \mu_t = \frac{2}{3}\mu_Q + \frac{1}{3}\mu_B, \tag{6.31}$$

$$\mu_d = \mu_s = \mu_b = -\frac{1}{3}\mu_Q + \frac{1}{3}\mu_B, \tag{6.32}$$

$$\mu_f = -\mu_Q + \mu_{L_f}, \tag{6.33}$$

$$\mu_{\nu_f} = \mu_{L_f}, \tag{6.34}$$

$$\mu_W = \mu_Q. \tag{6.35}$$

Consequently, the chemical potentials of the globally conserved quantities in the quark phase are

$$\mu_B(T > T_{\mathrm{QCD}}) = \mu_u + 2\mu_d, \tag{6.36}$$

$$\mu_Q(T > T_{\mathrm{QCD}}) = \mu_u - \mu_d, \tag{6.37}$$

$$\mu_{L_f}(T > T_{\mathrm{QCD}}) = \mu_{\nu_f}. \tag{6.38}$$

The conserved quantum numbers in the hadron phase are described by

$$\mu_Q(n_p + n_\pi + n_K + \cdots - n_e - n_\mu) + \mu_B(n_p + n_n) + \sum_f \mu_{L_f}(n_f + n_{\nu_f}) = \sum_b \mu_b n_b + \sum_m \mu_m n_m + \sum_l \mu_l n_l.$$

As above, a comparison of the coefficients leads to

$$\mu_B(T < T_{QCD}) = \mu_n, \tag{6.39}$$

$$\mu_Q(T < T_{QCD}) = \mu_p - \mu_n = \mu_\pi, \tag{6.40}$$

$$\mu_{L_f}(T < T_{QCD}) = \mu_{\nu_f}. \tag{6.41}$$

In the following we take a closer look on the chemical potentials of the conserved charges and on the effect of a large lepton asymmetry on them at temperatures close to the QCD transition.

6.3.1 Baryochemical potential

The baryochemical potential μ_B depends in general linearly on b and l.

In the quark phase, taking only three quarks (u,d,s), electrons and muons into account (and neglecting their masses), we insert (6.12) and (6.13) into (6.36) to find $\mu_B(T > T_{\rm QCD}) = 3bs(T)/2T^2$. Thus, it seems that the baryochemical potential would just depend on the baryon asymmetry, as one could naively expect. However, if we go to a slightly higher temperature, such that we have to include charm and tau, we find from (6.15) and (6.16) that

$$\mu_B(T \gg T_{\rm QCD}) = \left(\frac{39}{4}b - l\right)\frac{s(T)}{8T^2}. \tag{6.42}$$

In general, $\mu_B = \mu_B(b, l)$. Thus, for $|l| \gg b$, the order of magnitude of the baryochemical potential is set by the lepton asymmetry, and not as naively expected by the baryon asymmetry.

This can be understood by the following consideration: increasing the lepton flavour asymmetries, the corresponding chemical potentials are forced to react, see (6.9) to (6.11). On the other hand, electric charge and baryon number must not be changed. A large net charge in the leptons must be compensated by a large and opposite net charge carried by quarks, in a way that the baryon asymmetry remains tiny. That makes it very difficult to add a baryon without disturbing that fine balance, and that is why the baryochemical potential (6.36) grows as large as the lepton asymmetry.

Neglecting the physical masses of the particles would have a strong effect on μ_B, as shown in figure 6.2. While the simple analytic approach with $m = 0$ gives $\mu_B \propto T$ (see (6.42)), the numerical results with physical quark masses shows in the low temperature regime of the quark phase a different behaviour. The non-relativistic particles give rise to an increase of μ_B below $T \sim 3$ GeV, i.e. charm, bottom quarks and τs play an important role. However neglecting the heavy quarks, but taking the physical masses of the strange quark and the muon into account gives a reasonable approximation at the QCD scale (see figure 6.2).

In the hadron phase at low temperatures, but above temperatures of a few MeV, the difference in the masses and chemical potentials of the proton and neutron is negligible and one can assume $m = m_p \approx m_n$ and $\mu_B = \mu_n \approx \mu_p$, as given by (6.30) after pions and muons disappeared from the thermal bath. Thus, the baryochemical potential becomes

$$\mu_B(T < m_\pi/3) \approx m - T \ln\left[\frac{c(T)}{2bs(T)}\right]. \tag{6.43}$$

In the low temperature regime, μ_B is linear in T and approaches the nucleon mass m.

Let us now turn to a more detailed numerical study. We evaluate $\mu_B(T)$

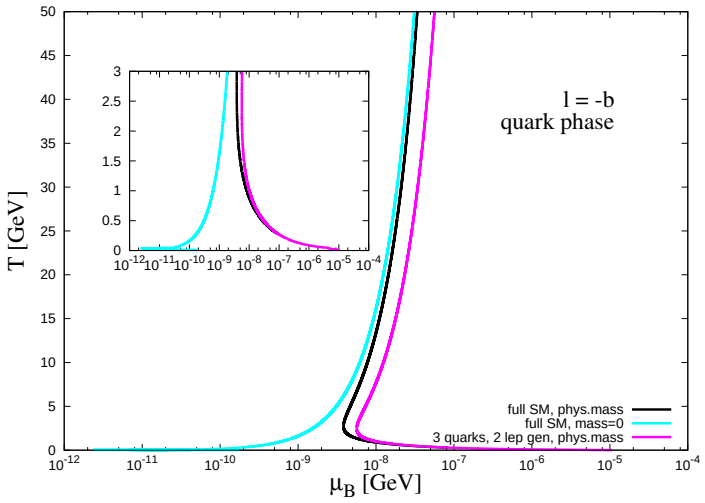

Figure 6.2: Trajectory of the quark phase in the $\mu_B - T$ plane for the $l = -b$ scenario. We compare several approximations to the exact result (black line). At high temperatures all particles can be assumed to be massless (blue line), while below $\sim$ 5 GeV mass thresholds are important. Below 1 GeV the universe is well described by three quark (up, down, strange) and two lepton (electron, muon) flavours only (magenta line).

numerically in the quark and hadron phases, i.e. expressions (6.36) and (6.39) respectively, for various values of l.

If there is no baryo- or leptogenesis after sphaleron processes cease, the pure standard model predicts a negative value for l. The influence of the sign of l on the baryochemical potential is displayed in figure 6.3. In order to illustrate the effect of the sign, we choose a rather "large" value for the lepton asymmetrie $l = \pm 3 \times 10^{-2}$. For negative l, μ_B is positive for all temperatures. In contrast, for positive values of l, μ_B can take negative values. For the high temperature regime, this is easily seen from (6.42). In the hadron phase, μ_B approaches the nucleon mass at low temperatures, independently of the value of l. While a positive l always allows for a point of coexistence of the quark and hadron phase at a temperature of $\sim$ 200 MeV, the trajectories of the $l < 0$ case would meet at a much lower temperature.

Figure 6.4 shows the case of negative lepton asymmetry for different values of l. The influence of the lepton flavour asymmetry on the baryochemical potential is evident. The point of coexistence moves to larger baryochemical potentials and lower temperatures as $|l|$ increases (not all crossings are

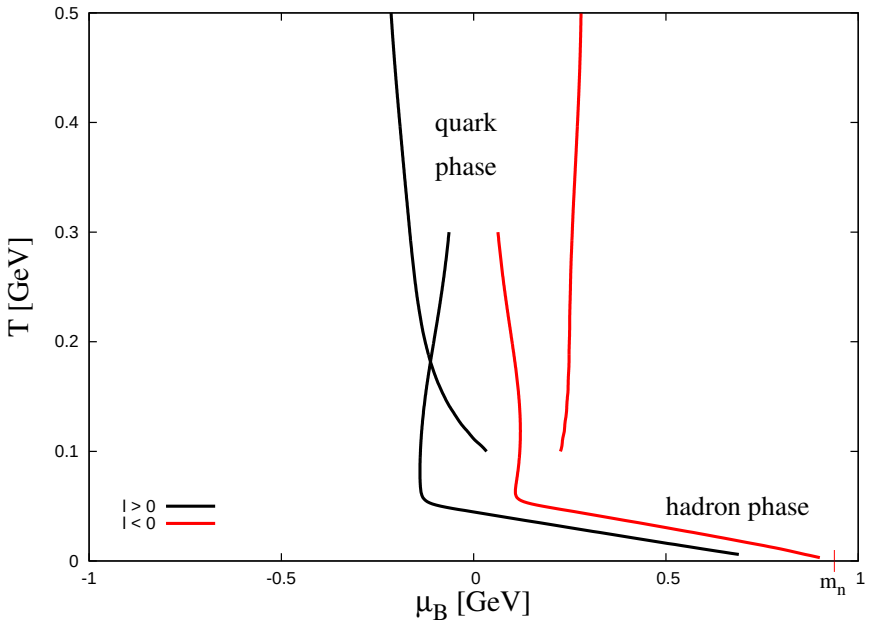

Figure 6.3: Evolution of the baryochemical potential in the quark and hadron phase for large lepton asymmetry $l = \pm 3 \times 10^{-2}$. Lepton asymmetries of different signs lead to qualitatively different trajectories. While the trajectories of the quark and hadron phase cross for positive l, they miss each other for negative l in the expected temperature region at ~ 200 MeV.

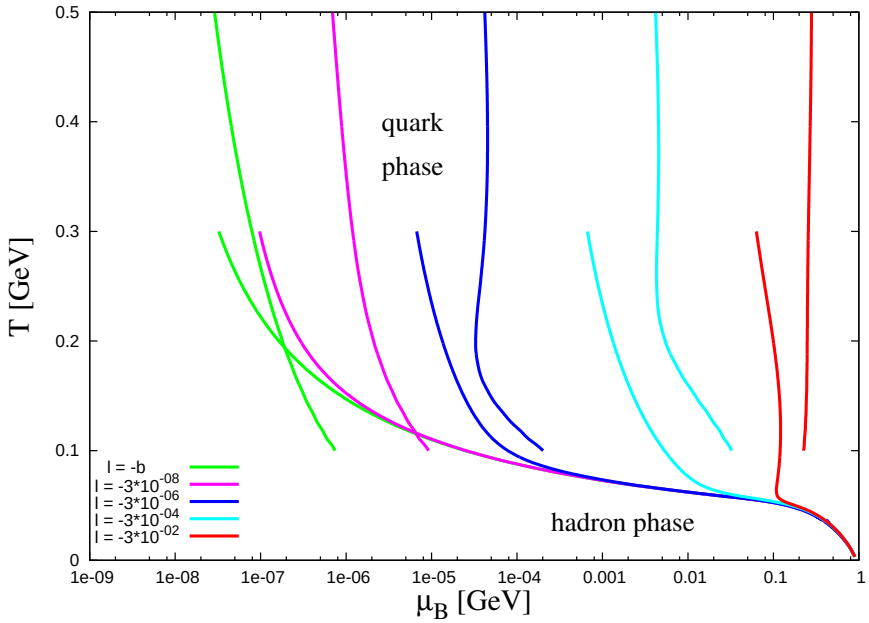

Figure 6.4: Evolution of the baryochemical potential for negative lepton asymmetries. Above the pion threshold, the trajectories of both phases depend strongly on the lepton asymmetry. For lower temperatures the lepton asymmetry is negligible.

shown in the figure). Shortly after the transition to the hadron phase, the trajectories are still heavily affected by the lepton asymmetry, as pions and other mesons can carry a net charge density. For temperatures below the pion threshold, $T < m_\pi/3 \approx 50\text{MeV}$, the hadron phase follows a unique trajectory, as predicted by (6.43).

6.3.2 Charge chemical potential

We associate with the globally conserved and vanishing charge of the Universe the charge chemical potential μ_Q, which is the energy needed to add a charge unit to a thermalised state at fixed volume and entropy.

For $T > T_{QCD}$ it depends, like the baryochemical potential, on μ_u and μ_d. But the effect of a large lepton asymmetry on the evolution is bigger because of the missing factor of two for μ_d. From the approximations (6.12) and (6.13), it follows for the case of three quark and two lepton flavour, $\mu_Q = ls(T)/4T^2$. Taking, as above, the charm and tau into account and using (6.15) and (6.16) we find:

$$\mu_Q(T \ll T_{\text{QCD}}) = \left(-\frac{3}{4}b + l\right)\frac{s(T)}{4T^2}. \tag{6.44}$$

The charge chemical potential is now depending on b too, and does not even vanish in the case $b = l$, as one could naively expect. Taking the particle masses into account has the same effect, namely $\mu_Q = \mu_Q(b, l)$ in general.

Actually, the lattice simulations that have been used to conclude that the cosmic QCD transition would be a crossover have been done with three dynamical quarks. They implicitly assume $l = 0$ and are typically performed at $\mu_Q = 0$. However, as we have seen above, including the mass of the strange quark already spoils that argument. We thus have to revisit the question of the order of the cosmic QCD transition.

After the QCD transition, a charge unit can be added to the Universe in the form of either a charged pion, muon or electron. While adding an electron or muon also affects the lepton asymmetry, the pions do not care about baryon and lepton number. At $T \approx m_\pi/3 \approx 50$ MeV the pions are annihilated and the charge neutrality has to be ensured by protons and electrons. Using (6.28), (6.29) and (6.40) one gets

$$\mu_Q(T < T_{\text{QCD}}) = (-9b + 2l)\,\frac{s(T)}{4T^2 + \frac{9c(T)}{T}\exp[-\text{m/T}]}. \tag{6.45}$$

The dependence on the sign of l is shown in figure 6.5. In the quark phase it behaves like $\mu_Q \propto l/T^2$, so that the sign of l fixes the sign of μ_Q. Figure 6.6 shows the dependence of μ_Q for negative l. A negative value of l implies a

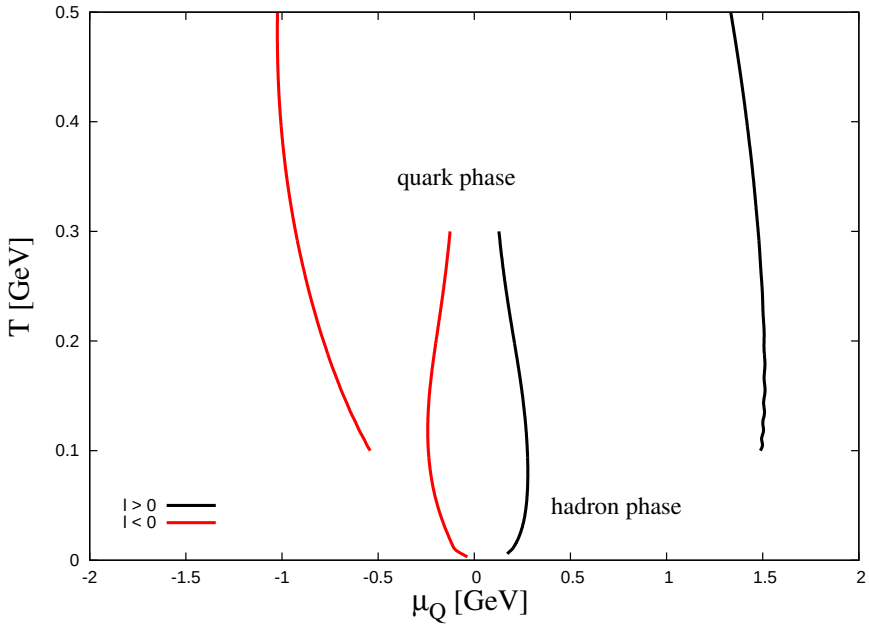

Figure 6.5: Evolution of the charge chemical potential for $l = \pm 3 \times 10^{-2}$. The trajectories of the quark and hadron phase miss each other for both signs of l.

negative charge chemical potential. It is interesting that there does not exist any point of coexistence for all the studied cases.

6.3.3 Leptochemical potentials

With each lepton flavour a chemical potential is associated. It is the energy needed to add a lepton of a certain flavour to a thermalised state at fixed volume and entropy. The cheapest way to add a lepton of some flavour is to add a corresponding neutrino, see (6.38) and (6.41). While for the case of three light quarks and two charged leptons at temperatures just above the QCD transition, $\mu_{L_e} = \mu_{L_\mu} = \mu_{L_\tau}/2 = ls(T)/2T^2$ from (6.14) and (6.11), including the charm and tau at higher temperatures leads to (6.18)

$$\mu_{L_f}(T \ll T_{\mathrm{QCD}}) = \left(l - \frac{1}{4}b\right) \frac{s(T)}{2T^2} \tag{6.46}$$

for all three lepton flavours. Again, taking the finite masses of quarks and charged lepton into account shows that $\mu_{L_f} = \mu_{L_f}(b, l)$.

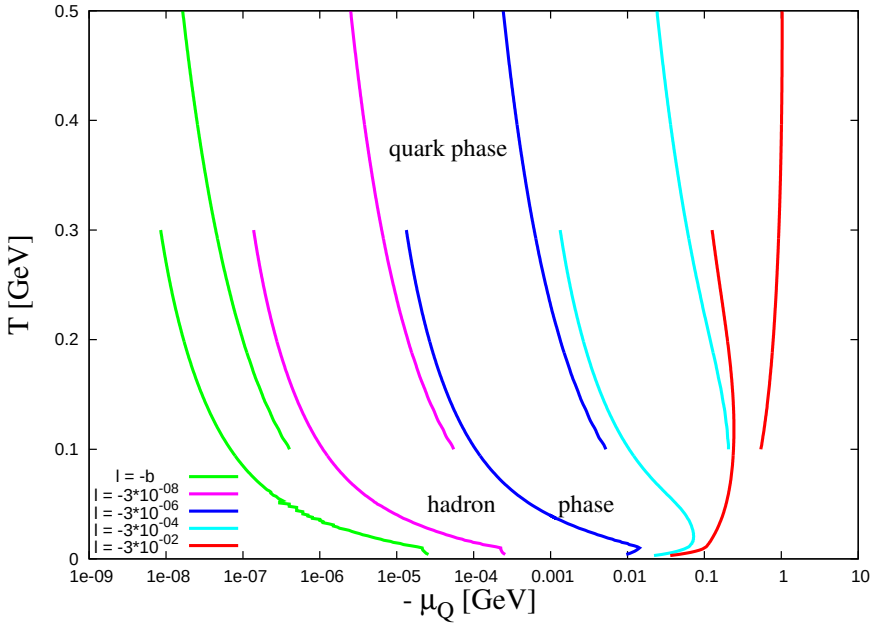

Figure 6.6: Evolution of the charge chemical potential for negative values of l.

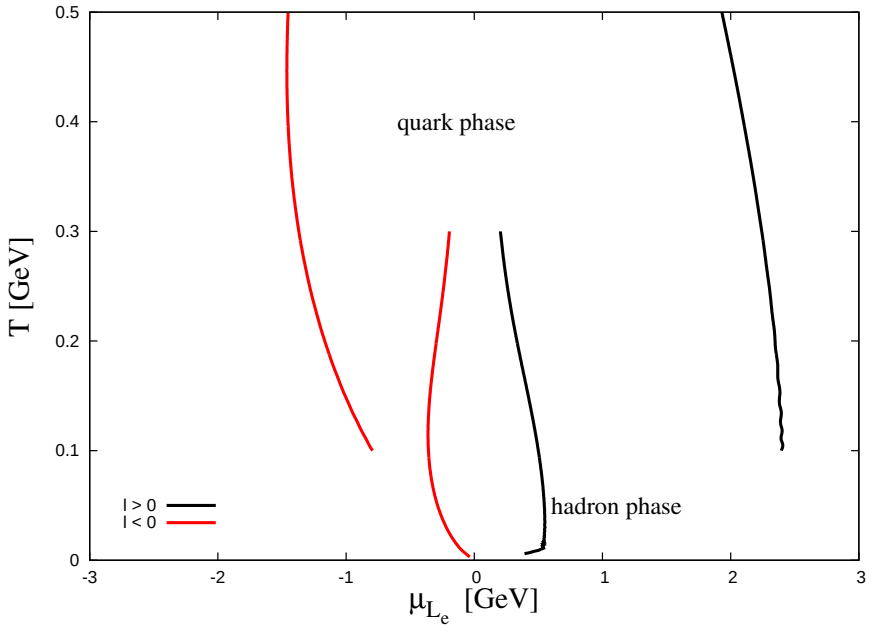

Figure 6.7: Evolution of the leptochemical potential associated with the first lepton generation for $l = \pm 3 \times 10^{-2}$.

After the annihilation of the tau and myon, the flavour asymmetries survives in the neutrino sector. Only the asymmetry in the electron flavour can be divided into electron and electron neutrino asymmetry. This changes with the onset of the neutrino oscillations at $T \sim 10$MeV. The flavours oscillate and the three neutrino sectors become linked via $\nu_e \rightleftharpoons \nu_\mu \rightleftharpoons \nu_\tau$ and lepton flavour is no longer a conserved quantum number. However, the total lepton number still is (if neutrinos are not their own anti-particles, i.e. are not Majorana particles).

6.4 Consequences for the cosmic QCD transition

Our findings question some of the established results about the dynamics of the cosmic QCD transition. For the scenario $l \sim -b$ we found for the barychemical potential a crossing of the quark and hadron phase trajectories at $T \approx 170$ MeV (figure 6.4). This seems to be consistent with a crossover found

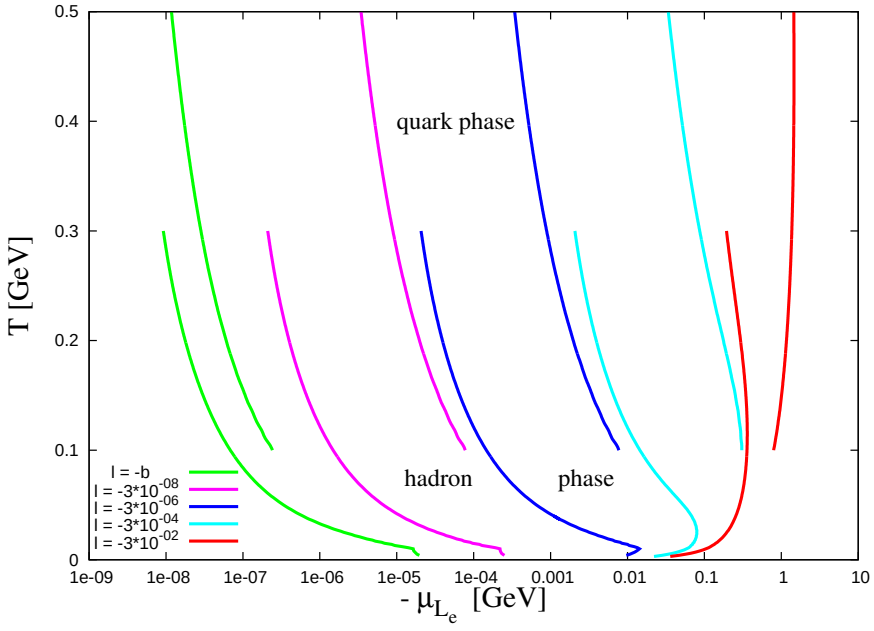

Figure 6.8: Evolution of the leptochemical potential associated with the first lepton generation for negative l.

by lattice simulations, but the trajectories for the charge and leptochemical potentials do not cross at $T \sim 200$ MeV. For a homogeneous universe this would require a jump from the quark- to the hadron trajectory, which would lead to a phase transition. In our simple model, due to $\mu_Q \neq 0$ a phase transition for $l \sim -b$ cannot be excluded. However, as we have neglected interactions in our analysis, the trajectories might be modified close to $T \sim \Lambda_{QCD}$ and our findings just tell us that the situation of $\mu_Q \neq 0$ and $\mu_{L_f} \neq 0$ has to be studied carefully. For the tiny baryon asymmetry and a small lepton asymmetry it would in principle be possible to revisit the question of the order of the QCD transition at $\mu_Q \neq 0$ by means of lattice QCD.

So far it seems, that increasing the lepton asymmetry leads to a decrease of the critical temperature. The opposite effect occurs at the electroweak transition, shown in [Gyn03].

The sign of a possible l asymmetry is important for the dynamics of the transition, as is obvious form figures 6.3, 6.5 and 6.7. However, for large $|l|$ or for positive l, the trajectories of the quark and hadron phases do not cross in the $\mu_B - T$ plane (at least not at $T > 100$ MeV. This might again suggest that the transition would become first order. This is also consistent with the speculation on the existence of a critical end point. Lepton asymmetries of the order of 10^{-2} might put the early Universe in the vicinity of this critical end point.

It is clear that the phase diagram for the cosmic phase transition lives in 5 dimensions for a charge neutral universe (3 lepton flavour asymmetries, the baryon asymmetry and temperature). So far just a two dimensional slice of it has been studied in greater detail.

Chapter 7

Leptons and WIMP Freeze Out

A wide variety of observations point to the existence of a dark matter particle. Several different candidates have been proposed with masses varying from 10^{-6}eV for Axions [Sik08] to 10^{16}GeV WIMPzillas [KT94].
The maybe best motivated candidate is a weakly interacting massive particle (WIMP) with a mass $m_\chi = \mathcal{O}(\text{GeV} - \text{TeV})$. One reason is that the so called hierarchy problem of the standard model suggests the existence of an additional particle with a mass around the weak scale. Such a weak scale particle, if produced thermally, would have an abundance today, similar to the measured dark matter density[GHS05].
Such an additional weak scale mass particle could be the lightest non-standard model particle in supersymmetric extensions if R-parity is conserved. These so called LSPs would be a neutral weakly interacting particle. If they would have strong or electromagnetic interactions they would be bound to ordinary matter today, forming anomalously heavy isotopes. Since experimental data show the non-existence of significance, we focus in the following on neutral WIMPS[1] Supersymmetry provides only a few not coloured and electrical neutral candidates. The sneutrino is one candidate, which is in the minimal supersymmetric standard model already experimentally as a dark matter excluded. The gravitino is another candidate, difficult to exclude. For an overview on dark matter candidates see for example [Ste09].
The remaining supersymmetric candidates are the neutralinos χ, a linear combination of the Bino, Wino, and the supersymmetric Higgs partners [Oli99]. We will focus on this candidate, explicitly on the relic abundance. The relic abundance of any particle in the early universe is determined by the Boltzmann equation. The annihilation of a particle in the early universe continue, until the annihilation rate drops below the Hubble rate. This time point

[1]Note that in principle a dark matter candidate can be charged. For discussion see for example [DEES90, SGED90, CK09].

is usually referred as chemical decoupling, in the following denoted by the subscript *cd*. If this annihilation occurs only through weak interactions, a particle with mass m_χ stops annihilating at $T \simeq m_\chi/20$ [Hoo09]. Below this temperature, the number density is only diluted by the expansion of the universe remains fixed. The change in the number density is described by a Boltzmann equation

$$\frac{dn}{dt} = -3Hn - \langle \sigma v \rangle \, (n^2 - n_{eq}^2), \tag{7.1}$$

with the Hubble parameter H, the total annihilation cross section σ and the relative velocity of the annihilating particles v. The subscript eq denotes the equilibrium density. The Hubble parameter is calculated from the thermodynamic properties of the earlier universe, which change by introducing large lepton asymmetry. In the following we want to investigate the influence of large asymmetries on the relativistic degrees of freedom g_*.

Changing the boundary condition of the ensemble of standard model particles should also then influence the WIMP interaction and hence the chemical freeze out. A large asymmetry between leptons and anti-leptons is such a boundary condition which might play even the dominant role in determining the relic abundance of a WIMPs as we will show.

7.1 Large lepton (flavour) asymmetries and effective relativistic degrees of freedom

Let us now take a closer look at the contribution of lepton flavour asymmetries on the effective relativistic degrees of freedom contributing to the total energy density of a Stefan-Boltzmann gas,

$$g_*(T, \{\mu_i\}) \equiv \frac{30}{\pi^2 T^4} \epsilon(T, \{\mu_i\}). \tag{7.2}$$

Together with the solution $\mu_i = \mu_i(T; b, l_e, l_\mu, l_\tau)$ we find

$$g_* = g_*(T; b, l_e, l_\mu, l_\tau). \tag{7.3}$$

Large lepton flavour asymmetries generically lead to large chemical potentials of all fermion species. and to an increase of g_*, due to non-vanishing chemical potentials,

$$g_*(T, \{\mu_i\}) \quad = g_*(T, 0) + \Delta g_*(T, \{\mu_i\}), \tag{7.4}$$

with

$$g_*(T,\{0\}) = \sum_{i=\text{bosons}} g_i + \frac{7}{8}\sum_{i=\text{fermions}} g_i, \tag{7.5}$$

and

$$\Delta g_*(T,\{\mu_i\}) = \sum_i g_i \left[\frac{15}{4}\left(\frac{\mu_i}{\pi T}\right)^2 + \frac{15}{8}\left(\frac{\mu_i}{\pi T}\right)^4\right]. \tag{7.6}$$

Any nonzero Δg_* would therefore increase the total energy density and thus the Hubble expansion rate.

For an analytic estimate of the effect of lepton flavour asymmetries, we neglect all masses of quarks and leptons and assume that all lepton flavour asymmetries are small enough to justify $\mu_i/(\pi T) \ll 1$. We assume $m_W/3 > T > m_b/3$, thus $g_* = 345/4$. From the conservation of charge, baryon number and lepton flavour we find

$$\begin{aligned}
0 &= \frac{1}{3}T^2(4\mu_u - 3\mu_d - \mu_e - \mu_\mu - \mu_\tau) + \mathcal{O}(\mu_i^3), && (7.7)\\
\frac{23\pi^2}{6}T^3 b &= \frac{1}{3}T^2(2\mu_u + 3\mu_d) + \mathcal{O}(b\mu_i^2, \mu_i^3), && (7.8)\\
\frac{23\pi^2}{6}T^3 l_f &= \frac{1}{6}T^2(2\mu_f + \mu_{\nu_f}) + \mathcal{O}(l_f\mu_i^2, \mu_i^3). && (7.9)
\end{aligned}$$

Solving this set of equations results in

$$\begin{aligned}
\frac{\mu_d}{\pi T} &= \pi\left[\frac{5}{2}b - \frac{2}{3}l\right], && (7.10)\\
\frac{\mu_u}{\pi T} &= \pi\left[2b + l\right], && (7.11)\\
\frac{\mu_f}{\pi T} &= \pi\left[\frac{1}{6}b - \frac{5}{9}l + \frac{23}{3}l_f\right], && (7.12)\\
\frac{\mu_{\nu_f}}{\pi T} &= \pi\left[-\frac{1}{3}b + \frac{10}{9}l + \frac{23}{3}l_f\right]. && (7.13)
\end{aligned}$$

It becomes apparent that lepton (flavour) densities large compared to the baryon density affect not only the number densities of leptonic species, but also those of quarks. This can lead to increase of the effective degrees of freedom in the energy density and the entropy density.

7.1.1 Flavour symmetric lepton asymmetry

As a first step we investigate again the analytic approach to see how the flavour distribute on the different fermionic chemical potentials. Let us first

assume that all lepton flavour numbers are the same, $l_e = l_\mu = l_\tau = l/3$. We also assume $b \ll |l| \ll 1$ and put $b = 0$. This results in

$$\frac{\mu_d}{\pi T} = -\frac{2\pi}{3} l, \tag{7.14}$$

$$\frac{\mu_u}{\pi T} = \pi l, \tag{7.15}$$

$$\frac{\mu_f}{\pi T} = 2\pi l, \tag{7.16}$$

$$\frac{\mu_{\nu_f}}{\pi T} = \frac{11\pi}{3} l, \tag{7.17}$$

and allows us to estimate the change in the effective degrees of freedom,

$$\Delta g_*(T, b = 0, l_f = l/3) = \frac{1265}{2} \pi^2 l^2 \approx 6.2 \times 10^3 l^2. \tag{7.18}$$

Thus $\Delta g_*/g_* \approx 760 l^2$, which we assumed to be small for the purpose of the analytic apprximation, i.e. $l < 10^{-2}$.

For lepton asymmetries $l > 10^{-2}$ we rely on a numerical solution of the five conservation equations and include all particles from the standard model of particle physics with their measured physical masses (the unknown masses of the Higgs and the neutrinos are irrelevant in the regime of interest). We solved the equations (3.33) to (3.35) using (3.17) and (3.22).

The numerical results for the effective helicity degrees of are shown in figure 7.1. We found that an asymmetry $l_f = 0.01$ leads to a small deviation from the standard case with $b = l = l_f = 0$. If we apply the experimentally given upper bound for the electron neutrino asymmetry to all flavours, we found for $l_f = 0.1$ approximately additional 50 degrees of freedom for the early universe between $1 < T < 50$ GeV. We see, that our analytic estimates predict a much higher deviation, due to the fact, that we it does not take the chemical potential ion the entropy into account. Also the relativistic approach for the net particle density $n = T^2\mu/3$ is not valid, since $\mu/T \ll 1$ is not valid any more. Taking the whole numerics into account reduces thee effect predicted by the analytic approach, but still leads to remarkable deviations from the standard scenario $l = l_f = b = 0$ Wee see that the plateau between between 3 and 10 GeV for $l_f < 0.01$ is in good agreement with our estimate $g_* = 345/4 = 86,25$.

7.1.2 Flavour asymmetric lepton asymmetry

Let us now have a closer look at situations in which at least one of the three flavour lepton numbers satisfies $|l_f| \gg b$, but we restrict to $|l_f| \leq 1$ for all

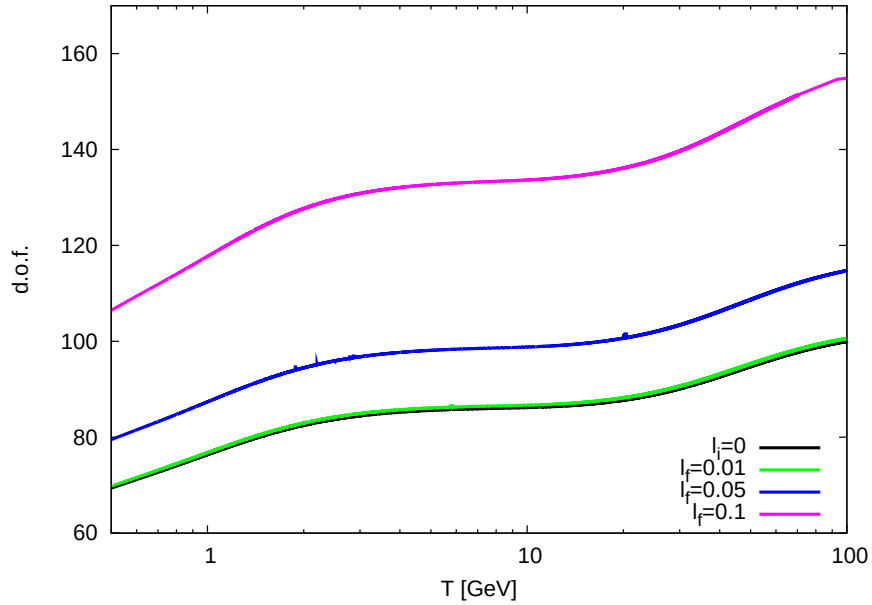

Figure 7.1: The numerical solution for the flavour symmetric case $l = 3l_f$. The effective degrees of freedom of all particles in chemical equilibrium versus the temperature in GeV on logarithmic scale. The black line corresponds to standard case, where lepton asymmetries are neglected. The blue line shows the influence of $l_f = 0.01$, the green $l_f = 0.05$ and the red $l_f = 0.1$.

flavours. For simplicity we can put $b = 0$. The first interesting situation is that one flavour asymmetry dominates, say $l_\tau \neq 0$ and the other flavour asymmetries vanish. In that case we would find that the quark chemical potentials are effected:

$$\frac{\mu_d}{\pi T} = -\frac{2\pi}{3} l_\tau, \tag{7.19}$$
$$\frac{\mu_u}{\pi T} = \pi l_\tau, \tag{7.20}$$
$$\frac{\mu_{e,\mu}}{T} = -\frac{5\pi}{9} l_\tau, \tag{7.21}$$
$$\frac{\mu_\tau}{T} = \frac{64\pi}{9} l_\tau, \tag{7.22}$$
$$\frac{\mu_{\nu_{e,\mu}}}{T} = \frac{10\pi}{9} l_\tau, \tag{7.23}$$
$$\frac{\mu_{\nu_\tau}}{T} = \frac{79\pi}{9} l_\tau. \tag{7.24}$$

The numerical results for this situation are presented in figure 7.2. We see again a tiny deviation from the standard case for $l_\tau = 0.01$. For $l_\tau = 0.1$ there would be around 10 more degrees of freedom. The effect is smaller compared to symmetric case since the total l is smaller.

Another interesting case would be $l = 0$, but $l_\mu = -l_\tau \neq 0$. In that case quark chemical potentials would not be affected:

$$\mu_d = \mu_u = \mu_e = \mu_{\nu_e} = 0, \quad \frac{\mu_f}{\pi T} = \frac{\mu_{\nu_f}}{\pi T} = \frac{23\pi}{3} l_f, \quad f = \mu, \tau. \tag{7.25}$$

In that case $\Delta g_* = 5(23\pi)^2 l_\tau^2 \approx 2.6 \times 10^4 l_\tau^2$. As we assumed for the analytic approximation that the modification is small, its regime of validity is limited to $|l_\tau| < 10^{-2}$. The numerical results for vanishing l, but non-vanishing lepton flavour asymmetry are presented in figure 7.3. In the calculations for the degrees of freedom the sign of a possible asymmetry does not play any role, since they enter squared. For $l_\mu = -l_\tau = 0.1$ additional 20 degrees of freedom appear. What makes this scenario the most interesting, is the possibility for even larger asymmetries. If we assume $l_\mu = -l_\tau = 1$ we find more then 600 additional degrees of freedom, shown in figure 7.4. This is the most extreme case and it is the question, how physical it is. The Universe would probably be in a fermi-condensate state which might be only a local solution, but no global.

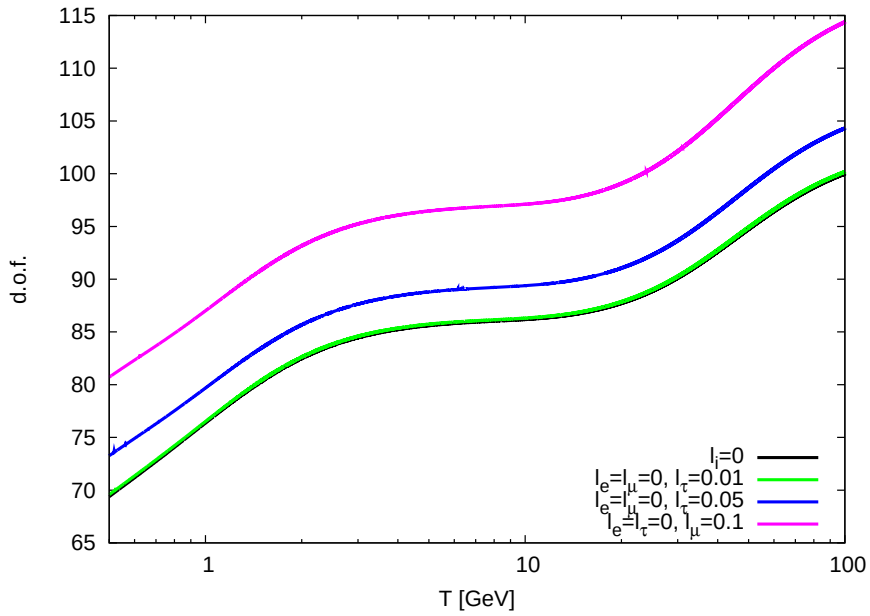

Figure 7.2: The numerical solution for the flavour symmetric case $l = l_\tau$. The effective degrees of freedom of all particles in chemical equilibrium versus the temperature in GeV on logarithmic scale. The black line corresponds to standard case, where lepton flavour asymmetries are neglected. The green line shows the influence of $l_\tau = 0.01$, the blue stands for $l_\tau = 0.05$ and the red for $l_\tau = 0.1$.

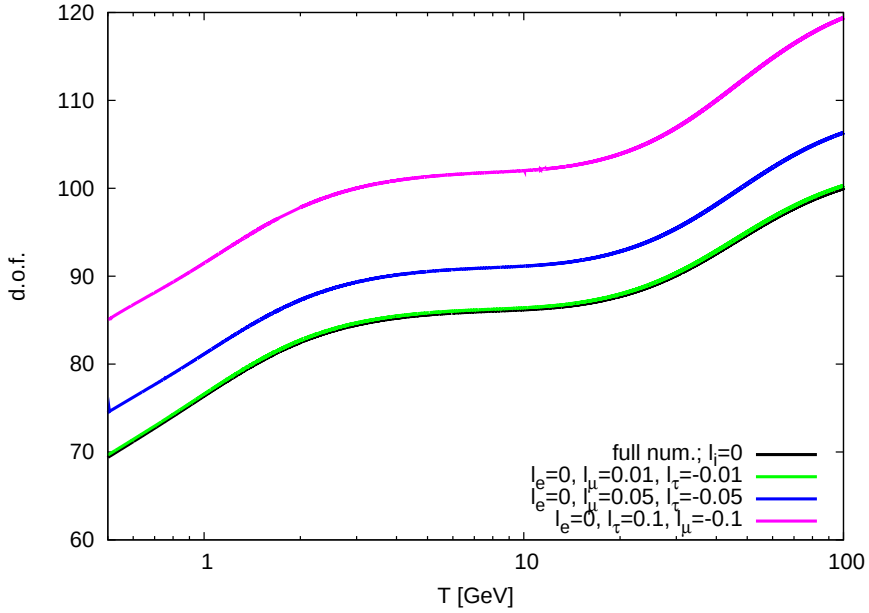

Figure 7.3: The numerical solution for the flavour symmetric case $l_\mu = -l_\tau$ and $l = l_e = 0$. The effective degrees of freedom of all particles in chemical equilibrium versus the temperature in GeV on logarithmic scale. The black line corresponds to standard case, where lepton flavour asymmetries are neglected. The green line shows the influence of $l_\tau = 0.01$, the blue stands for $l_\tau = 0.05$ and the red for $l_\tau = 0.1$.

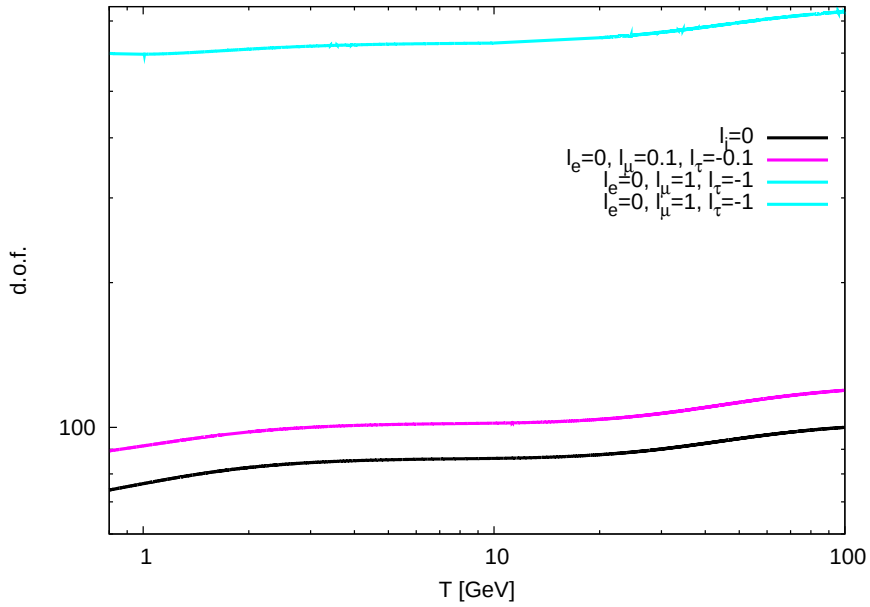

Figure 7.4: The numerical solution for the flavour symmetric case $l_\mu = -l_\tau$ and $l = l_e = 0$ including $|l_\tau| = 1$ (blue line). Compared to the standard case, around 600 additional degrees of freedom appear.

7.2 Effect on decoupling of WIMP Dark Matter

Let us now have a look, how these large effects on the degrees of freedom enter in the relic abundance of WIMPs. Recalling equation (7.1), the relic abundance also depends on parameters in the supersymmetric Standard Model. To determine the relic density, it is necessary to obtain a general annihilation cross-section for neutralinos. This has been done for example in [JKG96, MOS92]. In the following we assume the WIMP to be the single component Dark Matter particle, without asymmetry between WIMPs and anti-WIMPs. In the hot early universe these particles with masses typically between 10 and 1000 GeV are in thermal and chemical equilibrium with the radiation content. Their chemical freeze out, when WIMPs decouple chemically from the radiation plasma, happens at $T_{\rm fo} \simeq m/20$ GeV, leading to a mass dependent interval of $0.4< T_{\rm fo} <40$ GeV (see e.g. [GHS05]).

To calculate the relic density, we assume annihilations of the WIMPs $X\bar{X} \rightarrow \cdots$ with a typical weak interaction cross section $\sigma \propto G_{\rm F}^2$. The number density is described by a Boltzmann equation

$$\dot{n} + 3Hn = -\langle\sigma|v|\rangle\,(n^2 - n_{\rm eq}^2). \tag{7.26}$$

There are no closed analytical solutions to this equations, but one can get fairly good analytical and numerical estimates. Note that density of WIMPS id conserved

$$\left(\frac{n_\chi}{s}\right)_0 = \left(\frac{n_\chi}{s}\right)_{\rm fo}, \tag{7.27}$$

where the subscript 0 denotes the value today. The relative relic abundance of WIMPS today is defined as

$$\Omega_\chi h^2 = \frac{m_\chi n_\chi}{\rho_c} \tag{7.28}$$

$$= \frac{1}{0.264 m_{Pl}} \left(\frac{s}{\rho_c\ h^{-1}}\right)_0 \left(\frac{1}{\langle\sigma|v|\rangle\ {g_*}^{1/2}}\right)_{\rm fo}. \tag{7.29}$$

The abundance of a WIMP particle is inverse proportionally to its annihilation cross section, a more strongly interacting particle stays longer in equilibrium. But also to the helicty degrees of freedom at the temperature of freeze out. The dependence on helicity degrees of freedom is apparent in the denominator, but there is also an implicit dependence $\propto \ln(1/g_*)$ [GHS05]. An effect of order few percent in g_* translates to a few percent difference in the relic abundance of WIMP dark matter. We refer the reader for more details to [JKG96, GHS05].

We show in figures 7.5 to 7.7 for several freeze out temperatures and large lepton asymmetries the effect on the relic density compared to the standard case $\Omega_{\rm DM}(l = l_f = 0)$. Therefore we plotted the ratio $\Omega_{\rm DM}(l, l_f)/\Omega_{\rm DM}(l = l_f = 0)$. We see that the comparable huge effect in the degrees of freedom acts as a damping factor. In figure 7.5 we set $l_e = l_\mu = l_\tau = l_f$ and evaluated the ratio for $l_f \leq 0.1$. We observe an effect of order 1 % for $l_f = 0.01$ and the largest effect of almost 20% for $l_f = 1$.
If we reduce the asymmetry to be just in two flavour, $l_e = 0$ and $_\mu = -l_\tau \leq 0.1$, we reduce the effect to 10% for $l_\mu = 0.1$. We observe in figure **??** at the temperature of the τ freeze out that the effect gets a little larger. The electric neutrality forces the increase the chemical potential for the electron and muon. Note that the total lepton asymmetry in this scenario $l = 0$.
A comparable smaller but still relevant effect is observed for the asymmetry in one flavour, $l_\tau \leq 0.1$. Still the effect can be up to order 5 %, shown in figure 7.6.

7.3 Consequences for the relic abundance and density of WIMPS

The evolution of $Y_\chi = n_\chi/s$ is shown schematically in figure **??**. As the universe expands and cools down, n_χ decreases at least as R^3. Therefore, the annihilation rate quenches and the abundance freezes out. The reaction rates are not longer sufficient to keep the particles in equilibrium and the ratio $n\chi/s$ stays constant. The impact of the cross section on the comoving number density is shown in figure **??**. Assuming the current entropy density to be $s\_0 \simeq 4000$ cm$^-3$ and the critical density today as $\rho_c \simeq 10^{-5}h^2$ GeV cm^{-3} with the Hubble constant in units of $h \simeq 100$ km s^{-1} Mpc^{-1} and neglecting the effect of large chemical potentials on the helicity degrees of freedom, one gets the present mass density in units of the critical density $\Omega_\chi h^2 = m_\chi n_\chi/\rho_c \simeq 3 \times 10^{-27}$cm^{3}s^{-1}/ $\langle\sigma$v$\rangle$. The influence of the cross section on the comoving number density is shown in figure **??**. Increasing $\langle\sigma v\rangle$ leads to a smaller number density. For more details on the annihilation cross sections of WIMP candidates, we refer to [JKG96] We have shown in this chapter, that also chemical potentials at the freeze out time are an additional damping factor. With this second damping factor, one could now allow smaller cross section, so far excluded since they do not end up in the correct relic density, and trigger Ω_χ with the lepton asymmetry to the correct value. The distribution of individual flavour asymmetries we used here as an example is from the physical point of view fully justified and in no

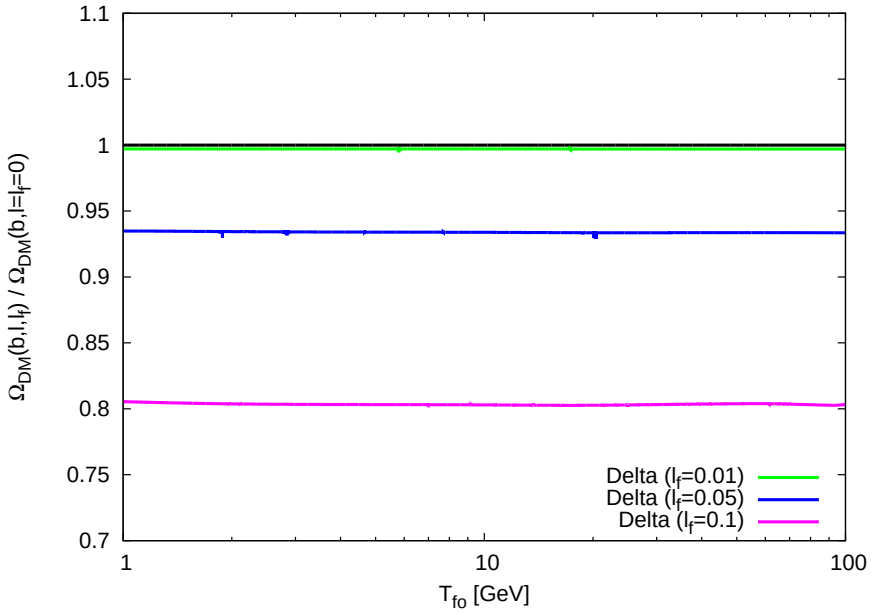

Figure 7.5: Effect of lepton asymmetries $l_e = l_\mu = l_\tau = l_f \leq 0.1$ on the relic WIMP dark matter abundance. We plotted ratio $\Omega_{\rm DM}(l, l_f)/\Omega_{\rm DM}(l = l_f = 0)$ for different freeze out temperatures $T_{\rm fo}$. The observational allowed asymmetries of $l_f = 0.1$ cause a reduction of the relic abundance of almost 20 %.

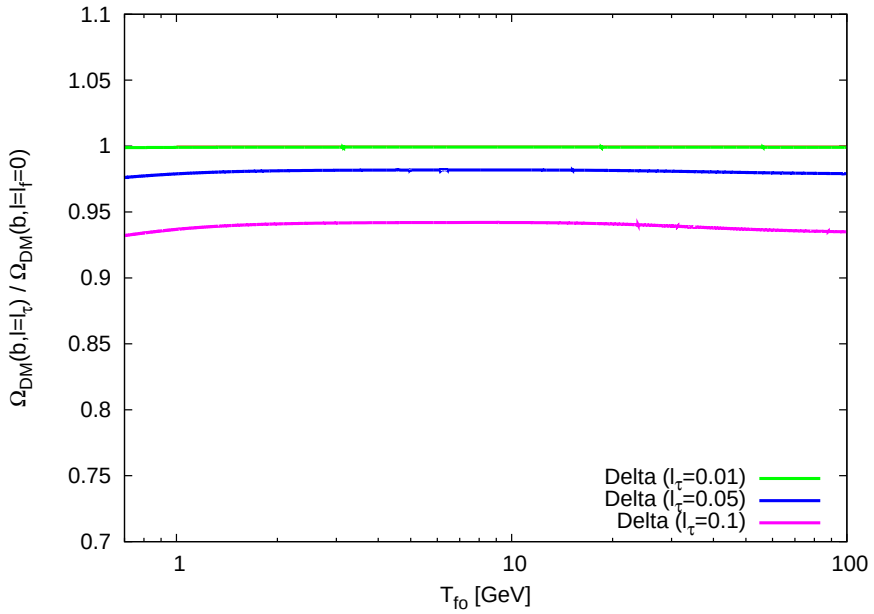

Figure 7.6: Effect of a lepton asymmetry in just one flavour, here $l_\tau \leq 0.1$ on the relic WIMP dark matter abundance. We plotted the ratio $\Omega_{\rm DM}(l, l_f)/\Omega_{\rm DM}(l = l_f = 0)$ for different freeze out temperatures $T_{\rm fo}$. The effect is smaller than for the three flavour case, but also the total lepton asymmetry $l = \sum_f l_f$ is here smaller. An asymmetry in the tau flavour of $l_f = 0.1$ causes a reduction of the relic abundance of $\mathcal{O}(5\%)$. Due to the annihilation of the charged tau at $T \simeq m_\tau/3$, we see an increasing effect for lower freeze out temperatures.

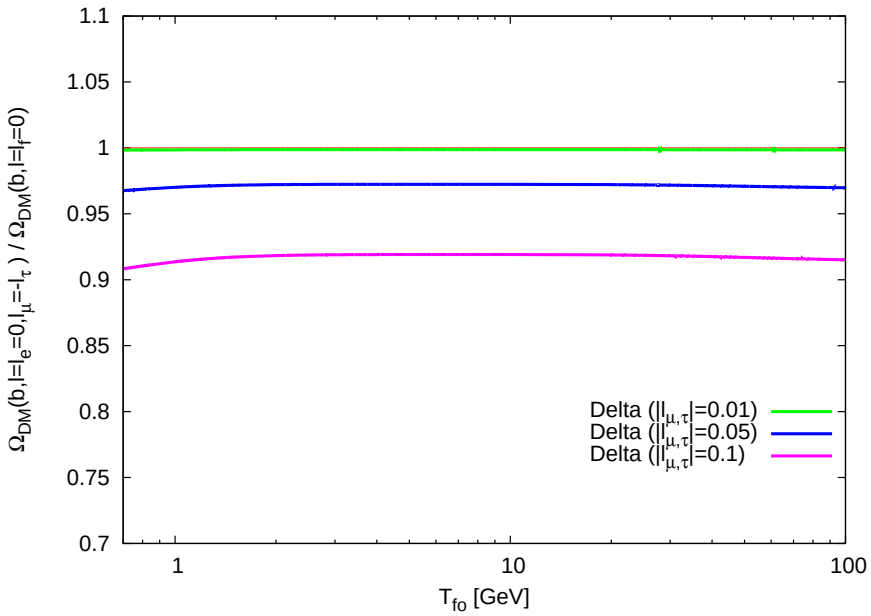

Figure 7.7: Effect of a lepton asymmetry in two flavours $-l_\mu = l_\tau = l_f \leq 0.1$ on the relic WIMP dark matter abundance. We plotted the ratio $\Omega_{\rm DM}(l, l_f)/\Omega_{\rm DM}(l = l_f = 0)$ for different freeze out temperatures $T_{\rm fo}$. We find for $l_f = 0.1$ an 7% effect, slightly incresing to $\approx 8\%$, again due to the tau annihilations at lower freeze out temperatures.

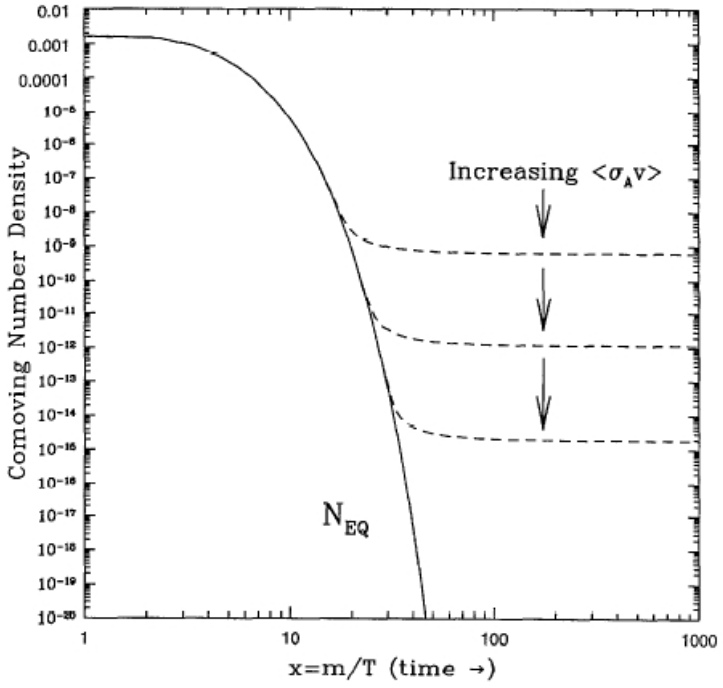

Figure 7.8: Shown here are solutions to the Boltzmann equation for the comoving number density in the early universe. On the x-axis is the ratio between the WIMP mass and the temperature plotted. We see that increasing $\langle \sigma v \rangle$ decreases the number density.

contradiction to any experimental data from CMB, BBN, ^{4}He-abundance or LSS [SS08]. It is also not in contradiction with a possible flavour equilibration before BBN [DHP$^+$02, ABB02, Won02]. But even if oscillations are not or only partial efficient, the asymmetries are still within the experimental boundaries.

Dark Matter candidates, excluded for having too small annihilation cross sections should be investigated again under the aspect of possible lepton flavour asymmetries.

Chapter 8

Conclusion

With this work we closed a gap in the description of large lepton asymmetries and their influence on the dynamics of the early universe. In the standard model of cosmology there are no L and/or B violating processes after the electroweak phase transition at T 200 GeV and before the onset of neutrino oscillation at $T \simeq 10$ MeV. Thus, any neutrino flavour asymmetry is conserved during this interesting epoch of the first 0.01 second of the universe, in which the WIMP decouples from the Standard Model particles and quarks confine to hadrons.

We know very little about the actual lepton asymmetry of the Universe. A large lepton asymmetry $|l| \gg b$ is compatible with constraints from primordial nucleosynthesis and the CMB if $|l| < \mathcal{O}(0.1)$.

We have shown in chapter 5.2.2 that such an asymmetry may significantly affect the dynamics of the cosmic QCD transition. The cosmic trajectory in the μ_B-T plane depends on the lepton flavour asymmetries l_f, besides the baryon asymmetry b.

Depending on the, yet unknown, structure of the QCD phase diagram and especially on the position of a hypothetical critical end point, a large lepton asymmetry might result in a first order QCD transition in the early Universe. This seems possible for $|l| \simeq 0.02$. Many formerly suggested cosmological consequences of a first order QCD transition would be possible (formation of relics, effects on nucleosynthesis, generation of magnetic fields, generation of gravitational waves, etc. [Sch03]).

So far, the conclusions from lattice QCD simulations at $\mu_Q = 0$ and $\mu_B \ll T$ have been used to conclude that the cosmic QCD transition is a crossover [AEF$^+$06]. We have shown that the cosmic trajectory has $\mu_Q \neq 0$. In the case of efficient sphaleron processes μ_Q is tiny, in the case of a large lepton asymmetry, μ_Q can be large and it is unclear if the conclusion that the cosmic QCD transition is a crossover remains true. For $|l| > 10^{-4}$, the

charge chemical potential differs between the quark and the hadron phase by more than 100 MeV (the QCD scale) at temperatures around the QCD scale (see figure 6.6).

A detailed understanding of the consequences of $|l| \gg b$ on the QCD transition could allow us to rule out or find evidence for leptogenesis scenarios that lead to a large lepton asymmetry.

We have also shown, that the unknown lepton asymmetry can have a huge effect on the relic abundance of the WIMP dark matter. Even if the total lepton asymmetry is of the same order as the baryon asymmetry, but individual flavour asymmetries $l_i \leq \mathcal{O}(0.01)$, we observed a few percent effect.

While for the cosmic QCD transition only the total lepton asymmetry $\sum_f l_f$ is of interest, the individual lepton flavour asymmetries may additionally change the relic abundance of WIMP dark matter. We have shown, that for individual asymmetries of $l_f = 0.05$ the damping of the relic density of WIMP dark matter with respect to $l_f = 0$ is in the few percent range. If the asymmetry is in more than one flavour, the effect grows and we observed even for $l_\mu = -l_\tau = 0.01$ a one percent effect. If for all three flavour $l_f = 0.1$ we found a decrease of almost 20 per cent.

This suggests, that cross sections, excluded because they lead to a too large relic density, might be relevant again. A large lepton asymmetry can compensate this by decreasing the abundance to the correct value. In turn, some large $\langle \sigma v \rangle$ might be excluded if the lepton (flavour) asymmetry is too large.

A deeper and more detailed investigation of the allowed region for $\langle \sigma v \rangle$ for different dark matter candidates is needed to obtain more rigorous bounds on the interplay of $\langle \sigma v \rangle$ with large chemical potentials induced by large lepton flavour asymmetries.

A more detailed understanding is needed of the cosmological consequences for the extreme case $l_\mu = -l_\tau = \mathcal{O}(1)$. The resulting fermi-condensate might be an interesting scenario for inhomogeneous cosmo-dynamics. One could imagine, that locally these states might be possible.

In this work we assumed that all globally conserved quantum numbers are also conserved locally and we have put the focus on the case of equal lepton flavour asymmetries. Dropping the latter, obviously leads to a somewhat richer phenomenology, which is beyond the scope of this work. While the local conservation of electric charge and baryon number are probably excellent approximations, the local conservation of lepton number is not correct if distance scales below the neutrino mean free path are considered. Consequently, as soon as inhomogeneities become important (and they will in the case of a first order phase transitions, as cold spots are more likely to nucleate bubbles of the new phase [IS01]) it would be more realistic to describe an

inhomogeneous universe with regions of different l_f. These different regions would be equilibrated via the neutrinos, so that possible bubbles of different l_f at the QCD phase transition would have a minimal radius $d_{\nu-\mathrm{mfp}} \simeq 1$ m [IS01]. This has to be compared to the size of the Universe at this time, $d_H \simeq 10$ km [Sch03]. Although giving rise to small effects only, precise measurements of the abundance of primordial light elements might be sensitive to inhomogeneities produced during the QCD transition, as they might lead to inhomogeneous nucleosynthesis.

There might also be interesting effects from inhomogeneous distributions of large lepton flavour asymmetries. Regions with larger differences in the lepton flavour asymmetry would result in different relic WIMP dark matter abundances. Thus, even if the WIMPs are homogeneous distributed before their chemical freeze out, an inhomogeneous lepton flavour asymmetry leads to an inhomogeneous distribution of the relic abundance.

Obviously, the consequences of a large lepton asymmetry on the physics of the early Universe between the electroweak transition and neutrino oscillations have been overlooked so far. This calls for a reinvestigation of many of the suggested effects of the cosmic QCD transition and might allow us to improve the limits on the universal lepton flavour asymmetries (before neutrino oscillations start). Deeper understanding of WIMP dark matter freeze out might allow us to get further insights to lepton flavour asymmetries.

Chapter 9

Outlook

Apart from the before discussed further investigations on the QCD transition and the relic WIMP density, there are more interesting cosmic scenarios including large particle asymmetries.

The written software provides the possibility to investigate another interesting effect large lepton flavour asymmetry in one flavour might have. Assuming neutrino oscillations to ensure full flavour equilibration of a one flavour asymmetry, lets say $l_e = l_\mu = 0$ but $l_\tau = \mathcal{O}(0.3)$ to $l_e = l_\mu = l_\tau$. A deeper investigation of the consequences might be interesting.

We assumed in this work the baryon asymmetry to be small ($\mathcal{O}(10^{-10})$) after the electroweak transition. There are scenarios described in the literature, where this asymmetry could also be large and diluted at the QCD-transition via a short period of inflation to the actual observed value [BCVM00, Kam00, BSB11]. Assuming that this idea is compatible with cosmological observations, it would be interesting to investigate the effect of an additional large μ_b on the relic WIMP density. It might turn out to be large, if the neutrino asymmetry is located in one flavour.

It might also be interesting to investigate the effect on the WIMP asymmetry allowing also chemical potentials for WIMPs. Models with WIMP and anti-WIMP particles have recently been discussed in the literature, see for example [KLZ09], and it was investigated how the relic abundance might be [IDC11]. There is clearly a dependence on the WIMP chemical potential in Ω_{DM} [GHS05] and it would be interesting to investigate the effect large lepton asymmetries would have on these scenarios.

Appendix A

Numerics

In this work we calculated the equilibrium thermodynamic variables for the Standard Model particles with global conserved baryon, lepton flavour number and electric charge. We solved equations (3.33), (3.34) and (3.35) for the exact equations for particle net numbers (3.17) and entropy (3.22) for any given lepton flavour number the observed baryon asymmetry and $q = 0$.

We performed the calculations of the quark phase for temperatures 200 GeV $> T >$ 100 MeV and for the hadron phase at 300 MeV $> T >$ 1 MeV.

We review in the following the used methods and describe the written software. The used programming language is C and all used programs are on the CD including comments.

A.1 Numerical methods

To calculate the chemical potentials we split the universe in three parts. From the electroweak phase transition to the QCD transition, where the three lepton flavour are conserved and quarks are free. The second from the QCD transition to the onset of neutrino oscillations, where the τ´s are already annihilated and l_τ effects only the neutrinos. At this time all quarks are bound to hadrons and mesons. We take resonances up to the Kaons K^0_* with masses $m_{K^0_*} = 1414$ MeV. And the third epoch after neutrino oscillation until BBN, where only the total lepton lumber is conserved. The programs on the CD are ew.c, qcd.c, nu.c, respectively. The equations to solve reduce from 5 to four and finally to three, respectively. For an overview how the programs work, we explain in the following in more detail the quark phase between the electroweak and QCD transition.

The core program to solve the five dimensional non-linear integral equation is described below. For further details we refer to [PTVF96]. For a

successful compiling the following packages are needed

```
include <stdio.h>
include <math.h>
include "nr.h"
include "nrutil.h"
```

The Methode to solve the nonlinear equations is *Broydn´s* method, a variant of Newton´s method (for a detailed description see [PTVF96]). It is a multidimensional secant method and looking for global minima as the best solution. The function is called by

```
broydn(mu,N,&check,funcv);
```

and makes use of further routines, shown in the diagram below The argument

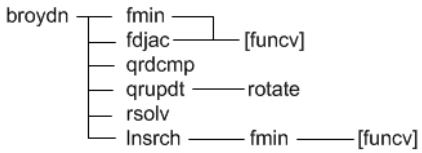

Figure A.1: Diagram of the dependence of the function broydn on further functions.

of *broydn* consists of

```
{mu,N,&check,funcv}.
```

The first variable *mu* is the starting condition for the variation. For our calculation it is a five-dimensional vector, indicated by the second variable, the integer *N*. The third expression &check is an integer with value 1 or 0 and is the break-down criteria for the function. If the value is 1, there is either no progress made by the routine, or the function *fmin* is convergent. In both cases the calculations stop and a new and better initial value has to be chosen. The value *funcv* is the system of equations which has to be set to zero, has the same dimension N as the vector *mu*.

The initial guesses for the vector *mu* is defined in the program for example as:

```
mu=vector(1,N);
  mu[1]=2.e-07;        /*mu e  */
  mu[2]=4.e-07;        /*mu u  */        /*initial guess*/
  mu[3]=-4.e-07;       /*mu nu e */
  mu[4]=-1.e-07;       /*mu nu myon*/
  mu[5]=-1.5e-07;      /*mu nu tau*/
```

representing the five independent chemical potentials in the quark phase. These values are varied starting from the given initial guess to set the equation vector zero. The routine *funcv* is called with the function

```
funcv(N,mu,f);
```

where the integer N is the dimension of the vector, *mu* the vector with the initial guess and f is the vector of equations, defined in *void funcv(int n,double mu[], double f[])* with entries for f

```
f[1]=Ne+Nnue-(myk1*entropy);
f[2]=Nmuon+Nnumuon-(myk2*entropy);
f[3]=Ntau+Nnutau-(myk3*entropy);
f[4]=Ncharm+Nup-Ne-Nmuon-Ntau-(myc*entropy);
f[5]=Nup+Ndown+Ncharm+Nstrange+Nbottom-(3*myc*entropy);
```

The net particle densities *Ne, Nue...* are defined in *funcv* as doubles, for example for the electron

```
double Ne = ((4/(Pi*Pi))*sinh(mu[1]/myT)*netto(mu[1],myT,electron));.
```

The double *netto* is called with the chemical potential *mu*, The temperature *myT* and the electron mass *electron*. The function *netto* is a Gauss-Laguerre integral and defined as

```
double netto (double mu, double T, double masse){
  double E,  netto2;
  int    n=25;
  int    i;
  double x[n],w[n];

  gala(x, w, n);
  netto2=0.0;
  for(i=0;i<n;i++)
    {
```

```
      netto2 += (w[i]*integ(x[i],mu,T,masse)*exp(x[i]));
    }
  return netto2;.
}
```

The routine is *gala(x, w, n)* the Gauss-Laguerre integration. The function *integ(x[i],mu,T,masse)* is the function which is integrated.

```
double integ(double E, double mu, double T, double masse)
{
return(T*((T*E+masse)*sqrt(T*T*E*E+2*T*E*masse)*exp(E+(masse/T)))
       /((exp(E+((masse-mu)/T))+1)*(exp(E+((masse+mu)/T)))+1));
}
```

The entropy is calculated exact for fermions and bosons by *myg* and *mygbos*, respectively.

For the two other periods of the universe one has only to change the particles and the system of equation.

```
  f[1]= Ne + Nnue - (myk1*entropy);
  f[2]= Nmyon + Nnumyon - (myk2*entropy);
  f[3]= Np + Nn - (myc*entropy);
  f[4]= Np - Ne - Nmyon + Npion;
```

for the universe between the QCD transition and the onset of neutrino oscillations and Dimensionen

```
  f[1]= Ne + Nnu - (myk*entropy);
  f[2]= Np + Nn - (myc*entropy);
  f[3]= Np - Ne;
```

for the epoch after neutrino oscillation and before BBN. Compiling the programs with the gnucompiler command

```
 gcc -o name *.c -lm
```

creates, opens and writes a file with the temperatures and solutions for the chemical potentials and/or corresponding particle densities. With the chemical potentials, the remaining thermodynamical variables for the different lepton asymmetries can be calculated,like the energy density or the pressure. See programs on the CD for more details.

The program join.c reads in files with solutions for several lepton asymmetries and creates a new file with selected solutions. This makes it easier to compare different solutions with graphic programs like for example gnu-plot.

A.1.1 Numerical results

Taking all particle masses into account, equations (6.2) to (6.6) and (6.19) to (6.22) have to been solved numerically. To avoid numerical instabilities the net particle densities in (**??**) are rewritten as

$$n = \frac{g}{2\pi} \sinh\left[\frac{\mu}{\mathrm{T}}\right] \exp\left[-\frac{\mathrm{m}}{\mathrm{T}}\right] (\mathrm{Tm})^{3/2} \mathrm{I}(\mathrm{T}, \mu),$$

where

$$I(T,\mu) = \int_0^\infty \frac{(1+\frac{T}{m}x)\sqrt{(1+\frac{T}{m}x)x}}{\left(\exp[\mathrm{x}-\frac{\mu}{\mathrm{T}}]+\exp[-\frac{\mathrm{m}}{\mathrm{T}}]\right)\left(\exp[\mathrm{x}+\frac{\mu}{\mathrm{T}}]+\exp[-\frac{\mathrm{m}}{\mathrm{T}}]\right)}\mathrm{d}x.$$

For the quark phase we consider the temperature interval 200 GeV $>$ $T > 10$ MeV with all SM particles. All particle masses are adopted from the Particle Data Group [N$^+$10]. We restrict our study to the case of an equal flavour asymmetries $l_e = l_\mu = l_\tau = l/3$ for our studies concerning the QCD transition and choose additionally flavour asymmetric distribution for the WIMP freeze out epoch. The baryon asymmetry is fixed to $b = 9 \times 10^{-11}$ and the charge is always set to zero in all our numerical calculations. As already discussed above, if sphaleron processes are efficient and no additional baryon or leptogenesis happens after they stop, the generic value of $l = -\frac{51}{28}b$ [HT90]. This leads to a universe dominated by antimatter in the leptonic sector and matter in the baryonic sector. Since it is the most common scenario, we choose this to show some numerical results. Below we discuss two examples $l = -b$ and $l = 3 \times 10^{-4}$.

The evolution of the net lepton densities in the quark-gluon phase is shown in figure A.2 for $l = -b$. At high temperatures there is no difference between the three lepton flavours. A negative net particle density means, that more antiparticles than particles exists. Below $\sim m_\tau/3 \approx 600$ MeV the tau leptons disappear, giving rise to an increase of net tau neutrino density, in order to keep l_τ constant. At the same time the number of positrons and positive muons increases in order to balance the positive charge that can no longer reside in the tau sector. To conserve flavour this is compensated by a corresponding change in the neutrino sector.

The net quark densities for this case are shown in figure A.3. The two different quark types u and d start at different points. If the temperature reaches the mass threshold of a quark species, it annihilates or decays and the remaining up- or down-like quarks increase their number densities to keep charge neutrality. For example the strange and down quarks react on the bottom disappearance. The picture shows, that considering only u, d, and

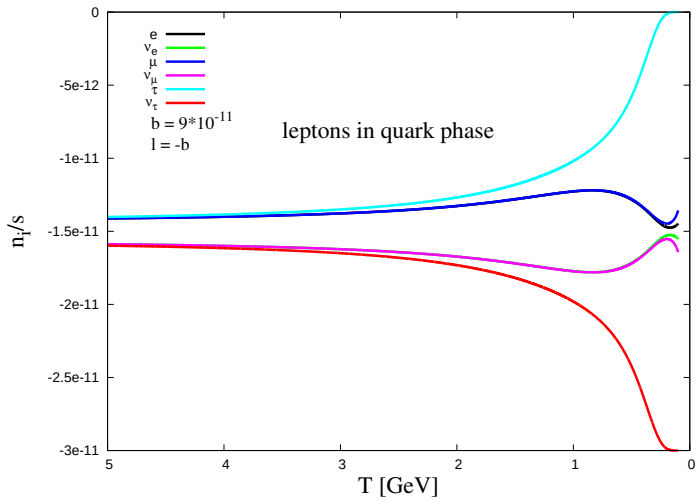

Figure A.2: Evolution of net lepton densities n_i in the quark phase for $l = -b$. We plot them with respect to the entropy density $s(T)$.

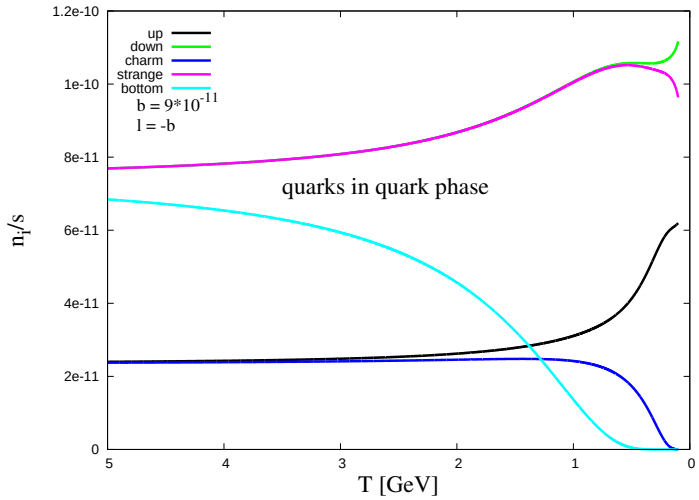

Figure A.3: Evolution of net quark densities in the quark phase for $l = -b$.

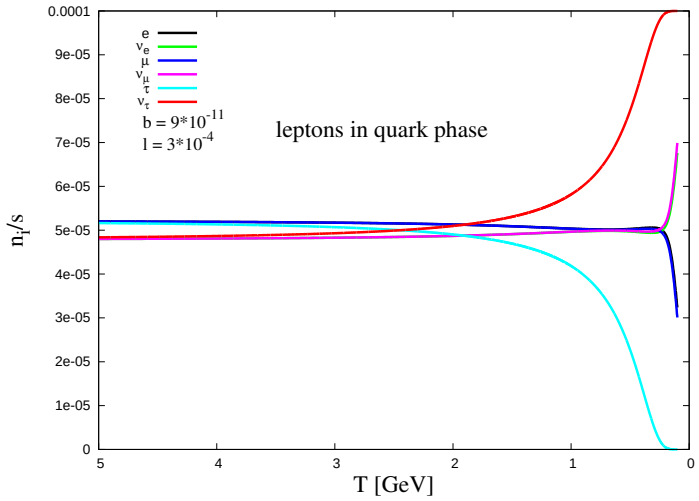

Figure A.4: Evolution of net lepton densities in the quark phase for $l = 3 \times 10^{-4}$. The order of magnitudes is very different from the case $l = -b$ and the sign is reversed.

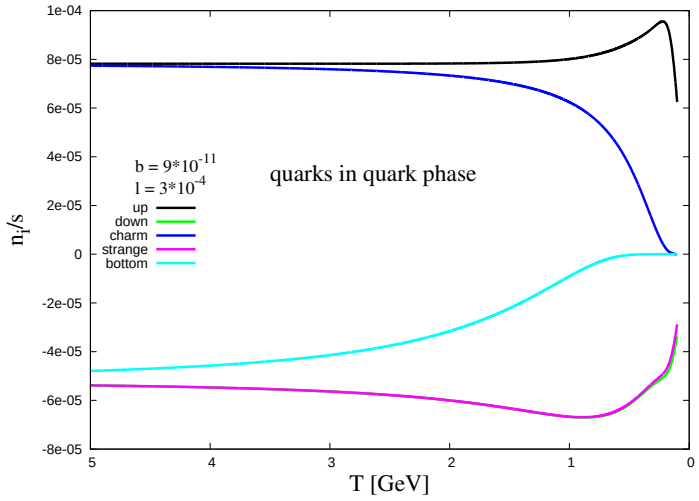

Figure A.5: Evolution of net quark densities in the quark phase for $l = 3 \times 10^{-4}$. In comparison to the $l = -b$ scenario, we find a very different behaviour of the net quark densities. Charge neutrality and the tiny baryon asymmetry force the net densities of down-like quarks to negative values.

s quarks around the QCD transition at $T_{\mathrm{QCD}} \sim 200$ MeV is a reasonable approximation.

Increasing the lepton asymmetry leads to drastically changes of net particle densities. In figures A.4 and A.5 their evolution in the quark-gluon phase are shown for $l = 3 \times 10^{-4}$. A positive lepton asymmetry leads to a dominance of negatively charged leptons. It comes without surprise that the net lepton densities react in a direct way, as they obviously depend on l_f. However, the quarks change their net densities by an comparable amount, as already indicated by our previous estimates (6.12) and (6.13). The net down-like quark densities become negative to react on the higher densities of the up-type quarks. The densities of the up types has to increase as an reaction of large lepton asymmetry to reach the charge neutrality. The different signs of the quark chemical potential for large l are also indicated by (6.12) and (6.13). Our numerical calculations confirm the analytic approach (6.12) to (6.14) and show that large lepton asymmetries influence the net quark densities strongly.

Let us now turn to the hadron phase. The numerical solution for all relevant particles in the hadron phase are shown in figures (A.6) and (A.7). We consider the evolution form 300 MeV down to 1 MeV. Below $T \sim 10$ MeV effects of neutrino oscillations become relevant, which are not included in this work. For these calculations we took all hadrons listed by the Particle Data Group up to the mass of $m_{K^*} = 1414$ MeV into account.

The figures show the evolution of net particle densities for $l = -b$ and $l = 3\times10^{-4}$, respectively. Again it can be seen, that $l = -b$ leads to an antimatter dominated universe in the leptonic sector until the pion disappearance (not shown in the figure). At the lowest temperatures considered, the electron density is strongly linked with the baryon number via the charge neutrality of the Universe. The inclusion of light mesons like pions and kaons is also important to understand the split between proton and neutron densities at temperatures close to the QCD transition. This is another effect that is not obvious from the very beginning. As pions are effectively massless, they can carry negative charge density in order to compensate for the positive charge density in protons and positrons. The influence of larger l on the net particle densities of the neutron and proton can be clearly seen, as the evolution differs in the high temperature regime. For low temperatures their evolution is independent of l, as indicated by (6.29). The effect of large l on μ_p and μ_n for small T is negligibly.

Our numerical calculation fits the analytic approaches for both phases well. There is clearly an influence of large l on quarks and hadrons.

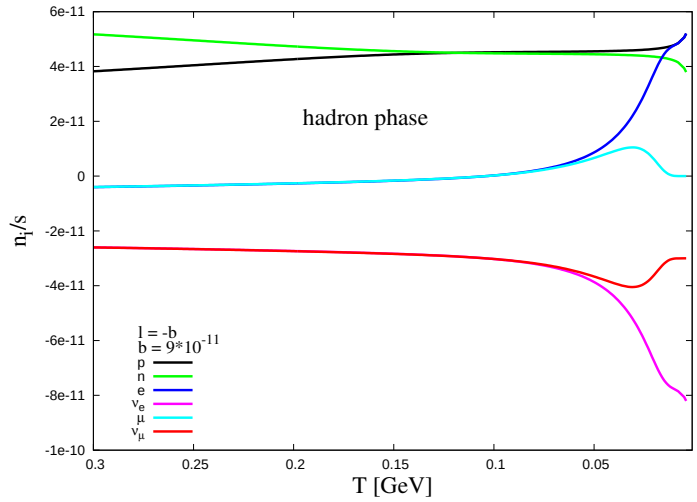

Figure A.6: Evolution of net particle densities in the hadron phase for $l = -b$.

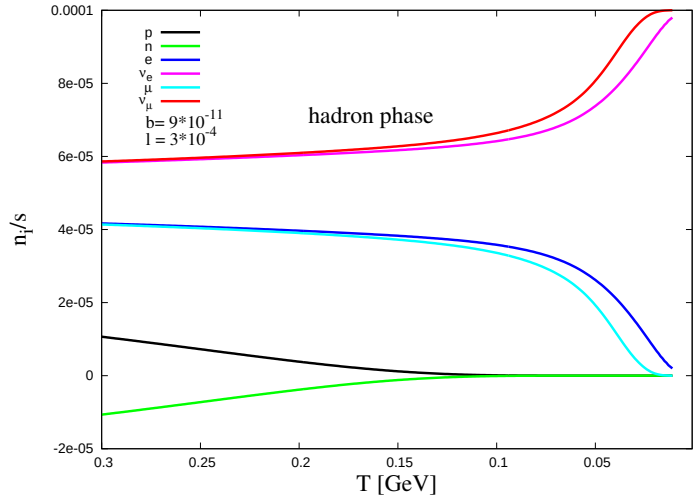

Figure A.7: Evolution of net particle densities in the hadron phase for $l = 3 \times 10^{-4}$. The influence of a larger l on the net particle densities of the neutron and proton can be seen clearly.

List of Figures

Bibliography

[ABB02] Kevork N. Abazajian, John F. Beacom, and Nicole F. Bell. Stringent constraints on cosmological neutrino anti-neutrino asymmetries from synchronized flavor transformation. *Phys.Rev.*, D66:013008, 2002. astro-ph/0203442.

[ABFW05] Kevork Abazajian, Nicole F. Bell, George M. Fuller, and Yvonne Y.Y. Wong. Cosmological lepton asymmetry, primordial nucleosynthesis, and sterile neutrinos. *Phys.Rev.*, D72:063004, 2005. astro-ph/0410175.

[AD85] Ian Affleck and Michael Dine. A New Mechanism for Baryogenesis. *Nucl.Phys.*, B249:361, 1985.

[AEF+06] Y. Aoki, G. Endrodi, Z. Fodor, S.D. Katz, and K.K. Szabo. The Order of the quantum chromodynamics transition predicted by the standard model of particle physics. *Nature*, 443:675–678, 2006. hep-lat/0611014.

[AFKS06] Y. Aoki, Z. Fodor, S.D. Katz, and K.K. Szabo. The QCD transition temperature: Results with physical masses in the continuum limit. *Phys.Lett.*, B643:46–54, 2006. hep-lat/0609068.

[AH85] J. H. Applegate and C. J. Hogan. Relics of cosmic quark condensation. *Phys. Rev.*, D31:3037–3045, 1985.

[ASRS08] Mark G. Alford, Andreas Schmitt, Krishna Rajagopal, and Thomas Schafer. Color superconductivity in dense quark matter. *Rev.Mod.Phys.*, 80:1455–1515, 2008. arXiv:0709.4635.

[BBS91] K.G. Begeman, A.H. Broeils, and R.H. Sanders. Extended rotation curves of spiral galaxies: Dark haloes and modified dynamics. *Mon.Not.Roy.Astron.Soc.*, 249:523, 1991.

[BCVM00] N. Borghini, W. N. Cottingham, and R. Vinh Mau. Possible cosmological implications of the quark-hadron phase transition. *J. Phys.*, G26:771, 2000.

[Ber88] Jeremy Bernstein. *Kinetic theory in the expanding universe.* Cambridge Univ. Pr., Cambridge, 1988.

[BHS05] Gianfranco Bertone, Dan Hooper, and Joseph Silk. Particle dark matter: Evidence, candidates and constraints. *Phys.Rept.*, 405:279–390, 2005. hep-ph/0404175.

[BS01] Annamaria Borriello and Paolo Salucci. The Dark matter distribution in disk galaxies. *Mon.Not.Roy.Astron.Soc.*, 323:285, 2001. astro-ph/0001082.

[BSB11] Tillmann Boeckel and Jurgen Schaffner-Bielich. A little inflation at the cosmological QCD phase transition. 2011.

[CC06] Yi-Zen Chu and Marco Cirelli. Sterile neutrinos, lepton asymmetries, primordial elements: How much of each? *Phys.Rev.*, D74:085015, 2006. astro-ph/0608206.

[CCG99] Alberto Casas, Wai Yan Cheng, and Graciela Gelmini. Generation of large lepton asymmetries. *Nucl.Phys.*, B538:297–308, 1999. hep-ph/9709289.

[CD92] M.V. Chizhov and A.D. Dolgov. Baryogenesis and large scale structure of the universe. *Nucl.Phys.*, B372:521–532, 1992.

[CDRG98] Andrew G. Cohen, A. De Rujula, and S.L. Glashow. A Matter - antimatter universe? *Astrophys.J.*, 495:539–549, 1998. astro-ph/9707087.

[Cer06] Precision electroweak measurements on the Z resonance. *Phys. Rept.*, 427:257–454, 2006. hep-ex/0509008.

[CGMO99] Bruce A. Campbell, Mary K. Gaillard, Hitoshi Murayama, and Keith A. Olive. Regulating the baryon asymmetry in no scale Affleck-Dine baryogenesis. *Nucl.Phys.*, B538:351–367, 1999. hep-ph/9805300.

[Che10] Hsin-Chia Cheng. 2009 TASI Lecture – Introduction to Extra Dimensions. 2010. arXiv:1003.1162.

[CK09] Leonid Chuzhoy and Edward W. Kolb. Reopening the window on charged dark matter. *JCAP*, 0907:014, 2009. arXiv:0809.0436.

[Cli06] James M. Cline. Baryogenesis. 2006. hep-ph/0609145.

[DEC79] Jr. Davis, R., J.C. Evans, and B.T. Cleveland. The solar neutrino problem. *AIP Conf.Proc.*, 52:17–27, 1979.

[DEES90] Savas Dimopoulos, David Eichler, Rahim Esmailzadeh, and Glenn D. Starkman. Getting a charge out of Dark Matter. *Phys.Rev.*, D41:2388, 1990.

[dFP07] P. de Forcrand and O. Philipsen. Exploring the details of the QCD phase diagram. *Eur.Phys.J.*, A31:804–809, 2007.

[DHH68] Jr. Davis, Raymond, Don S. Harmer, and Kenneth C. Hoffman. Search for neutrinos from the sun. *Phys.Rev.Lett.*, 20:1205–1209, 1968.

[DHP+02] A.D. Dolgov, S.H. Hansen, S. Pastor, S.T. Petcov, G.G. Raffelt, et al. Cosmological bounds on neutrino degeneracy improved by flavor oscillations. *Nucl.Phys.*, B632:363–382, 2002. hep-ph/0201287.

[DHS+10] J. Dunkley, R. Hlozek, J. Sievers, V. Acquaviva, P.A.R. Ade, et al. The Atacama Cosmology Telescope: Cosmological Parameters from the 2008 Power Spectra. 2010. 1009.0866.

[F+99] Y. Fukuda et al. Constraints on neutrino oscillation parameters from the measurement of day night solar neutrino fluxes at Super-Kamiokande. *Phys.Rev.Lett.*, 82:1810–1814, 1999. hep-ex/9812009.

[FK04] Z. Fodor and S.D. Katz. Critical point of QCD at finite T and mu, lattice results for physical quark masses. *JHEP*, 0404:050, 2004. hep-lat/0402006.

[FR02] Michael J. Fromerth and Johann Rafelski. Hadronization of the quark Universe. 2002. astro-ph/0211346.

[GGdHPGV00] M.C. Gonzalez-Garcia, P.C. de Holanda, Carlos Pena-Garay, and J.W.F. Valle. Status of the MSW solutions of the solar neutrino problem. *Nucl.Phys.*, B573:3–26, 2000. hep-ph/9906469.

[GHS05] Anne M. Green, Stefan Hofmann, and Dominik J. Schwarz. The First wimpy halos. *JCAP*, 0508:003, 2005. astro-ph/0503387.

[Gut81] Alan H. Guth. The Inflationary Universe: A Possible Solution to the Horizon and Flatness Problems. *Phys.Rev.*, D23:347–356, 1981.

[Gyn03] A. Gynther. Electroweak phase diagram at finite lepton number density. *Phys.Rev.*, D68:016001, 2003. hep-ph/0303019.

[HMM+02] S.H. Hansen, G. Mangano, A. Melchiorri, G. Miele, and O. Pisanti. Constraining neutrino physics with BBN and CMBR. *Phys.Rev.*, D65:023511, 2002. astro-ph/0105385.

[HMRW10] Steen Hannestad, Alessandro Mirizzi, Georg G. Raffelt, and Yvonne Y. Y. Wong. Neutrino and axion hot dark matter bounds after WMAP-7. *JCAP*, 1008:001, 2010. arXiv:1004.0695.

[Hoo09] Dan Hooper. TASI 2008 Lectures on Dark Matter. pages 709–764, 2009. arXiv:0901.4090.

[HT90] Jeffrey A. Harvey and Michael S. Turner. Cosmological baryon and lepton number in the presence of electroweak fermion number violation. *Phys.Rev.*, D42:3344–3349, 1990.

[HYG02] Henk Hoekstra, Howard Yee, and Mike Gladders. Current status of weak gravitational lensing. *New Astron.Rev.*, 46:767–781, 2002. astro-ph/0205205.

[IDC11] Hoernisa Iminniyaz, Manuel Drees, and Xuelei Chen. Relic Abundance of Asymmetric Dark Matter. 2011. arxiv:1104.5548.

[IS01] J. Ignatius and Dominik J. Schwarz. The QCD phase transition in the inhomogeneous universe. *Phys.Rev.Lett.*, 86:2216–2219, 2001. hep-ph/0004259.

[IT10] Y.I. Izotov and T.X. Thuan. The primordial abundance of 4He: evidence for non-standard big bang nucleosynthesis. *Astrophys.J.*, 710:L67–L71, 2010. arXiv:1001.4440.

[Jac07] Neal Jackson. The hubble constant. *Living Reviews in Relativity*, 10(4), 2007.

[JKG96] Gerard Jungman, Marc Kamionkowski, and Kim Griest. Supersymmetric dark matter. *Phys.Rept.*, 267:195–373, 1996. hep-ph/9506380.

[K+11] E. Komatsu et al. Seven-Year Wilkinson Microwave Anisotropy Probe (WMAP) Observations: Cosmological Interpretation. *Astrophys.J.Suppl.*, 192:18, 2011.

[Kam00] Burkhard Kampfer. Cosmic phase transitions. *Annalen Phys.*, 9:605–635, 2000.

[Kar07] Frithjof Karsch. Transition temperature in QCD with physical light and strange quark masses. *J.Phys.G*, G34:S627–S630, 2007.

[Kar09] Frithjof Karsch. Lattice results on QCD at high temperature and non-zero baryon number density. *Prog.Part.Nucl.Phys.*, 62:503–511, 2009.

[KLRS96] K. Kajantie, M. Laine, K. Rummukainen, and Mikhail E. Shaposhnikov. Is there a hot electroweak phase transition at m(H) larger or equal to m(W)? *Phys.Rev.Lett.*, 77:2887–2890, 1996. hep-ph/9605288.

[KLS10] Lawrence M. Krauss, Cecilia Lunardini, and Christel Smith. Neutrinos, WMAP, and BBN. *Phys.Rev.D*, 2010. 1009.4666.

[KLZ09] David E. Kaplan, Markus A. Luty, and Kathryn M. Zurek. Asymmetric Dark Matter. *Phys.Rev.*, D79:115016, 2009.

[KT94] E.W. Kolb and M.S. Turner. *The Early Universe*. Westview Press, 1994.

[Lin76] Andrei D. Linde. High Density and High Temperature Symmetry Behavior in Gauge Theories. *Phys.Rev.*, D14:3345, 1976.

[Lin82] Andrei D. Linde. A New Inflationary Universe Scenario: A Possible Solution of the Horizon, Flatness, Homogeneity, Isotropy and Primordial Monopole Problems. *Phys.Lett.*, B108:389–393, 1982.

[LS94] Jiang Liu and Gino Segre. Baryon asymmetry of the universe and large lepton asymmetries. *Phys.Lett.*, B338:259–262, 1994.

[McD99] John McDonald. Symmetry nonrestoration via order 10**-10 B and L asymmetries. *Phys.Lett.*, B463:225–229, 1999. hep-ph/9907358.

[McD00] John McDonald. Naturally large cosmological neutrino asymmetries in the MSSM. *Phys.Rev.Lett.*, 84:4798–4801, 2000. hep-ph/9908300.

[MMBP04] R. Benton Metcalf, Leonidas A. Moustakas, Andrew J. Bunker, and Ian R. Parry. Spectroscopic gravitational lensing and limits on the dark matter substructure in Q2237+0305. *Astrophys.J.*, 607:43–59, 2004. astro-ph/0309738.

[MOS92] John McDonald, Keith A. Olive, and Mark Srednicki. Relic densities of neutralinos. *Phys.Lett.*, B283:80–84, 1992.

[MRMR99] John March-Russell, Hitoshi Murayama, and Antonio Riotto. The Small observed baryon asymmetry from a large lepton asymmetry. *JHEP*, 9911:015, 1999. hep-ph/9908396.

[Muk05] V. Mukhanov. *Physical Foundation of Cosmology*. Cambridge University Press, 2005.

[N+10] K Nakamura et al. Review of particle physics. *J.Phys.G*, G37:075021, 2010.

[Oli99] Keith A. Olive. Introduction to supersymmetry: Astrophysical and phenomenological constraints. 1999. hep-ph/9911307.

[OSTW91] Keith A. Olive, David N. Schramm, David Thomas, and Terry P. Walker. Neutrino degeneracy and cosmological nucleosynthesis, revisited. *Phys.Lett.*, B265:239–244, 1991.

[Par08] Stephen J. Parke. *Neutrino oscillation phenomenology*. World Scientific, 2008.

[Pau78] W. Pauli. Dear radioactive ladies and gentlemen. *Phys.Today*, 31N9:27, 1978.

[Phi07] Owe Philipsen. Exploring the QCD phase diagram. *PoS*, CPOD07:028, 2007. arXiv:0710.1217.

[PQ77] R.D. Peccei and Helen R. Quinn. CP Conservation in the Presence of Instantons. *Phys.Rev.Lett.*, 38:1440–1443, 1977.

[PR03] P.J.E. Peebles and Bharat Ratra. The Cosmological constant and dark energy. *Rev.Mod.Phys.*, 75:559–606, 2003. astro-ph/0207347.

[PTVF96] W.H. Press, S.A. Teukolsky, W.T. Vetterling, and B.P Flannery. *Numerical Recipes in C*, volume 2nd Edition, reprinted 1996. Cambridge University Press, 1996.

[Sak67] A. D. Sakharov. Violation of cp invariance, c asymmetry, and baryon asymmetry of the universe. *Pisma Zh. Eksp. Teor. Fiz.*, 5:32–35, 1967.

[Sch98] Dominik J. Schwarz. Evolution of gravitational waves through cosmological transitions. *Mod.Phys.Lett.*, A13:2771–2778, 1998. gr-qc/9709027.

[Sch03] Dominik J. Schwarz. The first second of the universe. *Annalen Phys.*, 12:220–270, 2003. astro-ph/0303574.

[Sch06] Christian Schmidt. QCD thermodynamics at zero and non-zero density. *PoS*, CPOD2006:002, 2006. hep-lat/0701019.

[SF06a] E. R. Siegel and James N. Fry. Can electric charges and currents survive in an inhomogeneous universe? 2006. astro-ph/0609031.

[SF06b] E.R. Siegel and J.N. Fry. Cosmological structure formation creates large-scale magnetic fields. *Astrophys. J.*, 651:627–635, 2006. astro-ph/0604526.

[SGED90] Glenn D. Starkman, Andrew Gould, Rahim Esmailzadeh, and Savas Dimopoulos. Opening the Window on Strongly Interacting Dark Matter. *Phys.Rev.*, D41:3594, 1990.

[Sik08] Pierre Sikivie. Axion Cosmology. *Lect.Notes Phys.*, 741:19–50, 2008. astro-ph/0610440.

[SMFB06] Constantinos Skordis, D.F. Mota, P.G. Ferreira, and C. Boehm. Large Scale Structure in Bekenstein's theory of relativistic Modified Newtonian Dynamics. *Phys.Rev.Lett.*, 96:011301, 2006. astro-ph/0505519.

[SR05] Pasquale D. Serpico and Georg G. Raffelt. Lepton asymmetry and primordial nucleosynthesis in the era of precision cosmology. *Phys.Rev.*, D71:127301, 2005. astro-ph/0506162.

[SS08] Vimal Simha and Gary Steigman. Constraining The Universal Lepton Asymmetry. *JCAP*, 0808:011, 2008. arXiv:0806.0179.

[SSW97] Christoph Schmid, Dominik J. Schwarz, and Peter Widerin. Peaks above the Harrison-Zel'dovich spectrum due to the quark - gluon to hadron transition. *Phys.Rev.Lett.*, 78:791–794, 1997. astro-ph/9606125.

[Ste06] M. A. Stephanov. Qcd phase diagram: An overview. *PoS*, LAT2006:024, 2006. hep-lat/0701002.

[Ste07] Gary Steigman. Primordial Nucleosynthesis in the Precision Cosmology Era. *Ann.Rev.Nucl.Part.Sci.*, 57:463–491, 2007. arXiv:0712.1100.

[Ste09] Frank Daniel Steffen. Dark Matter Candidates - Axions, Neutralinos, Gravitinos, and Axinos. *Eur.Phys.J.*, C59:557–588, 2009. arXiv:0811.3347.

[T+04] Max Tegmark et al. The 3-D power spectrum of galaxies from the SDSS. *Astrophys.J.*, 606:702–740, 2004. astro-ph/0310725.

[Wei72] S. Weinberg. *Gravitation and Cosmology, Principles and Applications of the General Theory of Relativity*. John Wiley and Sons Inc., 1972.

[Wit84] Edward Witten. Cosmic separation of phases. *Phys. Rev.*, D30:272–285, 1984.

[WK06] Yuki Watanabe and Eiichiro Komatsu. Improved Calculation of the Primordial Gravitational Wave Spectrum in the Standard Model. *Phys.Rev.*, D73:123515, 2006. astro-ph/0604176.

[Won02] Yvonne Y.Y. Wong. Analytical treatment of neutrino asymmetry equilibration from flavor oscillations in the early universe. *Phys.Rev.*, D66:025015, 2002. hep-ph/0203180.

[Zar00] K. Zarembo. Lepton asymmetry of the universe and charged quark gluon plasma. *Phys.Lett.*, B493:375–379, 2000. hep-ph/0008264.

[Zhi03] Ariel R. Zhitnitsky. Dark matter as dense color superconductor. *Nucl.Phys.Proc.Suppl.*, 124:99–102, 2003. astro-ph/0204218.